

REDUCTION OF FALSE ARRHYTHMIA ALARMS ON PATIENT  
MONITORING SYSTEMS IN INTENSIVE CARE UNITS BY USING  
FUZZY LOGIC ALGORITHMS

A THESIS SUBMITTED TO  
THE GRADUATE SCHOOL OF NATURAL AND APPLIED SCIENCES  
OF  
MIDDLE EAST TECHNICAL UNIVERSITY

BY

ERDEM YANAR

IN PARTIAL FULFILLMENT OF THE REQUIREMENTS  
FOR  
THE DEGREE OF MASTER OF SCIENCE  
IN  
ELECTRICAL AND ELECTRONICS ENGINEERING

JANUARY 2018



Approval of the thesis:

**REDUCTION OF FALSE ARRHYTHMIA ALARMS ON PATIENT  
MONITORING SYSTEMS IN INTENSIVE CARE UNITS BY USING  
FUZZY LOGIC ALGORITHMS**

submitted by **ERDEM YANAR** in partial fulfillment of the requirements for  
the degree of **Master of Science in Electrical and Electronics Engineer-  
ing Department, Middle East Technical University** by,

Prof. Dr. Gülbin Dural Ünver \_\_\_\_\_  
Dean, Graduate School of **Natural and Applied Sciences**

Prof. Dr. Tolga Çiloğlu \_\_\_\_\_  
Head of Department, **Electrical and Electronics Eng.**

Assoc. Prof. Dr. Yeşim Serinağaoğlu Doğrusöz \_\_\_\_\_  
Supervisor, **Electrical Electronics Eng. Dept., METU**

**Examining Committee Members:**

Prof. Dr. Murat Eyüboğlu \_\_\_\_\_  
Electrical and Electronics Engineering Department, METU

Assoc. Prof. Dr. Yeşim Serinağaoğlu Doğrusöz \_\_\_\_\_  
Electrical and Electronics Engineering Department, METU

Prof. Dr. Nevzat Gençer \_\_\_\_\_  
Electrical and Electronics Engineering Department, METU

Prof. Dr. Tolga Çiloğlu \_\_\_\_\_  
Electrical and Electronics Engineering Department, METU

Assist. Prof. Dr. Özlem Birgül \_\_\_\_\_  
Biomedical Engineering Department, Ankara University

**Date:** \_\_\_\_\_

I hereby declare that all information in this document has been obtained and presented in accordance with academic rules and ethical conduct. I also declare that, as required by these rules and conduct, I have fully cited and referenced all material and results that are not original to this work.

Name, Last Name: ERDEM YANAR

Signature :

## ABSTRACT

### REDUCTION OF FALSE ARRHYTHMIA ALARMS ON PATIENT MONITORING SYSTEMS IN INTENSIVE CARE UNITS BY USING FUZZY LOGIC ALGORITHMS

YANAR, Erdem

M.S., Department of Electrical and Electronics Engineering

Supervisor : Assoc. Prof. Dr. Yeşim Serinağaoğlu Doğrusöz

January 2018, 132 pages

Generally in hospitals, monitoring devices in the intensive care units (ICU) have high rates of false arrhythmia alarms independent of their brands and prices. These falsely issued alarms have financial and physiological effects such as redundant usage of hospital resources and hassling patients' rest, reducing sensitivity of the hospital staff to potential emergency cases, which is named as "false alarm fatigue". According to Deshmene et al. (2009), 43% of arrhythmia alarms in ICUs are false. Moreover, This rate reaches 90% in some of the arrhythmia types. In our study, we considered that the alarms are triggered by five life threatening conditions, which are asystole (ASY), bradycardia (EBR), tachycardia (ETC), ventricular tachycardia (VTA), ventricular flutter/fibrillation (VFB). These alarms are usually triggered by analysis of ECG and pulsatile waveforms recorded by patient monitoring equipments, which have standard alarm triggering criteria such as instantaneous thresholds on the predictor values. Most

of the ICU false alarms are caused by single channel artifacts. In this study, we aim to fuse ECG features with information from other independent signals and get more robust alarm algorithms for ICUs. Pulsatile waveforms, which are highly correlated signals, can be used to corroborate the alarm category and to suppress significant number of false ECG alarms in ICUs. Photoplethysmogram (PPG), arterial blood pressure (ABP) or both PPG, and ABP can be used for this purpose. These waveforms are the least noisy pressure signals available in certain ICUs, and rarely contain ECG-related artifacts. We implemented four different algorithms that use information from ECG, PPG and ABP waveforms. We trained and tested these algorithms on Physionet Challenge 2015 database, which consists of 5 main arrhythmia types and total of 750 recordings. These algorithms have main analysis steps as: pre-processing (bandpass filters to remove baseline artifacts, scaling to normalize the amplitude of waveforms), beat detection, alarm decision (for the generic algorithm). Our results show that if we use only ECG data of the whole dataset, we can obtain 88.3% sensitivity and 77.4% specificity with negligible difference in results between two simultaneous ECG channels. When we use ECG with ABP and PPG combinations, our sensitivity was increased by 8% but specificity decreased by 4%. When we use ECG with PPG combinations, our sensitivity was increased by 6.7% but specificity decreased by 7.9%. These improved methods obtained in this work are around the tolerances accepted by expert physicians, and slightly outperform the results of EBR and VFB cases by the other known algorithms evaluated with the same database.

Keywords: False alarm reduction, Signal quality assessment, ECG (Electrocardiogram); Intensive Care Unit; Blood pressure

# ÖZ

## YOĞUN BAKIM ÜNİTELERİNDEKİ HASTA BAŞI MONİTÖRLERİNDE YANLIŞ ARİTMİ ALARMLARININ BULANIK MANTIK ALGORİTMALARI KULLANILARAK AZALTILMASI

YANAR, Erdem

Yüksek Lisans, Elektrik ve Elektronik Mühendisliği Bölümü

Tez Yöneticisi : Doç. Dr. Yeşim Serinağaoğlu Doğrusöz

Ocak 2018 , 132 sayfa

Günümüz hastane ünitelerinde gelişmiş medikal cihazlar, görüntüleme, tanı ve tedavi açısından önem arz etmektedir. Bunlardan Hasta Başı Monitörleri (HBM) gelişmiş sinyal işleme algoritmaları ve sensörleriyle erken tanı imkanı sağlayarak ve alarm vererek özellikle yoğun bakım ünitelerinin ihtiyaçlarını karşılamaktadırlar. Bu sayede hastalardaki kritik ve olağandışı reaksiyonlara anında müdahale edilebilmektedir. Fakat bu cihazlarda algılayıcı uçlarda temassızlık, hastanın fiziksel hareketi, veya cihazdaki algoritmanın hatası sonucu yanlış alarmlar ortaya çıkabilmekte acil bir durum olmadığı halde cihaz alarm verebilmektedir. Yapılan bir araştırmaya göre hasta başı monitörlerinin verdiği alarmların %43'ünün

yanlış alarm olduğu, hatta bu oranın bazı durumlarda %90'lara kadar çıkabildiği saptanmıştır. Bu da hastane kaynaklarının boşa harcanmasına, hastane personelinin tepki süresinin uzamasına ve alarmların sıradan olarak algılanmasına yol açmaktadır. Yukarıda bahsedilen insan veya cihaz kaynaklı hataların azaltılması için elektrokardiyografi (EKG) verisi dışında ek verilerin de değerlendirilip, sonuçların füzyon edilmesi ile daha hassas sonuçlar elde edilebilmektedir. Bu çalışmada EKG verisinin, fotopletismografi (PPG) ve arteriyel kan basıncı (ABP) verilerinin analizi ile hasta başı monitörlerindeki beş temel aritmi (asistoli, bradikardi, taşikardi, ventriküler taşikardi, ventriküler fibrilasyon) için yanlış alarmların azaltılması amaçlanmaktadır. Bu doğrultuda dört farklı algoritma geliştirilmiş ve bu algoritmalar Physionet Challenge 2015 veri seti üzerinde eğitilip test edilmiştir. Yapılan araştırmalar sonunda veri setinden sadece EKG verisi kullanılarak %83.3 hassaslık ve %77.4 özgüllük elde edilmiştir. EKG ve PPG verileri birlikte kullanıldığında hassaslık %6.7 artırılırken buna karşılık özgüllükte %7.9 düşüş gözlemlenmiştir. EKG, PPG ve ABP verileri ile birlikte kullanıldığında hassaslık %8 artırılırken buna karşılık özgüllükte %4 düşüş gözlemlenmiştir. Bu çalışma kapsamında geliştirmiş olduğumuz metotlardan elde edilen sonuçlar, kardiyologların aritmi saptama istekleri içerisinde kalmakta olup aynı data bankasını kullanan literatürdeki diğer yöntemlere göre özellikle bradikardi ve ventriküler taşikardi alarmlarında daha iyi performans göstermektedir.

Anahtar Kelimeler: False alarm reduction, Signal quality assessment, ECG (Electrocardiogram); Intensive Care Unit; Blood pressure

To my wife and family

## ACKNOWLEDGMENTS

First of all, I would like to express my gratitude to my advisor Assoc. Prof. Dr. Yeşim Serinağaoğlu Doğrusöz for her guidance and motivation throughout the study. I would like to thank my employer, ASELSAN, for supporting this study. Last but not least, I would like to thank my wife Seda ATEŞ YANAR and my families (ATEŞ and YANAR) for their love and support which started the day we met and continue throughout my life.

# TABLE OF CONTENTS

ABSTRACT . . . . .	v
ÖZ . . . . .	vii
ACKNOWLEDGMENTS . . . . .	x
TABLE OF CONTENTS . . . . .	xi
LIST OF TABLES . . . . .	xv
LIST OF FIGURES . . . . .	xix
LIST OF ABBREVIATIONS . . . . .	xxii
CHAPTERS	
1 INTRODUCTION . . . . .	1
1.1 Physionet Challenge 2015 Databases . . . . .	4
1.2 Objective of the Thesis . . . . .	6
1.3 Contribution of Thesis . . . . .	8
1.4 Scope of the Study . . . . .	8
1.5 Outline of the Thesis . . . . .	9
2 BACKGROUND INFORMATION . . . . .	11
2.1 Medical Background . . . . .	11

2.1.1	Anatomy and Physiology of the Heart . . . . .	11
2.1.2	Electrical Activity of the Heart . . . . .	12
2.1.3	ECG Waveform Morphology . . . . .	13
2.1.4	ECG Waveform Measurement . . . . .	17
2.1.5	PPG Waveform Morphology and Pulse Oximetry	20
2.1.6	Arterial Blood Pressure (ABP) Waveform Mor- phology . . . . .	22
2.1.7	Arterial Blood Pressure Measurement . . . . .	23
2.1.8	Artifacts in Physiological Signals . . . . .	24
2.2	Signal Processing Background . . . . .	29
2.2.1	QRS Complex Enhancement Methods . . . . .	29
2.2.2	QRS Complex Detection Methods . . . . .	30
2.2.3	PPG Waveform Detection Methods . . . . .	30
2.2.4	ABP Waveform Detection Methods . . . . .	32
2.2.5	Literature Survey on False Arrhythmia Alarms Reduction . . . . .	34
2.2.6	Performance Evaluation . . . . .	42
3	METHODS . . . . .	45
3.1	Pre-Processing . . . . .	45
3.2	QRS Complex Detection . . . . .	46
3.3	PPG Detection . . . . .	51
3.4	ABP Detection . . . . .	53

3.5	Signal Integration . . . . .	54
3.6	Arrhythmia Type Based Processing and Classification . . . . .	58
3.6.1	Asystole Processing . . . . .	59
3.6.2	Bradycardia Processing . . . . .	60
3.6.3	Tachycardia Processing . . . . .	61
3.6.4	Ventricular Tachycardia Processing . . . . .	62
3.6.5	Ventricular Flutter or Fibrillation Processing . . . . .	63
4	PERFORMANCE EVALUATION . . . . .	65
4.1	QRS Complex, PPG, ABP, Detections Performances . . . . .	65
4.1.1	QRS Complex, PPG, ABP, Detection Based Methods Performances . . . . .	67
4.1.2	METU BEST Methods Performances . . . . .	80
4.1.3	Our Best Methods vs Cinc2015 Finalists Performances . . . . .	86
4.2	Limitations . . . . .	91
5	DISCUSSION AND CONCLUSIONS . . . . .	93
5.1	Summary and Discussions . . . . .	93
5.2	Conclusions . . . . .	96
5.3	Recommendations for Future Work . . . . .	97
	REFERENCES . . . . .	99

APPENDICES

A	MATLAB PHYSIONET TOOLBOX ALGORITHMS USED IN THE THESIS . . . . .	107
B	FEATURE EXTRACTION . . . . .	111
C	QRS COMPLEX ENHANCEMENT METHODS . . . . .	115
C.1	QRS Complex Detection Methods . . . . .	126

## LIST OF TABLES

### TABLES

Table 1.1	Data Set Alarm Definitions [17] . . . . .	5
Table 1.2	Data Set Alarms [17] . . . . .	6
Table 1.3	Pulsatile Waveform Distribution of the Dataset [17] . . . . .	6
Table 2.1	Einthoven Triangle Leads [10] . . . . .	18
Table 2.2	wabp.mat Function Performance . . . . .	33
Table 2.3	General Use of Parameters . . . . .	43
Table 3.1	Summary of various researches for ECG beat segmentation . .	47
Table 3.2	QRS complex performance comparison with several algorithms	47
Table 4.1	Training, Testing and Challenge Datasets Contents [17] . . . .	66
Table 4.2	Number of PPG/ABP signals in the Training, Testing Datasets [17] . . . . .	67
Table 4.3	General Arrhythmias Threshold and Tolerance Limit Parameters	68
Table 4.4	Only ECG Method Arrhythmia Based Parameters . . . . .	68
Table 4.5	Only ECG Method Training Results . . . . .	68
Table 4.6	Only ECG Method Testing Results . . . . .	69

Table 4.7 ONLY ECG Method for Challenge Case and Comparison with CinC2015 Best Results . . . . .	69
Table 4.8 Only PPG or ABP Method Arrhythmia Based Parameters . .	72
Table 4.9 Only PPG/ABP Method Training Results . . . . .	72
Table 4.10 Only PPG/ABP Method Testing Results . . . . .	72
Table 4.11 ONLY PPG/ABP Method for Challenge Case . . . . .	73
Table 4.12 Main PPG/ABP Secondary ECG Method Training Results . .	77
Table 4.13 Main PPG/ABP Secondary ECG Method Testing Results . .	77
Table 4.14 MAIN PPG OR ABP SECONDARY ECG Method for Chal- lenge Case . . . . .	78
Table 4.15 Main ECG and Secondary PPG or ABP Method Arrhythmia Based Parameters . . . . .	79
Table 4.16 Main ECG Secondary PPG/ABP Method Training Results . .	79
Table 4.17 Main ECG Secondary PPG/ABP Method Testing Results . .	79
Table 4.18 MAIN ECG SECONDARY PPG AND ABP Method for Chal- lenge Case . . . . .	79
Table 4.19 METU BEST Method Training Results . . . . .	80
Table 4.20 METU BEST Method Testing Results . . . . .	80
Table 4.21 METU BEST Method Arrhythmia Based Parameters . . . . .	81
Table 4.22 METU BEST Method for Challenge Case . . . . .	81
Table 4.23 METU BEST Generic Method Training Results . . . . .	82
Table 4.24 METU BEST Generic Method Testing Results . . . . .	82
Table 4.25 METU BEST (without using ABP signal) Method Arrhythmia Based Parameters . . . . .	82

Table 4.26 METU BEST (without using ABP signal) Method Training Results . . . . .	83
Table 4.27 METU BEST (without using ABP signal) Method Testing Results	83
Table 4.28 METU BEST (without using ABP signal) Method for Challenge Case . . . . .	83
Table 4.29 METU BEST (without using ABP signal) Generic Method Training Results . . . . .	85
Table 4.30 METU BEST (without using ABP signal) Generic Method Testing Results . . . . .	85
Table 4.31 METU BEST (without using ABP signal) Generic Method Results in Challenge Case . . . . .	86
Table 4.32 Asystole Case Comparison . . . . .	87
Table 4.33 Bradycardia Case Comparison . . . . .	88
Table 4.34 Tachycardia Case Comparison . . . . .	89
Table 4.35 Ventricular-Tachycardia Case Comparison . . . . .	90
Table 4.36 Ventricular-Flutter/Fibrillation Case Comparison . . . . .	91
Table A.1 jSQI.m . . . . .	107
Table A.2 abpfeature.m . . . . .	108
Table A.3 rdmat.m . . . . .	109
Table A.4 wabp.m . . . . .	110
Table B.1 ABP Features . . . . .	111
Table B.2 SQI Logic . . . . .	112
Table B.3 Asystole Case Comparison . . . . .	112

Table B.4 Bradycardia Case Comparison . . . . .	113
Table B.5 Tachycardia Case Comparison . . . . .	113
Table B.6 Ventricular-Tachycardia Case Comparison . . . . .	114
Table B.7 Ventricular-Flutter/Fibrillation Case Comparison . . . . .	114

# LIST OF FIGURES

## FIGURES

Figure 2.1 P wave, QRS Complex, T wave and Their Intervals Illustration [10] . . . . .	14
Figure 2.2 P waves Examples [10] . . . . .	14
Figure 2.3 Various QRS complexes in the ECG [10] . . . . .	15
Figure 2.4 ST segments in the ECG [10] . . . . .	17
Figure 2.5 12 Lead Measurement Points [10] . . . . .	21
Figure 2.6 PPG Hemoglobin Extinction Curves [73] . . . . .	22
Figure 2.7 ABP Waveform [60] . . . . .	23
Figure 2.8 Power Line and Motion Artifacts [35] . . . . .	25
Figure 2.9 Loose Electrode Contacts Artifacts [35] . . . . .	26
Figure 2.10 Loose Motion Artifacts [35] . . . . .	27
Figure 2.11 Respiration and Noise [35] . . . . .	27
Figure 2.12 EMG Noise [35] . . . . .	28
Figure 2.13 Instrumentation Saturation Noise [35] . . . . .	28
Figure 2.14 Onset Detection by using arctan [77] . . . . .	31
Figure 2.15 Block Diagram of The ABP Onset Time Detection Algorithm	32
Figure 2.16 Block ABP signal, SSF Comparison . . . . .	33

Figure 2.17 ECG signal for Asystole Case [22] . . . . .	34
Figure 2.18 ECG signal for Bradycardia Case [22] . . . . .	34
Figure 2.19 ECG signal for Tachycardia Case [22] . . . . .	35
Figure 2.20 ECG signal for Ventricular Tachycardia Case [22] . . . . .	35
Figure 2.21 ECG signal for Ventricular Tachycardia Case [22] . . . . .	36
Figure 3.1 Block Diagram of Pre-processing Step . . . . .	46
Figure 3.2 Block diagram of Hilbert Detector . . . . .	48
Figure 3.3 R wave equivalences in The Approach . . . . .	48
Figure 3.4 Block diagram of the proposed QRS detector . . . . .	51
Figure 3.5 Block Diagram of PPG Detection Step . . . . .	52
Figure 3.6 Block Diagram of ABP Detection Step . . . . .	54
Figure 3.7 Block diagram of Only ECG Method . . . . .	55
Figure 3.8 Block diagram of Only PPG/ABP Method . . . . .	56
Figure 3.9 Block diagram of Main decider PPG/ABP Secondary Decider ECG Algorithm . . . . .	57
Figure 3.10 Block diagram of Main decider ECG Secondary Decider PPG/ABP Method . . . . .	58
Figure 3.11 Block diagram of Asystole Process . . . . .	59
Figure 3.12 Block diagram of Extreme Bradycardia Process . . . . .	60
Figure 3.13 Block diagram of Extreme Tachycardia Process . . . . .	61
Figure 3.14 Block diagram of Ventricular Tachycardia Process . . . . .	62
Figure 3.15 Block diagram of Ventricular Flutter/Fibrillation Process . . . . .	63

Figure 4.1 Asystole FalsePositive sample(a219l) . . . . .	70
Figure 4.2 Asystole FalseNegative sample(a653l) . . . . .	70
Figure 4.3 Tachycardia FalsePositive sample(t409l) . . . . .	71
Figure 4.4 Tachycardia FalseNegative sample(t114s) . . . . .	72
Figure 4.5 Ventricular Tachycardia FalsePositive sample (v100s) . . . . .	74
Figure 4.6 Ventricular Tachycardia FalseNegative sample (v206s) . . . . .	74
Figure 4.7 Tachycardia FalsePositive sample (t503l) . . . . .	75
Figure 4.8 Tachycardia FalseNegative sample (t192s) . . . . .	76
Figure 4.9 Asystole FalsePositive sample (a103l) . . . . .	76
Figure 4.10 Asystole FalseNegative sample (a653l) . . . . .	77
Figure 4.11 Ventricular Tachycardia FalsePositive sample(a385l) . . . . .	84
Figure 4.12 Ventricular Tachycardia TrueNegative sample(v111l) . . . . .	85
Figure 4.13 Asystole Case Comparison . . . . .	87
Figure 4.14 Bradycardia Case Comparison . . . . .	88
Figure 4.15 Tachycardia Case Comparison . . . . .	89
Figure 4.16 Ventricular-Tachycardia Case Comparison . . . . .	90
Figure 4.17 Ventricular-Flutter/Fibrillation Case Comparison . . . . .	91
Figure A.1 The slope sum function (SSF),It aids in onset detection [80] .	109
Figure C.1 Multilayer Perception [44] . . . . .	128
Figure C.2 LVQ Network [44] . . . . .	128
Figure C.3 Singularity Work Flow [44] . . . . .	131

## LIST OF ABBREVIATIONS

ABP	Arterial Blood Pressure
PPG	Photoplethysmography
WHO	World Health Organization
CVD	Cardiovascular Disease
AHA	American Heart Association
ECG	Electrocardiography
PD	Photodiode
SPI	Serial Peripheral Interface
ADC	Analog to Digital Converter
FIR	Finite Impulse Response
PPI	Peak-to-Peak Interval
Se	Sensitivity
+P	Positive Predictivity
-P	Negative Predictivity
TP	True Positive
TN	True Negative
FN	False Negative
FP	False Positive
THV	Threshold Value
SVM	State Vector Machine
CVD	Cardiovascular Disease
MI	Myocardial Infarction
VCG	Vector Cardiogram
IMF	Intrinsic Mode Function
EMD	Empirical Mode Decomposition
RBF	Radial Basis Function
LVQ	Network and Learning Vector Quantization
MLP	Multilayer Perception

## CHAPTER 1

### INTRODUCTION

The intensive care unit (ICU) is a unit in the hospital such that seriously ill patients, or patients who have undergone a major surgical operation or a serious head injury are cared by specially trained staff with special devices. The ICU staff includes doctors, nurses, respiratory therapists, clinical nurse specialists, pharmacists, physical nurse practitioners, physician assistants, dietitians, social workers and chaplains. There are a lot of equipments in the ICUs, such as ventilators, infusion pumps, syringe pumps, blood warmers, defibrillator and patient monitors, which may seem overwhelming. Patient monitors, which are used to monitor their heart, blood pressure and respiratory rate, and ventilators, which are used to help some patients breathe until they are able to breathe on their own, are the main devices in ICUs.

Clinical alarms are the another important duty of these ICU patient monitoring devices. These alarm systems warn hospital staff when a patient, who may have heart and blood vessel problems (such as very low/high blood pressure, heart attack, or unstable heart rhythm), needs an emergency care or when a sudden abnormal event occurs in the patient condition. In other words, when any emergency case or an abnormal vital signal is detected, these systems are triggered and give an alarm. Patient monitoring devices, which display frequent measurements of a myriad of vital sign parameters such as heart rate, respiratory rate ( $SpO_2$ ), systolic, diastolic, and mean values for all available pressures, are the main devices of detection of these situations. When any of these individual parameters fall outside the ‘too low’ or ‘too high’ alarm thresholds for a few seconds, an alarm is triggered which may sound an audible tone or visual text message. They are usually ECG signal-based devices.

Falsely issued alarms are very common in these devices. These incessant alarms are triggered by something as motion artifact from activities such as brushing one's teeth or noises from power line interference (details are explained in subsection 2.1.8). There are generally three main problems associated with false arrhythmia alarms in ICUs. These problems are redundant usage of hospital resources, hassling patients rest and inhibiting sensitivity of the hospital staff to potential emergency cases [13]. In some cases, hospital staff turn off alarms or adjust settings outside of safety limits, which lead to terrible consequences like patient falls, delay in treatments or treatment errors. Nearly 90% of false alarms are patient monitor based [19]. According to statistics, 43% of arrhythmia alarms in ICUs are false, and it can be as high as 90% in some arrhythmia types [2]. Therefore, reducing the number of falsely issued alarms in patient monitoring devices is highly important and vital. These alarms can be handled by improving the ECG processing or examining other measurable waveforms, which shows that there are no critical signs of abnormalities in the cardiac function.

False arrhythmia alarm reduction approaches in literature can be divided into 4 main categories as: those that use only the ECG signals, those that use the ECG and ABP signals together, those that use ECG and PPG signals together and those that uses ECG, PPG and ABP signals together during processing with respect to the input signals used in the approaches. In ECG only approaches, the algorithm proposed by Krestava et al. [46] is used. The ECG signal quality is obtained by using 3 frequency bands, which are high frequency (for spikes from artifacts and pacemakers), medium frequency (for signal level and power-line interference), low frequency (for baseline wanders) ranges.

Secondary waveforms are not measured directly from the heart; therefore, these signals are not affected by the same types of artifacts and noises which appear in the ECG signals. Moreover, these secondary signals such as pulsatile waveforms can also be used to compute and compare morphology and timing features of the cardiac cycle with the ones calculated from, the ECG signals.

In ECG with multiple pulsatile signals (ABP and PPG) as input approaches, Zong et al. claimed that false arrhythmia alarm reduction rate can be improved by comparing ECG signal results with multiple pulsatile waveform results [80].

Therefore, if the main signal has low SQ, then the alternative or secondary signals can be used for alarm decision. There are mainly two signals convenient for this purpose. One of them is photoplethysmogram (PPG) waveform. The PPG waveform is a pulsatile signal, which is measured non-invasively by attaching a pulse oximeter to a patient's finger. The other one is the ABP waveform. ABP is a basic hemodynamic index often utilized to guide therapeutic interventions, especially in critically ill patients and obtained from an arterial catheter connected to a pressure transducer. These waveforms have different noise characteristics from each other due to differences in their measurement techniques and sensor locations. For example the PPG waveform measures the blood further down the arterial tree, where the ABP measurement point is located. Therefore, the PPG waveform appears like a low pass filtered and delayed form of an ABP waveform. Usability of the PPG and the ABP waveforms and their performances vary from case to case. For example, PPG waveforms could provide more information than ABP if there is premature ventricular beat pattern during measurement. This makes the ABP waveform noisier than the PPG waveform because the latter are less affected from the noise due to inefficiency of blood pumping resulting in less amplification to of the noise. However, if there is tachycardia pattern, probably the ABP waveform is more useful than the PPG waveform for alarm suppression [43]. Clifford et al. reported that to avoid misleading decisions in their ECG false alarms suppression framework, before using PPG and ABP waveforms they apply SQ measurements on these signals to decide their reliability [43]. Details of literature survey is given in subsection 2.2.5.

In ECG, ABP signals together input approach, Aboukhalil et al. have proposed a mathematical model and a framework, which use arterial blood pressure (ABP) waveforms to indicate false critical ECG arrhythmia alarms [2]. When ECG based alarms occur, in parallel, the algorithm calculates the signal quality (SQ) of the ABP waveform, which was recorded simultaneously with the ECG measurement. If the ABP SQ is over the threshold, which means ABP signal is proper to use, the algorithm computes and compares cardiac features with the triggered ECG alarm. If the ABP SQ value is under the threshold, which means ABP is not proper to use, and the ECG alarm is accepted as true. However, ABP measurement is not commonly collected at all hospitals from all patients.

According to Desmane et al. [23], only 60% of bed side monitors, which are connected to patients, measure ECG and ABP signals together because the ABP waveform measurement is invasive and not as simple as the ECG measurement. They used PPG signals, which are more general in use than ABP signals, instead of the ABP signals in addition to the ECG signals with a pulse oximeter.

In the integration of the results of each modality requires a robust decision algorithm. The signal integration algorithms introduced in this thesis form a decision scheme by using the PPG, ABP and ECG waveforms recorded in the ICU monitoring devices. We used a total of 750 records given in the dataset from Physionet Challenge 2015 (details are explained in Section 1.1 Physionet Challenge 2015 Databases).

In the literature, there is no direct comparison of these three signals (ECG, ABP, PPG) processing performances of false arrhythmia alarm reduction comparison on the same dataset. They usually compare combinations of two them, such as ECG+PPG versus ECG+ABP or only ECG versus ECG+ABP, ECG+PPG processing algorithms. The future health care solutions have trends to be mobile and computation efficient for worldwide usage without directly going to hospital and connected to wired devices. The main obstacle of these trends are cost efficient solution (without the need of high processing power and price of hardware) for implementing and generalizing these applications. To overcome these obstacle and improve the false arrhythmia alarm reduction, a variety of algorithms, which perform filtering, artifact detection, pulse onset identification, pulse feature extraction and then combining them by fuzzy logic, are specified for the purpose of usage can be used to determine high-quality segments of these waveforms, were developed from ones in the literature in this thesis. These have been modified in order to get the best performances for specific usage areas (explained in Section 4.1).

## 1.1 Physionet Challenge 2015 Databases

In this study, we need to compare our results with recent studies in the literature; therefore, we selected CinC2015 challenge 'Reducing False Arrhythmia Alarms in the ICU', which is the most important computing competition in the

cardiology era because the participants of challenge and the committee members are the pioneers in both medicine and engineering part of cardiology. The results of the challenge have recently been announced in 2016. The topic of the CinC2015 challenge was very similar with the scope of the thesis and provide a good chance to compare the results of the thesis with the results of the finalists of the challenge. The data set included 750 records from bedside monitors in the ICU, which were manufactured by the three biggest intensive care monitoring device manufacturers'. Each record contains ECG data from lead II, aVr, and PPG/ABP pulsatile waveforms. Each alarm was labeled by expert cardiologists as "false", "true" or "no comment" after reviewing the alarms for each arrhythmia type. The arrhythmia types were asystole (ASY), extreme bradycardia (EBR), extreme tachycardia (ETC), ventricular fibrillation or flutter (VFB), or ventricular tachycardia (VTA), whose features are shown in Table 1.1.

Table 1.1: Data Set Alarm Definitions [17]

Alarm Type	Alarm Definition
ASY	0 beats in 4s
EBR	$\geq 5$ beats, $HR < 40\text{bpm}$
ETC	$\geq 17$ beats, $HR > 140\text{bpm}$
VTA	$\geq 5$ ventricular beats, $HR > 100\text{bpm}$
VFB	Fibrillation waves

The dataset does not include more than three alarms of each of the five categories from any given patient, and alarms were at least 5 minutes apart (usually longer). In this way, the dataset does not address the issue of what to do with repeated alarms and how to use information from earlier alarms. An alarm was triggered 5 minutes from the beginning of each record. The exact time of the event that triggered the alarm varies somewhat from one record to another. However, the dataset meets the ANSI/AAMI EC13 Cardiac Monitor Standards [33], which defines that the onset of the event must be within 10 seconds of the alarm (i.e., between 4:50 and 5:00 of the record). All signals in the dataset are 250 Hz and 12 bit data. Some ECG signals in dataset may have pacemaker and other noise artifacts. Some pulsatile signals in the dataset have movement artifact, sensor disconnects and other events (such as line flushes or coagulation in the catheter). Each recording contains two ECG leads (which may or may not be

the leads that triggered the alarm) and one or more pulsatile waveforms (the photoplethysmogram and/or arterial blood pressure waveform). The detailed number of false, true alarms and signal type, which the data set consist of, for each arrhythmia type in the dataset is given Table 1.2. The distribution of signal type and distribution of the records is given in Table 1.3.

Table 1.2: Data Set Alarms [17]

CinC2015 Dataset (N=750)			
Alarm Type	Total	False	True
ASY	120	100	20
EBR	90	45	45
ETC	139	8	131
VTA	343	253	90
VFB	58	52	6
All Signals	750	458	292

Table 1.3: Pulsatile Waveform Distribution of the Dataset [17]

CinC2015 Dataset (N=750) Pulsatile Waveforms Distributions			
Alarm Type	Total	False	True
PPG Only	405	227	178
ABP Only	122	59	63
Both PPG and ABP	233	172	51
All Signals	750	458	292

Note: Each of N records included ECG signals.

## 1.2 Objective of the Thesis

In this study we tried to develop and modify a new method to solve the problem of high false alarm rates by increasing the sensitivity and specificity rates of ICU alarms. We focused on five types of life-threatening arrhythmia alarms, which were asystole, extreme bradycardia, extreme tachycardia, ventricular tachycardia, ventricular fibrillation or flutter. We used a database, which is given for CinC2015 challenge, of total 750 record for these five arrhythmia types. We used fuzzy logic methods with information from various waveforms, such as electrocardiogram, photoplethysmogram, and arterial blood pressure. We had three

steps in analysis of each type of waveforms.

For the ECG signal analysis, QRS detection was applied, which was based on Hilbert transform with first differential method after pre-processing of the signal. Signal quality (SQ) was calculated based on ECG specific rules. If the SQ was over the threshold, alarm decision rules for specific arrhythmia types were applied to decide whether alarm is false or true.

For the ABP signal `wabp.m` function in Physionet toolbox package of CinC2015 was used. Then with `abpfeature.m` function features of the signal were calculated. The SQ of the signal was calculated by `jsql.m` function. If the SQ was over the threshold, alarm decision rules for specific arrhythmia types were applied to decide the alarm is false or true.

For PPG signal, we quantile, which was explained in Appendix A, the signal to fit `wabp.m` function and calculated the heart beat, annotation times. The `ppgSQL.m` function was applied with these inputs and SQ of the pulsatile waveform was calculated. If the SQ was over the threshold, alarm decision rules for specific arrhythmia types were applied to decide the alarm is false or true.

In fusion part of our methods, we tried to fuse above algorithms to get more robust methods in terms of sensitivity and specificity. We grouped these methods in two categories as: QRS Complex, PPG, ABP, Detection Based Methods, METU BEST Methods by optimizing the method to the intended purpose of use. In the QRS Complex, PPG, ABP, Detection Based Methods, we have implemented Only ECG Method, Only PPG/ABP Method, Main PPG/ABP and Secondary ECG Method, Main ECG and Secondary PPG/ABP Method with respect to the signals used in the method. In the METU BEST Methods, we implemented METU BEST Method, METU BEST (without using ABP) Method, METU BEST Generic Method and, METU BEST (without using ABP) Generic Method (for devices unable to measure ABP signals) with respect to the purpose of the methods by modifying and mixing the first category methods for the purpose of usage and comparison with CinC2015 challenge finalists.

In the performance evaluation part, we triane and tested the above methods with training and testing datasets and compared the results with those of Cinc2015 challenge finalists' by performing our methods on the same training dataset. We explained the limitations of our methods and give examples of data, which our

methods failed.

### 1.3 Contribution of Thesis

With this thesis we made the following contributions to "False Arrhythmia Alarm reduction in ICU monitoring devices" studies:

- Fusing pulsatile waveforms such as ABP, PPG as a secondary decision part increases the specificity which is proven in the literature by comparing two of these three signals such as ECG versus ECG+ABP, ECG versus ECG+PPG or ECG+PPG versus ECG+ABP. We proved these comparisons by calculating the performances of processing ECG, PPG, ABP and their all combination of mixtures on the same database.
- Using ECG as the main and PPG as the secondary decision in fuzzy logic showed comparable results as our superior method which uses PPG/ABP as the secondary decision part. These comparable results made this method eligible to be implemented in any ICU monitoring device because these devices usually record ECG and PPG signals simultaneously. ABP signal is rarely used due to its hard implementation and cost.
- Developing a robust and using low processing power method can be used in the near future mobile health care devices for mobile patient monitoring (we implemented our method on a \$24 Texas Instrument watch).

### 1.4 Scope of the Study

The following topics are covered in this study:

- QRS detection step is improved by:
  - implementing a pre-processing step to suppress artifacts from the ECG signal to enhance the performances of the QRS detection method which is an improved version of Hilbert detector method.

applying signal quality indexes to decide usability of them in the detection method.

- Pulsatile Waveforms detection step is improved by:
  - implementing ABP detection method with MATLAB physionet toolbox,
  - implementing PPG detection method with some modification in MATLAB physionet toolbox,
  - applying signal quality indexes to decide usability of them in the detection method.
- Fusing the detection methods using individual waveforms to get a robust arrhythmia detection logic, which improved both sensitivity and specificity rates of our methods.
- Evaluate the performances of our robust fuzzy logic methods by testing and, comparing the results with the Physionet Challenge 2015 finalist scores who use the same challenge training database. The comparisons are made with respect to these parameters:
  - between the results obtained by each arrhythmia type performance,
  - between the overall score obtained by the total database evaluation.
- Arrhythmia classification step is added to get the generic performance of our methods in unknown arrhythmia detection and classification cases.
- Preparing a Real-time method in guide of the above developed Retrospective method made our methods applicable in pre-clinical or clinical usage because our methods only use the information from data before the alarms alarm occurs.

## 1.5 Outline of the Thesis

- In Chapter 1, introduction to the subject matter is given. Then the objective of this thesis is stated. Finally, outline of the thesis report is presented.

- In Chapter 2, background information is provided.
- In Chapter 3, details of the developed methods are explained.
- In Chapter 4, performance evaluation of the methods is provided.
- In Chapter 5, a brief summary on the performed study is given. This chapter also contains some concluding remarks and recommendations for future works.
- In Appendix A, Physionet Toolbox algorithms are given.

## CHAPTER 2

### BACKGROUND INFORMATION

This chapter starts with brief explanation of the medical and electro physiological background, followed by literature survey on QRS, PPG, ABP detection, signal integration methods, feature extraction and classification. Then continues with background information on performance evaluation features, training and testing signals (ECG, ABP and PPG waveforms) databases.

#### 2.1 Medical Background

In this part anatomy, physiology and electrical activity of the heart are briefly explained based on the information provided in [52] and [71].

##### 2.1.1 Anatomy and Physiology of the Heart

Heart is a vital organ that produces a wave of electrical activity to contract and pump blood throughout the body. It is located in the thorax; between the lungs, behind the sternum and the diaphragm.

Heart consists of two main parts; heart walls and valves. Walls consist of mainly cardiac muscle, called myocardium and some striations. Right atria, left atria, right ventricle and left ventricle are compartments of the heart.

Valves are the gates of the heart, which are tricuspid (located between right atrium and right ventricle), mitral (between left atrium and left ventricle), pulmonary (located between right ventricle and pulmonary artery) and aortic (located between left ventricle and aorta). There are two types of circulation

which are controlled by the heart, i.e., pulmonary and systemic circulation. Pulmonary circulation moves blood between the heart and the lungs. It transports the blood out from right ventricle to the lungs through pulmonary valve. Oxygenated blood enters to the left atrium from the lungs. Systemic circulation moves blood between the heart and the rest of the body. Oxygenated blood from the left ventricle is pumped to the whole body through aorta by the aortic valve. Then the deoxygenated blood from the body enters the right atrium and through tricuspid valve goes to right ventricle.

### **2.1.2 Electrical Activity of the Heart**

Mechanism of the electric activation in a heart muscle cell (myocyte) is the same as in a nerve cell. The distribution of ions across the cell membrane creates a potential difference across the membrane of the cell. This potential difference is called the transmembrane potential. The transmembrane becomes charged and its potential increases during impulse propagation with action potential impulses. An action potential is a carrier of the information providing the control and coordination of organs like heart. An action potential is a wave of electrical discharge that propagates along the membrane of a cell. Depolarization increases the membrane potential and re-polarization decreases the membrane potential so that the potential returns to its resting state.

In muscle cells, inflow of sodium ions through the cell membrane creates action potential with amplitude of 100 mV and duration of approximately 300 ms. Electrical activation between cardiac muscle cells propagates and mechanical contraction follows the electrical activation. Electrical activation consists of two main nodes interactions, which are Sinoatrial, Atria Ventricular nodes interactions. Sinoatrial node (SA node) consists of specialized, self-excitatory, pacemaker muscle cells and located at superior vena cava in the right atrium. These pacemaker cells stimulate electrical activation about 70 times in a minute in a normal heart. Stimulated action potentials propagate through the atria but not to the ventricles since there is a nonconducting barrier in the boundary between the atria and ventricles. AV node is located at the boundary between atria and ventricles. Similar to the SA node, AV node consists of specialized,

self-excitatory, pacemaker muscle cells stimulating electrical activation about 50 times in a minute. But if AV node is on the path of an electrical activity having higher frequency, the intrinsic frequency of the AV node does not appear. Since at normal conditions, the action potential stimulated by SA node pass through AV node and intrinsic frequency of AV node is about 50 times/min, which is lower than SA node frequency (70 times/min). The SA node behaves just as a normal conducting path from atria to ventricles. Action potential propagation from AV node to ventricles is through a specialized bundle system, called bundle of His and its branches are called Purkinje fibers.

### 2.1.3 ECG Waveform Morphology

In each cardiac cycle the flow of depolarization through the heart creates impulses which are composed of P, QRS and T waves as shown in Figure 2.1. These waves propagate in a different way with a delay through all blood circulation system. Therefore, the waves can be detected by surface electrodes on body skin. Then these detected signals are processed by an electrocardiograph which filters, amplifies and records them in the form of consecutive waveforms called ECG [10]. The ECG waveforms consist of main features which carry important information about heart beat morphology like respective P wave, QRS complex, T wave and their segment intervals. These features are depicted in Figure 2.1 and described in the following sections. Heart activity starts with atrial contraction (Systole) which propagates P wave. In cardiovascular diseases (CVDs) like in Figure 2.2, the P wave can appear in an abnormal waveform. These P wave abnormalities can be a sign of serious heart diseases. For example, negative P wave is an indication of an abnormality in polarization direction of atria. In other words, it is sign of, that pacemaker is not triggering the SA node or the AV node. Broadened or notch shape in P wave is an indication of delay in depolarization of the left atrium, which possibly arise from problems in conduction system. For example, if the measured ECG signals contain P waves, which have amplitudes, it is sign of right atrial enlargement (P pulmonale).

Moreover, in some situations P waves do not appear because there can be a

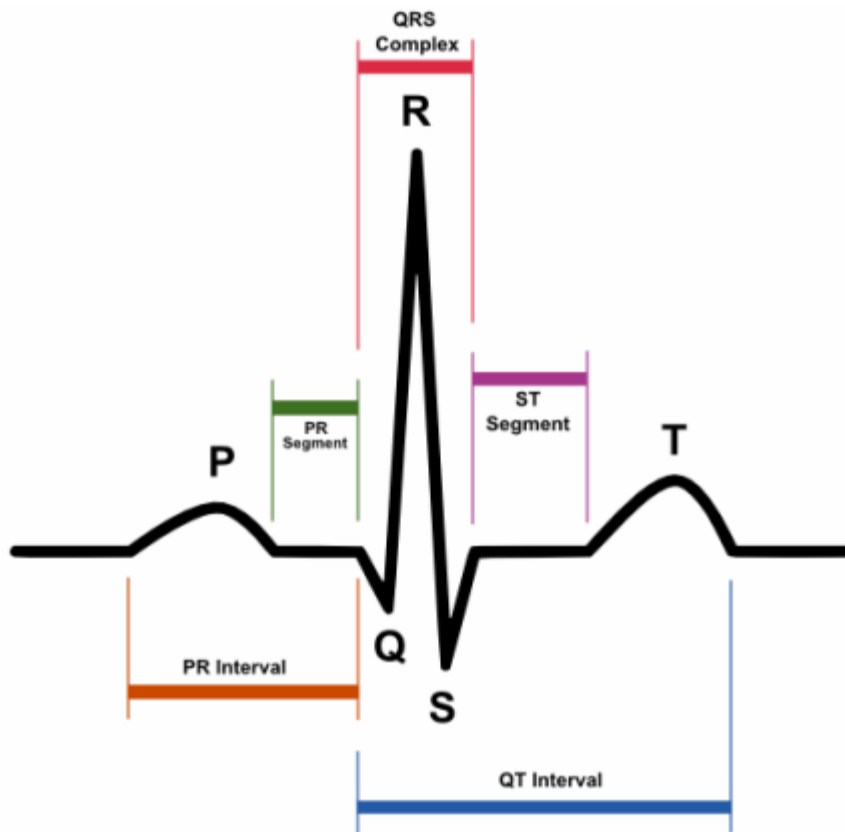


Figure 2.1: P wave, QRS Complex, T wave and Their Intervals Illustration [10]

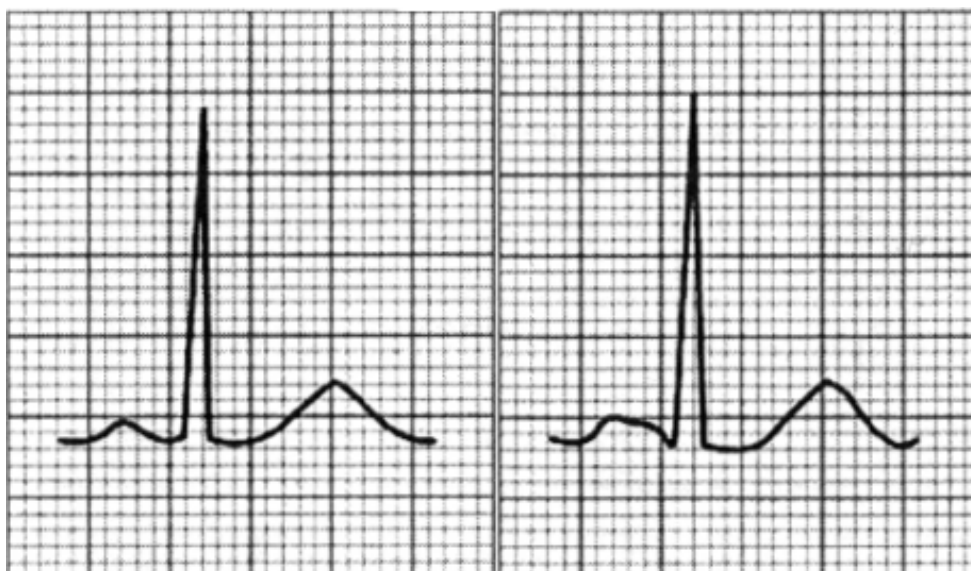


Figure 2.2: P waves Examples [10]

junctional rhythm or SA block. On the other hand, it can be early atrial flutter/fibrillation or temporary oscillations in the heart [10].

The QRS complexes are the most important waveforms reflecting electrical signal within the heart because of ventricular contraction (systole). Generally it is the basis of automatic heart rate detection algorithms [45]. The QRS gives important information of physiological action of the heart in each cycle (chamber). The summation of Q, R and S waves give QRS complex. Firstly, Q wave is defined as the first negative (downward) deflection. Secondly, R wave which followed Q wave, is the positive (upward) deflection. Finally, S wave is the any negative deflection just after the R wave. In some diagnosis, there are two or more R waves or no R wave in the ECG record at all like one QRS complex as depicted in Figure 2.3.

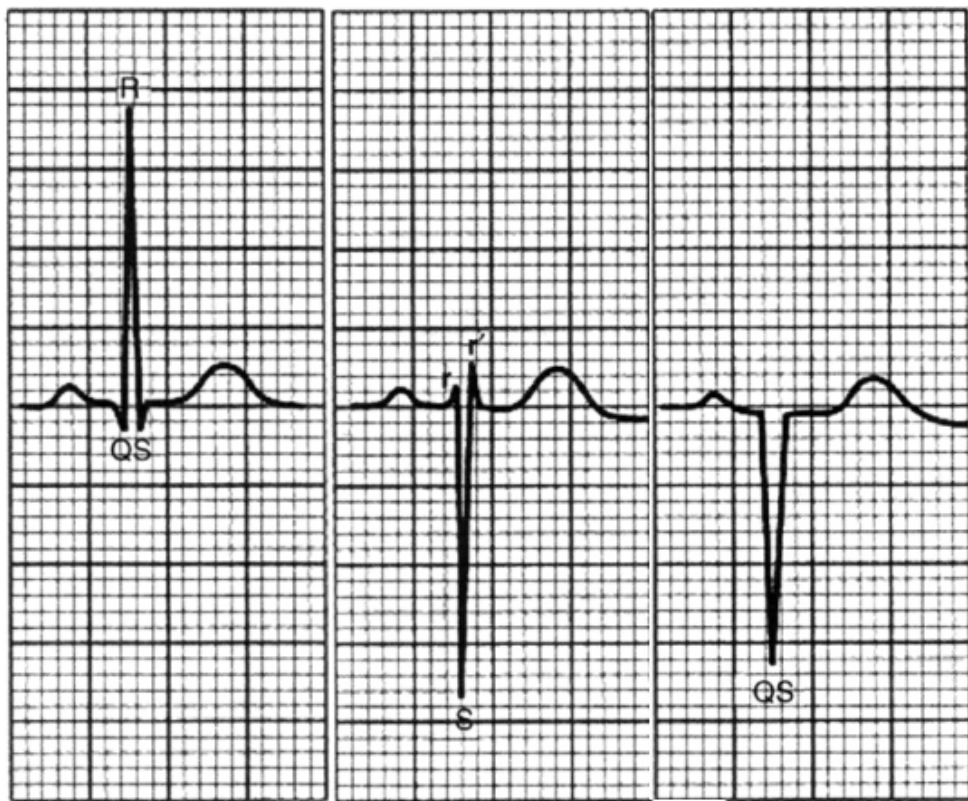


Figure 2.3: Various QRS complexes in the ECG [10]

Moreover, ECG signal measurements can be affected from the electrode or lead, which is used to measure the wave. For example, S wave seen from lead VI, which is located on the right hand side of the heart, is a large S wave because the electrode location is where forces of the left ventricular pass away. Normally, healthy Q waves have amplitude up to 2 mm or 0.03 s in width. Waves which are not in these limits usually are indication of myocardial infarction (MI). The

QRS complex is normally up to 0.1 s and its duration ranges are between 60 – 80 ms [10].

When ventricles relax (diastole) after ventricular contraction, T wave is generated like in the definition of T wave due to re-polarization. Unlikely Q and R waves are due to polarization. T wave normally have 0.25 – 0.35 s after ventricular depolarization. The lower heart chambers are electrically relaxing and preparing for their muscle contraction, during T wave. Atria re-polarization is difficult to observe because the larger QRS complex masks it during ventricular contraction. Moreover, the QRS complex and T wave are in the same direction because depolarization and re-polarization occurs in the opposite directions. Most researches showed that T waves amplitudes are generally lower than 5 mm. However, if they are taller than 5 mm it can be an indication of myocardial infarction (MI) or if T waves are also flattened, it can be an indication of myxoedema or hypokalaemia. Slight T wave inversion can be due to hyperventilation and smoking; however, it is usually because of heart walls infarctions like bundle branch block, MI and, ventricular hypertrophy [10].

Shape and the time interval of the waves are important in the evaluation of cardiac health. PQ interval is the time interval between the beginning of the P wave and the onset of the QRS complex. PR interval is the time of onset on atrial contraction. Atrial contraction is generally about 0.16 s [10]. If the heart tissue is scarred or inflamed, PR interval usually becomes longer. In other words, the depolarization wave need more time to propagate from atrial myocardium to AV node. If PR interval is shortened, this can be an indication of junctional tissue originated impulse or the Wolff-Parkinson-White syndrome [10]. The ST segment is usually a leveled signal straight line which starts with the QRS complex and ends with T wave. Various CVDs are reflected in this segment. This segment is shown in Figure 2.4. If the heart walls (muscles) are damaged or there is no enough blood, some disturbances appear in ventricular repolarization causing ST segments to be elevated or depressed depending on the observed ECG lead. Concave upward ST segments over many cardiac cycles is an indication of pericarditis. Shape of ST segment depression is characteristic to pathologies which can indicate ventricular hypertrophy, acute myocardial ischemia, and sinus tachycardia [10].

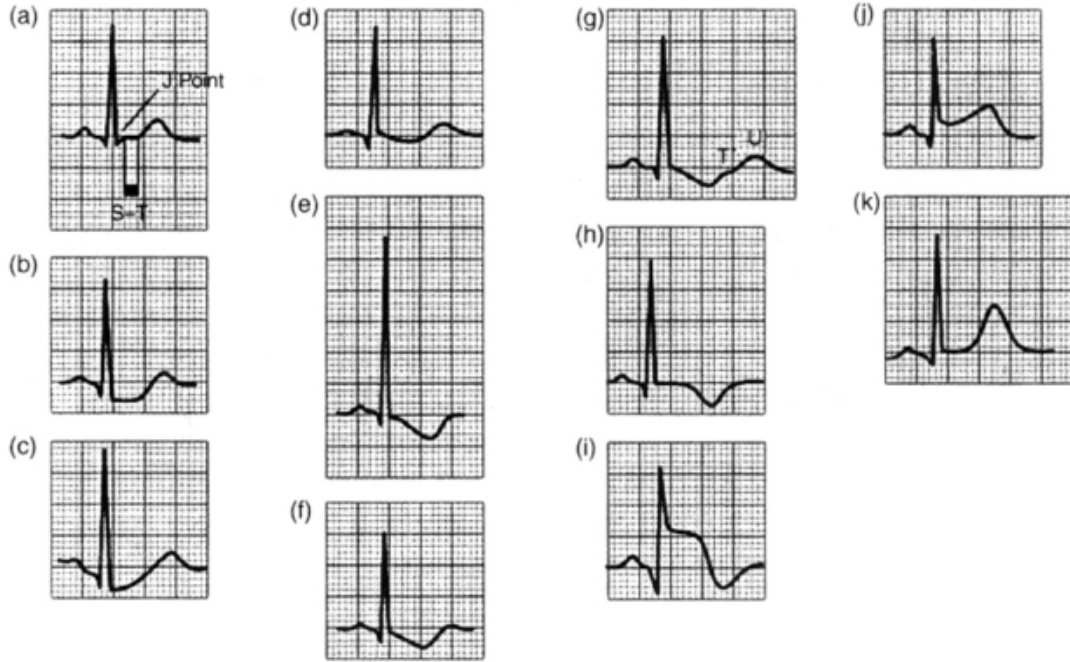


Figure 2.4: ST segments in the ECG [10]

#### 2.1.4 ECG Waveform Measurement

The ECG lead (electrodes) placement on the body surface affects the voltage obtained during a normal ECG monitoring [10]. There are different ways of lead placement and configurations to decrease contact impedance and increase the ECG signal. Generally three basic configurations are used in clinical applications. These are standard 12 – *lead* clinical ECG, Vector Cardiogram (VCG) and Monitoring ECG (1 or 2 leads) or bipolar leads (I, II, and III are electrodes attached to the limbs). These methods are based on 12 Leads ECG System which is the central of the field of the ECG.

12 Lead ECG System Consist of three main ECG Leads Placement and Calculation Methodologies:

- Einthoven Triangle:

This method was invented by Willem Einthoven who used the capillary electro-meter in his first ECG recordings. His application of the string galvanometer (which was invented by Clément Ader (Ader, 1897).) is the main contribution to clinical ECG-recording technology. The sensitivity

rates of his system was higher than the previous system which are using capillary electro-meter. He published the description of the first clinically ECG measuring system in 1908. They are bipolar. Leads are defined in Table 2.1.

Table 2.1: Einthoven Triangle Leads [10]

Lead	Positive Electrode +	Negative Electrode -
I	Left Arm (LA)	Right Arm (RA)
II	Left Leg (LL)	Right Arm (RA)
III	Left Leg (LL)	Left Arm (LA)

The mathematical equations of these leads are illustrated as:

$$\begin{aligned}
 V_I &= \phi_L - \phi_R \\
 V_{II} &= \phi_L - \phi_R \\
 V_{III} &= \phi_L - \phi_R
 \end{aligned}
 \tag{2.1}$$

where:

$V_I$  = the voltage of Lead I

$V_{II}$  = the voltage of Lead II

$V_{III}$  = the voltage of Lead III

$\phi_L$  = potential at the left arm

$\phi_R$  = potential at the right arm

$\phi_F$  = potential at the left foot

According to Kirchhoff's law these lead voltages have the following relationship:

$$V_I + V_{III} = V_{II} \tag{2.2}$$

These Einthoven's lead system lead vectors are based on the assumption that the heart is located in a homogeneous and infinite volume conductor (at the center of a homogeneous sphere representing the torso). For example, if the position of the left, right arms and left leg are at the vertices of an equilateral triangle and the heart is located at the center of this triangle, these lead vectors form an equilateral triangle.

- Wilson Terminal:

Electrocardiographic unipolar potentials were defined by Frank Norman Wilson in 1934. He and his colleges suggested the use of the central terminal as reference for these measurements. They are unipolar leads. This was achieved by connecting a 5000  $\Omega$  resistor from each terminal of the limb leads to a common point called the central terminal.

His suggestions were that unipolar potentials should be measured with respect to this terminal which approximates the potential at infinity. Although, this central terminal is not independent of the limbs potentials, it is the average of them. This can be easily proved by noting that in an ideal voltmeter there is no lead current. Therefore, the total current into the central terminal from these limb leads sum to zero to satisfy the conservation of current. Wilson used 5000  $\Omega$  resistances and got these equations:

$$I_R + I_L + I_F = \frac{\phi_{CT} - \phi_R}{5000} + \frac{\phi_{CT} - \phi_L}{5000} + \frac{\phi_{CT} - \phi_F}{5000} \quad (2.3)$$

$$\phi_{CT} = \frac{\phi_R + \phi_L + \phi_F}{3} \quad (2.4)$$

- Goldberger Augmented Leads:

In this method three additional limb leads,  $V_R$ ,  $V_L$ , and  $V_F$  are obtained by measuring the potential between each limb electrode and the Wilson central terminal. They are unipolar leads. For instance, the measurement from the left leg (foot) gives:

$$V_F = \phi_F - \phi_{CT} = \frac{2\phi_F - \phi_R - \phi_L}{3} \quad (2.5)$$

E. Goldberger observed that these signals can be augmented by omitting that resistance from the Wilson central terminal, which is connected to the measurement electrode in 1942. Potential of the  $aV_F$  is represented as:

$$V_{aV_F} = \phi_F - \phi_{CT/aV_F} = \phi_F - \frac{\phi_L + \phi_R}{2} = \frac{2\phi_F - \phi_L - \phi_R}{2} \quad (2.6)$$

- Precordial Leads Method:

Wilson introduced measuring the potentials from precordial leads close to

the heart in 1944. They are unipolar leads. These leads, which are defined from V1-V6 and located over the left chest.

Therefore, the 12-lead ECG system has eight truly independent and four redundant leads. The lead vectors for each lead are based on an idealized (spherical) volume conductor.

For example in lead I electrodes, the positive electrode is attached to the left arm and the negative to the right arm. Therefore, the potential voltage calculated by subtracting the right arm voltage from the left arm voltage [10]. An example of ECG waveforms, the potential difference calculated by subtracting positive voltage leads from a voltage, that it is ground (GND) or a Wilson terminal, which is a small voltage. It contains 3 limb lead electrodes [10].

Standard clinical ECG is implemented in hospital to a resting patient by using 12 leads (measured I, II, V1 to V6 and computed III, aVL, aVR and aVF). In vectorcardiogram (VCG), 3 orthogonal leads are used to obtain 3 dimensional vector model for the cardiac electrical activity. Main purpose of all these methods is for monitoring the cardiac electrical activity . Monitoring this activity via ECG is implemented by using 1 or 2 leads for arrhythmia analysis in a long term monitoring ICU. Monitoring ECG is generally battery or ambulatory powered application. Since main goal of monitoring ECG applications is to detect each heart beat and perform arrhythmia analysis, the leads in which the R wave is most apparent are selected; therefore, high signal to noise ratio is achieved. Moreover, in general lead II is the first choice for monitoring, because it has the highest R wave amplitude among other leads. Second lead is generally considered as a backup lead in case of a malfunction such as a loss of electrode contact in the lead II channels.

### **2.1.5 PPG Waveform Morphology and Pulse Oximetry**

Pulse oximetry was invented in the 1970s [23]. It was developed commercially in the 1980s [23]. Pulse oximetry is a non-invasive technique of predicting oxygen saturation values in clinical settings. The main idea of pulse oximetry is that hemoglobin absorbs specific frequency intervals of light waves. Hemoglobin is

bound reversibly to oxygen molecules in the blood, which is shown Figure 2.5.

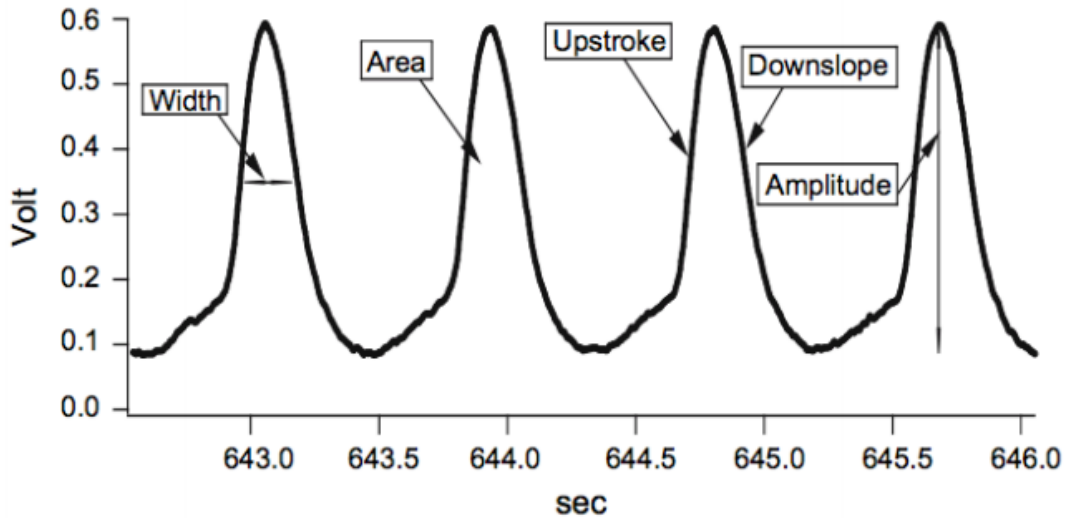


Figure 2.5: 12 Lead Measurement Points [10]

These oxygen molecules are released in capillary level to feed tissues in the cardiovascular system. These oxygen molecules shifting is changed in hemoglobin's charge densities, which effects their optical features [27]. For example, oxygenated hemoglobin ( $O_2Hb$ ) appear red, which means they absorbs blue region of light. Deoxygenated hemoglobin ( $RHb$ ) appear blue or darker, which means they absorb approximately all frequencies of in visible light. Moreover, there can be permanent bindings as carboxy hemoglobin ( $COHb$ ) and methemoglobin ( $MetHb$ ) which prove that different binding molecules with hemoglobin gives different frequencies of light absorption and give chance to detect the unknown bound molecules. The light absorption level of ( $RHb$ ) and ( $O_2Hb$ ) are very different for near infrared and red regions [73] as shown in Figure 2.6. This difference is used in pulse oximetry devices. They measure at least two wavelengths of light which are commonly around 660 nm and 940 nm. These reflected and transmitted light measurements are taken from the forehead, finger or the ear lobe.

The mathematical model of pulse oximetry relies on Beer-Lambert Law estimations [73]. Beer-Lambert Law states that the intensity of light transmitted

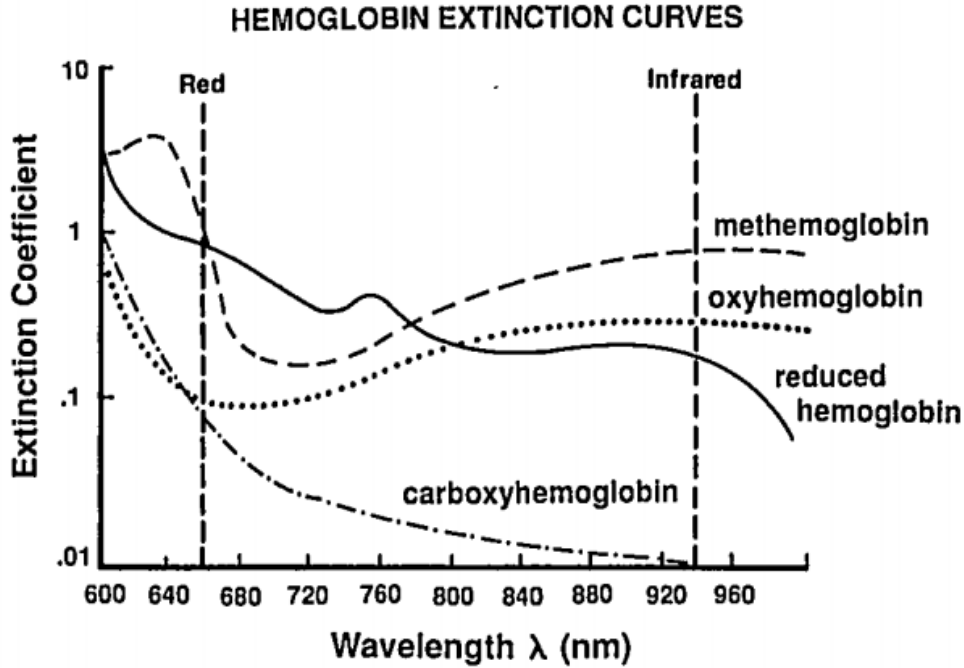


Figure 2.6: PPG Hemoglobin Extinction Curves [73]

through a material is scaled to the intensity of received light and exponentially involved with the absorption frequency interval of the given light. The equation consists of  $A$ , which is the amount of light absorbed by a sample,  $I$  (in  $W/m^2$ ), which is a scalar value based on the light intensity of the influenced subject, and  $I_0$ , which is the light intensity in the absence of the sample as shown below:

$$A = \log_{10} 3 \frac{I}{I_0} \quad (2.7)$$

### 2.1.6 Arterial Blood Pressure (ABP) Waveform Morphology

Cardiovascular control mechanism regulates the arterial blood pressure; therefore, the cardiovascular system depends on it. Figure 2.7 shows main features of cardiovascular system as ventricular volume, pressure changes in a typical cardiac cycle, heart sounds, electrocardiogram and venous pulse [49]. Arterial blood pressure is the force exerted by the blood on the wall of blood vessels during systole and diastole, which are the main phases of cardiac cycle. When the heart is pumping (contracting), the degree of pressure is called as the  $P_s$  (systolic blood pressure) and the phase is called as systole, which is around 1/3

of the cardiac cycle. On the other hand, when the heart is relaxed, the blood pressure is called as the  $P_d$  (diastolic blood pressure) and the phase called as diastole, which is around  $2/3$  of the cardiac cycle. The  $P_p$  (pulse pressure) is defined as  $P_s - P_d$ .  $P_m$  (mean pressure) is a time based average of arterial blood pressure during one cardiac cycle and it is approximately  $P_d + P_p/3$ . In normal subjects,  $P_s$  and  $P_d$  are around 120 mmHg and 80 mmHg.

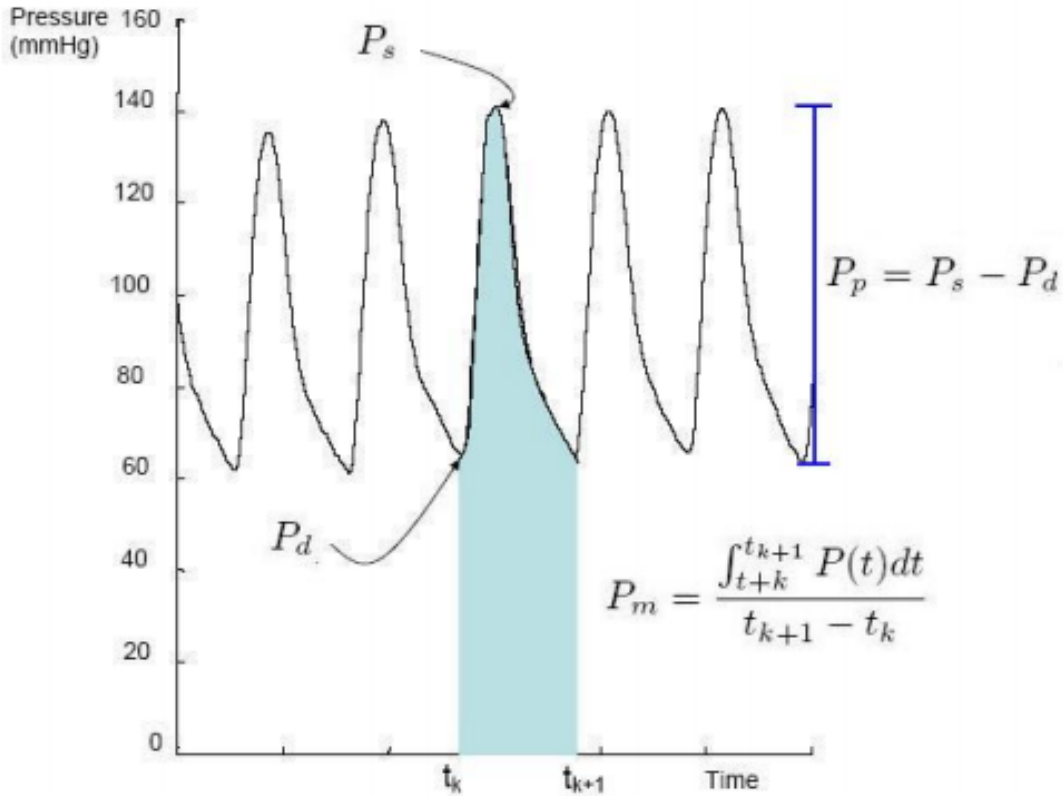


Figure 2.7: ABP Waveform [60]

### 2.1.7 Arterial Blood Pressure Measurement

ABP measurement techniques can be divided in to two main approaches: indirect (noninvasive) cuff devices and direct (invasive) arterial cannulation. Indirect cuff devices can be divided in to two types as manual and automated; or continuous and instant intermittent technique. In the manual method patient’s arm is grabbed with a cuff centered over the brachial artery and air is pumped in an inflatable rubber bag inside the cuff until the artery is closed. Then the air

pressure is released by opening the valve of the cuff until the pressure in the cuff is equal to the pressure of blood in the artery. In other words, the air pressure is released until the blood flow starts again and pulse sound is heard again. These sounds can only be heard by stethoscopes placed over a pulse point. There is also manometer on the cuff to measure the pressure of air inside it. During measurement, while releasing the pressure, when the first pulse sound is heard, the pressure value on the manometer is  $P_s$ . Then if you continue releasing the air, when the second pulse sound is heard, the pressure value on the manometer is  $P_d$ . In the automated version, the main difference is, that it does the manual parts automatically, other steps are the same as the manual version. This measurement system based on fluctuations around 20 mmHg baseline shift at night or during rest [9]. However, ICU connected patients take medicines for stability of their cardiovascular systems. Therefore, their heart rate and ABP ranges are limited than healthy subjects [43]. In invasive measurement method, ICU monitoring devices measure ABP waveforms by using a pressure transducer, which is connected invasively to an artery. For example, doctors choose femoral artery (radial artery) for measurement location because the risk of complications are less and cannulation procedure is easy [66].

### 2.1.8 Artifacts in Physiological Signals

ECG, PPG, ABP signals may be corrupted by various kinds of noise. Typical examples are: power line interference, electrode contact noise (loose of electrode contact noise, motion artifacts and baseline drift and ECG amplitude modulation with respiration), muscle contraction (electromyographic, (EMG) noise), instrumentation noise generated by electronic device used in signal processing, electro-surgical noise and other less significant noise sources. This section explains the origins and effects of these artifacts.

- **Power Line Interference:** Power line interferences consist of 60  $Hz$  (in the U.S.), 50  $Hz$  (in EU) pickup frequencies and harmonics which can be modeled as sinusoids [36] as shown Figure 2.8. Therefore, these noises have characteristics like amplitude and frequency, which might need

to be varied in a model of power line noises. These characteristics are generally consistent for a given measurement situation and, once they are calculated, they will not change during a detector evaluation, which make their removal easier from the measured signal.

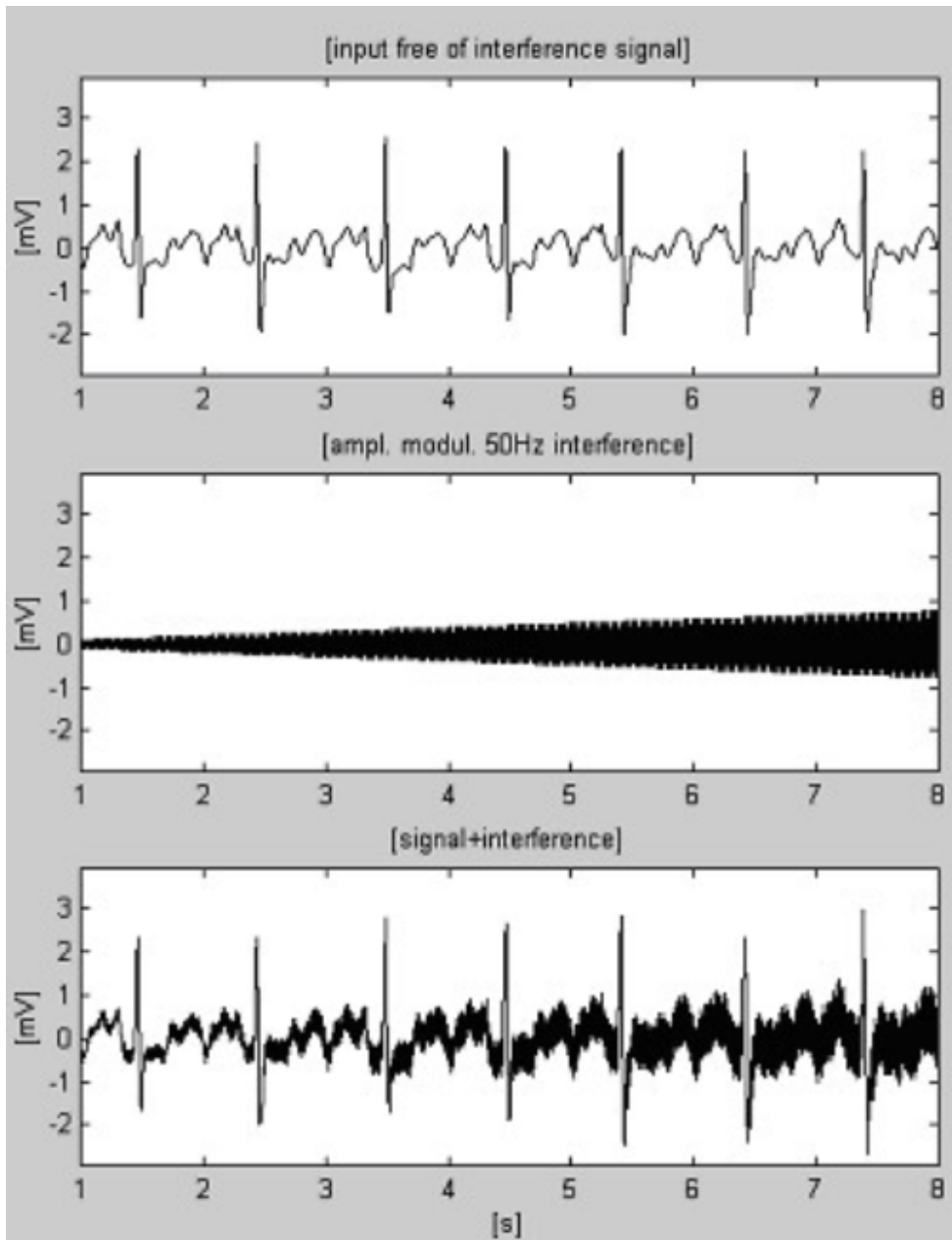


Figure 2.8: Power Line and Motion Artifacts [35]

- Electrode Contact Noises: These type of noises typically  $< 0.5 \text{ Hz}$  signals (except for the abrupt shifts due to motion). General examples are: loose of electrode contact noise, motion artifacts and baseline drift and ECG

amplitude modulation with respiration.

- **Loose of Electrode Contact Noise:** The transient interference due to loss of contact between the electrode and the subject's skin surface, which also disconnects the measurement from the subject is named as Loose of Electrode Contact Noise. This disconnection can be intermittent or permanent which are in and out contact because of unintended movement and vibration. The intermittent type of disconnections change the input of the electrode impedance suddenly. These sharp alterations produce significant artifacts and noises at the input. In addition, if the amplifier of the input is disconnected 50 Hz or 60 Hz interference affects the measurement system. This switching action at the measurement system input can result in large artifact since ECG signals capacitively coupled to the system. An example of electrode contact noise is shown in Figure 2.9

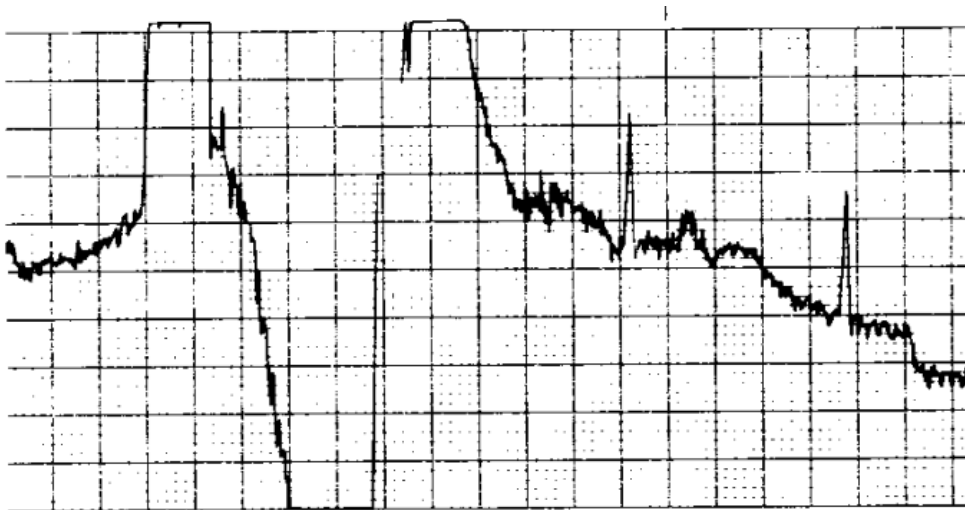


Figure 2.9: Loose Electrode Contacts Artifacts [35]

- **Motion Artifacts:** Baseline fluctuations occur by alternations between the electrode to skin distance (impedance) named as motion artifacts. Motion and movement of the subject without loss of the contact between skin and electrode is the main source of motion artifacts. A typical example is shown in Figure 2.10.

Because of this impedance alteration, the ECG amplifier takes different source of impedances, which forms a voltage divider with the

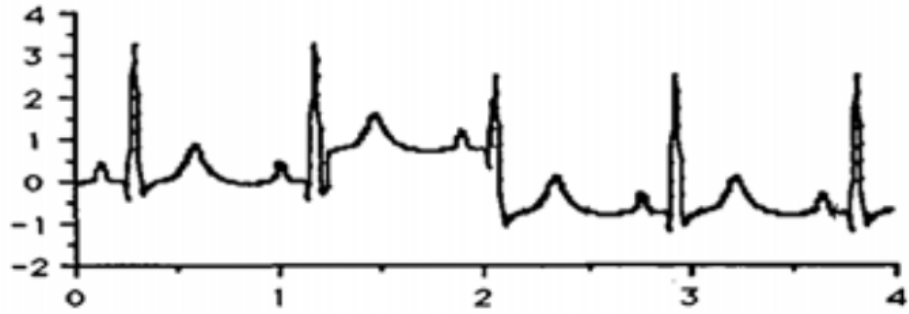


Figure 2.10: Loose Motion Artifacts [35]

amplifier input impedance. Therefore, the voltage depends on the fluctuations on the position of the electrode.

- **Baseline Drift and ECG Amplitude Modulation with Respiration:** The drift of the baseline with respiration can be represented as a sinusoidal component at the frequency of respiration added to the ECG signal. A typical example is shown in Figure 2.11.

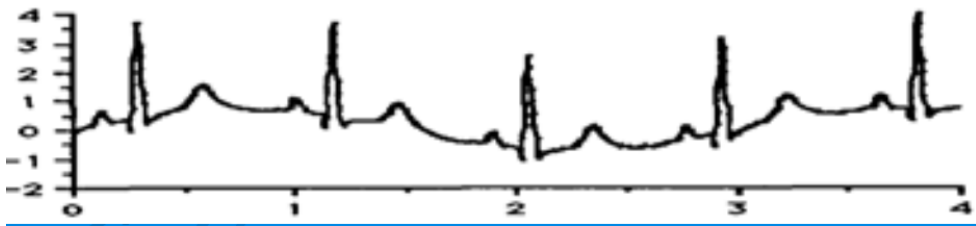


Figure 2.11: Respiration and Noise [35]

- **Muscle Contraction(Electromyography, EMG):** Muscle contractions cause artifactual millivolt level potentials. The baseline electromyogram is usually in the microvolt range. Therefore, it is usually insignificant. However, the surface EMG artifacts are around 10% of ECG signal potential and may interfere or corrupt the ECG, which affects the data processing and analysis. A typical example is shown in Figure 2.12.
- **Instrumentation Noise Generated by Electronic Devices used in Signal Processing:** Artifacts generated by electronic devices in the in-

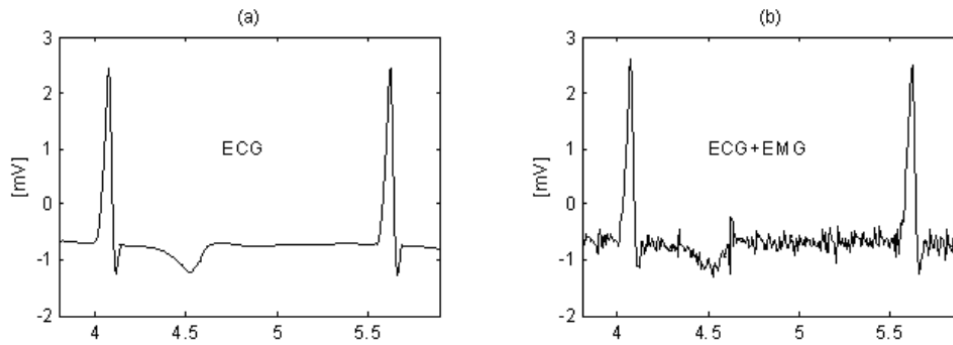


Figure 2.12: EMG Noise [35]

strumentation system are shown in Figure 2.13. These cannot be corrected by a QRS detection algorithm. The input amplifier has saturated and no information about the ECG can reach the detector. These kind of artifacts are generally caused by hardware error, disconnections of electrodes or cables. In this case an alarm must sound to alert the ECG technician to take corrective actions, such as check the connections and/or, reset the patient monitor.

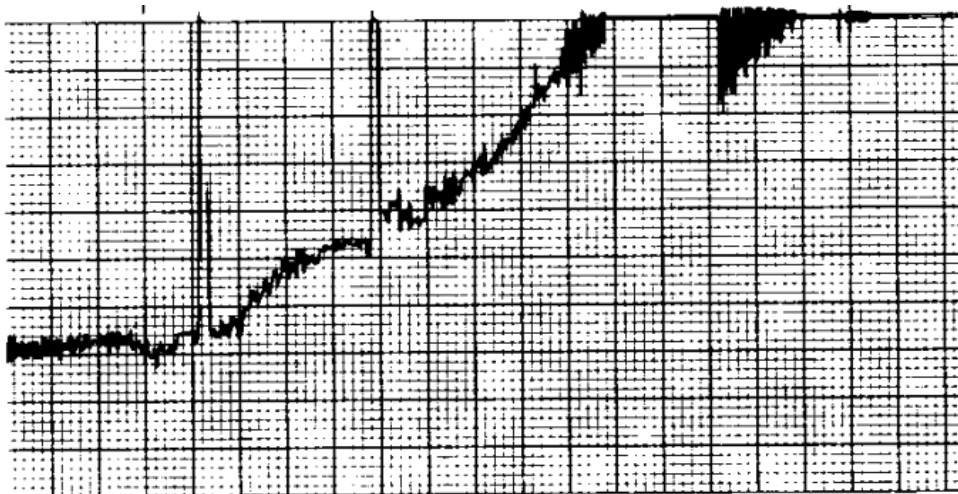


Figure 2.13: Instrumentation Saturation Noise [35]

- **Electro-surgical Noise and other less Significant Noise Sources:** Electro surgical noise can be represented as a high amplitude sine wave with frequency range between 0.1 – 1000 kHz. These noises are added to the ECG signal and destroy the ECG because the ECG sampling rate is between 250-1000 Hz.

- Other Noises: Flat/Zigzag lines are segments of signals having almost zero electrical activity. Segments of signal, having zero amplitude difference between two consecutive samples, for a duration of minimum two seconds, are classified as being "flat lines". Segments of signal, having alternating samples, for duration of minimum seconds, are classified as having zigzag lines.

## 2.2 Signal Processing Background

In this part QRS complex enhancement methods, QRS complex detection methods, PPG waveform detection methods, ABP waveform detection methods, literature survey and performance evaluation are briefly explained.

### 2.2.1 QRS Complex Enhancement Methods

ECG signals detection is affected by various kinds of artifacts as mentioned in section 2.1.8. Therefore, ECG signals have to be improved by filtering for noise suppression, R peak enhancement and QRS enhancement stages, which are prerequisites for detecting the QRS complex. This section introduces amplitude thresholding method, first derivative only approach, first and second derivative only approach, digital filters approach, mathematical morphology approach, empirical model decomposition, Hilbert transform approach, filter banks approach and wavelet transform approach.

These QRS enhancement algorithms are numerically inefficient if we want to remove all noise and achieve a proper less noisy ECG signal for QRS detection. As the main purpose of this work is to highlight a suitable QRS enhancement algorithms for a reliable ECG monitoring and also using it in a battery operated, portable devices, using Hilbert transform with first derivate only approaches gives a robustness for noise cancellation with medium level of numerical efficiency. Details about our implementation is given in Section 3.2. Other methods detailed explanations are given in Appendix C.

### 2.2.2 QRS Complex Detection Methods

After enhancing the QRS features using the previous algorithms explained in section 2.2.1 QRS Enhancement is the next step to detect the QRS complexes. Through the previous enhancement step, QRS complexes are filtered and magnified relative to other ECG features, artifacts and noise. There are many detection techniques in the literature. These methods are: thresholding, neural network, Hidden Markov Models, matched filters, syntactic method, zero crossing and singularity.

When you compare these QRS detection algorithms, they are divided in two category as numerically inefficient with high performance and numerically efficient with medium performance. As the main purpose of this work is to highlight a suitable QRS detection algorithms for a reliable ECG monitoring and also using it in a battery operated, portable devices, using Thresholding with adaptive thresholds approaches gives a robustness for R peak detection with medium level of numerical efficiency. Details about our implementation is given in Section 3.2. Other methods detailed explanations are given in Appendix C.1.

### 2.2.3 PPG Waveform Detection Methods

PPG signal was generated by periodic ejection of the heart, so it has a close relationship with the ejection period, from which the heart rate (HR) could be extracted. In another aspect, from these information, such as heart rate and onset times. You can decide state of the heart in terms of normal or abnormal activities like Arrhythmia detection. Therefore, many researches have been made to find and improve reliable, robust and fast PPG onset detection algorithm. The top authors and their works are explained below:

- In 2010 Farooq et al [32], proposed a time domain based algorithm to detect onset times and peaks of PPG with low computing cost. The core concept of this algorithm is that this algorithm based on obtaining a transformed PPG waveform which enhances the systolic rises of PPG to be a significant peaks and onsets of the original waveform more reliable and robust to

detect.

- Zhou et al. [79] proposed a novel algorithm based on the idea of raised from physiological phenomenon that the trend of PPG waveform changes sharply on the both side of the PPG onset points. For example, from a decreasing movement in the previous end diastolic step to a sharp rising movement in the coming early systolic step in PPG onset points are observed because of the arrival of arterial pulse. Therefore, they implement an adopted version of a published method [32] to detect the 1st derivative PPG peak points. Then in the near region of each 1st derivative PPG peak point, the waveform trend shifts between two sides of each point in this near region was computed. Then the onset points was defined as the one highest positive trend shift. The tendency of one side of a target was computed from the arctan angles between the target point and its nearby points on this side.

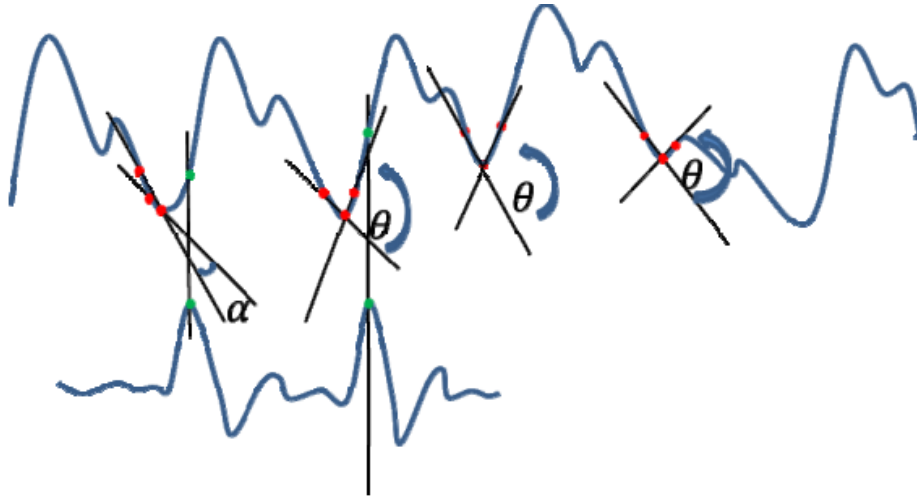


Figure 2.14: Onset Detection by using arctan [77]

- In 2015 Jang et al [42], proposed a pulse peak detection method, which has low complexity and simple based on cascading recursive digital filters and using slop sum function (SSF) with an adaptive filtering and thresholding diagram. The algorithm has four main steps. In the first step they eliminate noises in the PPG by applying cascaded low pass and high pass filters (3 dB cut-off frequencies of 11 Hz and 0.5 Hz). In the second step the filtered PPG signals are transformed by the SSF function, which en-

hances the upslope of the PPG signal and suppresses the remainder part for simplifying the detection of the pulse peaks. In the third step, SSF peaks are identified by thresholds, which are updated by applying median filter (with order of 5). This method adapts the thresholds against the variations of SSF amplitudes. In the final step pulse peaks are identified with in the interval of an onset index of the SSF signals to the following zero index. In order to handle with the redundant over detections and unnoticed information knowledge based rules post-processing is employed.

### 2.2.4 ABP Waveform Detection Methods

The ABP waveform contains rich information about the cardiovascular system, such as heart rate, systolic, mean, diastolic pressure and it can be used to get properties of the arterial vessel walls. Especially from heart rate and onset points computed from ABP can be used for determination of heart situation.

**wabp.m Algorithm:** This algorithm has been developed by Zong et. al. [80]. The ABP onset time detection divided in 3 steps which are show in Figure 2.15



Figure 2.15: Block Diagram of The ABP Onset Time Detection Algorithm

The purpose of the low pass filter is suppress high frequency that could affect the ABP onset detection. A second order recursive filter used as low pass filter, which have consisted of:

$$H(z) = \frac{(1 - z^{-5})^2}{(1 - z^{-1})^2} \quad (2.8)$$

$$|H(wT)| = \frac{(\sin(3wT))^2}{(\sin(\frac{wT}{2}))^2} \quad (2.9)$$

$$y_n = 2y_{n-1} - y_{n-2} + x_n - 2x_{n-5} + x_{n-10} \quad (2.10)$$

The purpose of the slope sum function (SSF) is to enhance the upslope of the ABP pulse and suppress the remainder of the pressure waveform. The weighted

and windowed slope sum function by time  $i$ ,  $z_i$  are given below:

$$z_i = \sum_{k=i-w}^i \Delta u_k \quad (2.11)$$

$$\Delta u_k = \begin{cases} \Delta y_k & \Delta y_k > 0 \\ \Delta y_k & \Delta y_k \leq 0 \end{cases} \quad (2.12)$$

To maximize the SSF,  $w$  should be chosen equal or very close to the typical duration of the upslope of the ABP pulse. The relationship between ABP and the SSF is shown in Figure 2.16

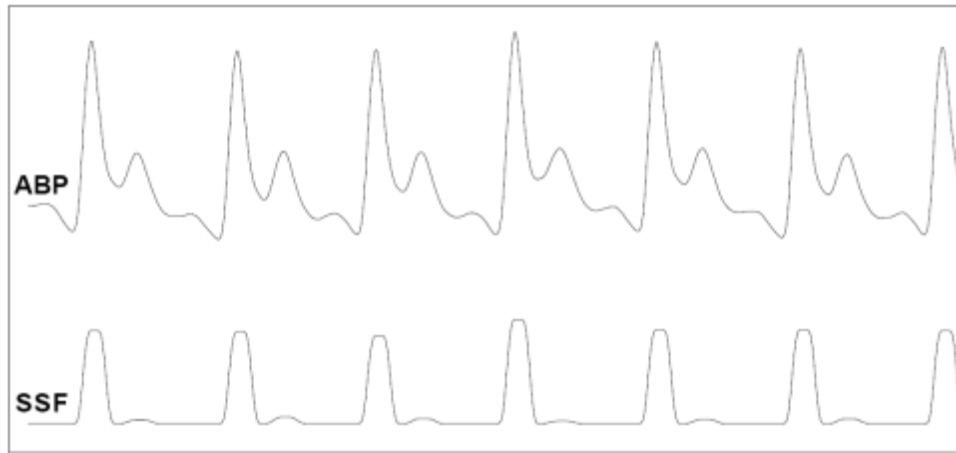


Figure 2.16: Block ABP signal, SSF Comparison

In the decision part, which is the final step, they divide it in two. Firstly, by adaptive thresholding the SSF pulses of appropriate amplitude detected from the SSF signal. Secondly, by employing a local search algorithm around the detection point to confirm the detection and identify the likely onset of the pulse. The algorithm performance shown in Table 2.2

Table 2.2: wabp.mat Function Performance

Volume	Sensitivity(%)	Positive Predictive Accuracy(%)
Gross	99.71	99.69
Average	99.71	99.72

### 2.2.5 Literature Survey on False Arrhythmia Alarms Reduction

Numerous works exist in the literature on the subject of design and implementation of false arrhythmia reduction in ICUs for asystole, extreme bradycardia, extreme tachycardia, ventricular tachycardia and ventricular flutter/fibrillation. Their explanation and figures are given as:

- ASY: The electrical activity of the heart is lost. There are no regularity, rate, P, T or QRS waves measurements as shown in Figure 2.17:

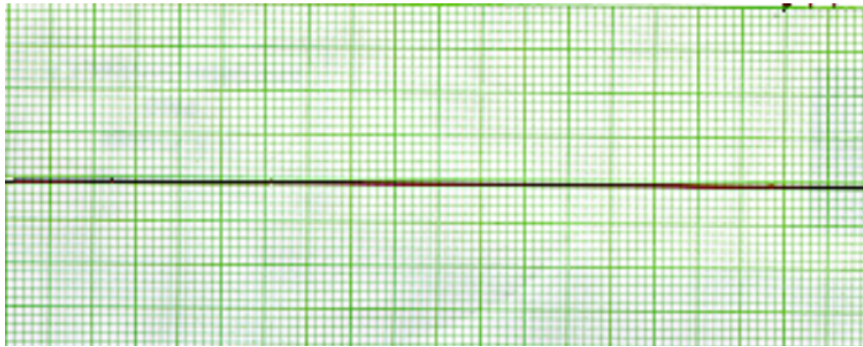


Figure 2.17: ECG signal for Asystole Case [22]

- EBR: Heart rate is less than 40 times per minute. The R-R intervals are constant and heart rhythms are regular. There is a uniform P wave before QRS complex as shown in Figure 2.18:



Figure 2.18: ECG signal for Bradycardia Case [22]

- ETC: Heart rate is greater than 100 times per minute. The R-R intervals are constant and heart rhythms are regular. There is a uniform P wave before QRS complex as shown in Figure 2.19:



Figure 2.19: ECG signal for Tachycardia Case [22]

- VTA: Heart rate is greater than 100 times per minute. The R-R intervals are constant and heart rhythms are usually regular but sometimes slightly irregular as shown in Figure 2.20:



Figure 2.20: ECG signal for Ventricular Tachycardia Case [22]

- VFB: Heart rate is greater than 100 times per minute. There are no discernible waves or complexes to calculate the regularity, and rhythms of the heart as shown in Figure 2.21:

Aboukhalil et al. [2] and Deshmane et. al. [23] applied a multi-parameter analysis on ECG and pulsatile waveforms and signal quality assessment technology to improve algorithms for alarm generation. However, both methods met the problem that alarms had high true alarm (TA) suppression rate while low false

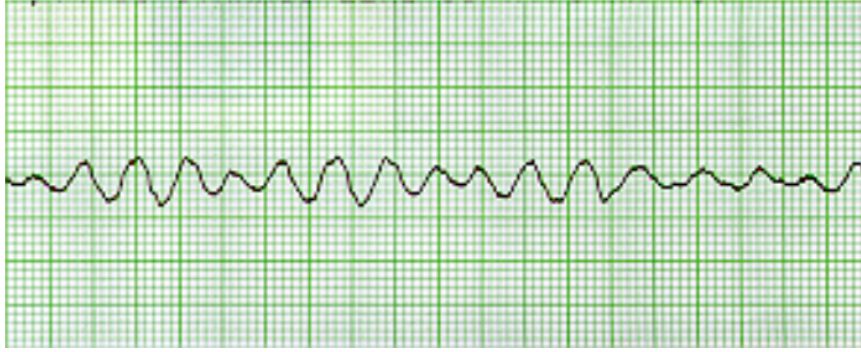


Figure 2.21: ECG signal for Ventricular Tachycardia Case [22]

alarm reduction rate because they only used morphological and timing information. The work described by Sayadi et al. [65] deployed a model-based filtering method to detecting alarms. Superior as the FA suppression rates are, this algorithm is computationally intensive. Qiao Li and Gari D. Clifford [17] extracted features from ECG, arterial blood pressure (ABP), and photoplethysmogram (PPG) and employed a machine learning approach. They achieved a ventricular tachycardia FA suppression of more than 30% with a true alarm suppression rate below 1%.

We also reviewed CinC2015 Challenge articles in terms of :

- Preprocessing and Signal Conditioning: All filters and other methods are applied before using the input in the main algorithm (beat detection) for removing the noise, artifacts and redundant signals in the original signal (such as P and T wave).
- Beat Detection: Processes that investigate QRS or R peaks are named as beat detection.
- Beat Classification: Process that are used to classify the detected beats as real or not real.
- Alarm Classification: Process that are used to classify the alarms as true or false by investigating classified beats properties.

According to Plesinger et al., in the pre-processing stage, noise and pacemaker activities were estimated between spectral content of the 50-70 Hz and bandpass

filtered to them. Pulsatile waveforms are low pass filtered cut-off frequency at either 5 or 20 Hz. In beat detection stage, ECG QRS detection were based on analysis of Fourier and Hilbert transform derived envelopes with a 110 ms refractory period between detection. Pulsatile signals based beat detection was evaluated on estimated temporal slope values. In beat classification stage, spectral features and descriptive residue statistics over 120 ms and 500 ms windows were used. In alarm classification stage, on ASY, VTA and VFB alarms, count of invalid features are used. Additionally, statistics of RR series, which are obtained from multiple channels are used. A set of heuristic rules was applied based on the derived RR series and the invalid region statistics. According to Kalidas and Tamil et al., In the pre-processing stage, a low pass filtered signal with cutoff frequency 1 Hz is subtracted from the original signal to remove baseline wanders. Alternating positive consecutive samples are tested to detect flat-line and zig-zag artifacts. In beat detection stage, the standard Pan and Tompkins 1985 algorithm was used to detect QRS complexes in the ECG. Pulsatile peaks were detected through first order differentiation. In alarm classification stage, No pulsatile signal information was used for VFB and VTA arrhythmia alarms. For each alarm type, an individual support vector machine and set heuristics was developed. The features used into these classifiers included the ECG-derived heart rate, and PPG-derived heart rate if morphology was considered valid (excluding the VFB and VTA alarms). The VFB and VTA alarms also included an additional set of features related to the power spectra of the ECG waveforms. According to Krasteva et al., in the pre-processing stage, the ECG channels were fused to form two data streams: a magnitude (second norm) and a velocity (second norm of the first order derivative). The ECG signal quality was estimated using 3 frequency bands on 4s interval windows: high frequency was used to estimate spikes from artifacts and pacemakers, medium frequency range was used to estimate the signal level and power line interference (with intra-beat temporal statistics used to estimate the power line noise level), and the low frequency band was used to estimate baseline wander. Pulsatile signal were low-pass filtered with a 1 Hz cutoff. The pulsatile signal quality was estimated with periodicity index, and mean peak-to-peak amplitude values. In the beat detection stage, a nonlinear filtering approach, with adaptively updated upper

and lower thresholds, was used for QRS detection. The beat detector had a conventional refractory period of 150 ms. In the beat classification stage, a beat classifier was developed for supra-ventricular and ventricular ectopic beats. A decision tree model was also used, based on features that included: information from template correlation matching, beat morphology features, and RR statistics. In alarm classification stage, an alarm classifier algorithm used a set of heuristic rules based on heart rate, dominant frequency for ventricular rate, phase, space area from both the ECG magnitude and velocity, and pulsatile quality metrics. According to Rodrigues and Couto et al., in the preprocessing stage, all signals were re-sampled to 125 Hz, and the ECG waveforms were processed for pacemaker detection and removal. Baseline noise was removed by first estimating it with a 125 sample median filter, followed by subtraction from the original signal. Flat signal regions were identified by thresholding on low variance over 2 second windows. In the beat detection stage, ECG QRS detection was performed using `gqrs` and `osea` software packages of Hamilton (2002). The beats on the pulsatile signals were detected with the `wabp` software. The authors developed their own specific beat detectors for ventricular fibrillation beats by fitting a parabola on 125 ms windows. Following the method of Li et al. (2008), a quality index was developed based on the fraction of matched beats from `gqrs.m` and the `osea` software packages Hamilton (2002) on the ECG channels. For pulsatile signals, the quality was estimated using the morphology of consecutive beats estimated from correlation and dynamic time warp analysis, per Li and Clifford (2012). The detected beats were fused based on quality indices and a tolerance window of 150 ms. Pulsatile beats were compensated with a delay estimated from initial detections. In the beat classification stage, it was based on a set of heuristics modified from the `osea` software package Hamilton (2002). These set of rules included statistics derived from inter-beat interval and QRS duration. Author also developed a four-category feature, termed ‘polarity’ that characterized the different types of phases of the R wave into: positive, negative, positive-negative, negative-positive (the last two representing biphasic R waves). In the alarm classification stage, It was calculated from a set of decision rules based on signal quality, but with priority weight given to ECG signals. According to Fallet et al., in the pre-processing stage, a filter, which was consisted of

50 Hz power line noise removal was used. For the calculations of spectral purity indices, the signal was down-sampled to 35 Hz and a 5-sample moving average filter was applied. The signal quality for the pulsatile waveforms was estimated through the ppgSQI and jSQI methods of Clifford et al. (2015) [17]. In the beat detection stage, the QRS component of the ECG signal was detected through a morphological analysis approach with an adaptive approach from Yazdani and Vesin (2014) [31]. Beat detection on the pulsatile signals was performed using the algorithm proposed by Arberet et al. (2013) [31]. The heart rate time series was then derived through a multi-channel oscillator based adaptive frequency tracking algorithm. In the beat classification stage, the spectral purity index Sörnmo and Laguna (2005) [55]; Goncharova and Barlow (1990) [31] used a feature to distinguish between normal, ventricular tachycardia, ventricular flutter/fibrillatory arrhythmia (the index was expected to be higher for abnormal rhythms). In the alarm classification stage, a set of heuristic rules was developed for the final alarm classification. In the case of ASY alarm, the algorithm applied majority voting based on the heart rate series from individual ECG and pulsatile channels. The pulsatile channels were only used if the quality was above a certain threshold. A linear discriminant analysis classifier was used for the retrospective event to corroborate the ECG output, but again, only if the pulsatile signal quality was sufficiently high. If the pulsatile quality was low, a set of heuristic thresholds was applied to the minimum heart rate from the last five consecutive beats using 16 seconds before and five seconds after the alarm. The extreme tachycardia alarm only used pulsatile waveforms: if the quality was good, the alarm was checked against the pulsatile rate, else it was defaulted to true. Ventricular flutter/fibrillatory alarms were checked through the maximum average spectral purity index calculation over a 3 second window, and no pulsatile information was used. Finally, ventricular tachycardia alarms used a set of Clifford et al. heuristic rules encompassing pulsatile waveform heart-rate series, as well as current versus previous values of the ECG spectral purity indexes. According to Hoog Antink et al., in the pre-processing stage, steps for this algorithm included re-sampling of the signals to 100 Hz, band-pass filtering with a pass-band region of 1-30 Hz. The signals were also normalized to zero mean and unit variance using statistics calculated on 5-minutes of data prior to

the alarm. In the beat detection stage, it was achieved through the Bayesian fusion of several inter-beat interval estimators that rely on self-similarity: lag adaptive short-time autocorrelation, average magnitude difference function, and maximum amplitude pairs Brüser et al. (2013). A quality metric based on the reliability of the fused estimates was derived from the peak height to area of the fused similarity curve. In the alarm classification stage, the classifiers chosen for the alarm validation included binary classification trees, regularized linear discriminant analysis, a support vector machine, and a random forest. The authors utilized a combination of both alarm specific and global classifiers (i.e., classifiers trained to detect a general false alarm). Their final choices were linear discriminant analysis for EBR, VFB, and VTA, a binary classifier for ETC, and a random forest model for ASY. A superset of 88 features was developed from: 24 beat-to-beat interval statistics and correlogram analysis of interval time series. From this superset, subsets were selected according to alarm types. According to Eerikäinen et al., in pre-processing stage, all signals were down-sampled to 125 Hz and the processing window length was optimized for each arrhythmia type (varying from 14 to 16 seconds prior to the alarm). Noise levels were estimated based on the power, which were estimated from the regions in between beats. In the beat detection stage, beat detection on the ECG waveforms were performed using a QRS detector based on wavelets and auto-regressive modeling of the R-peak. According to Eerikainen et al., the pulsatile peaks were detected via the open source detector wabp.m. In the alarm classification stage, a random forest classifier was trained for each of the five different types of alarms. The technique focused on comparing pairs of beats. Two beats were considered a match if they were within 100 ms of each other. Delays across channels were compensated, if the standard deviation of 10 consecutive beats was less than 5% of the mean delay. For the VTA and VFB alarms, only the F1 statistic between ECG leads was used, in addition to spectral purity indices. An alarm with an F1 equal to zero was identified to be false. According to Ansari et al. [4], in the pre-processing stage, steps consisted of re-sampling the signals to 125 Hz. The ECG signals were band-pass filtered between 0.5-40 Hz, while the pulsatile signals were band-pass filtered between 0.5-10 Hz. Baseline and trend estimation and subtraction was accomplished with a 250 point median filter. The authors

also removed pacemaker activity by thresholding on the peak amplitude. In the beat detection stage, he implemented 7 different QRS detectors for each ECG signal, and 3 peak detectors for each of the pressure signals. The fiducial points for all peaks were re-aligned by picking the maximum within 50 ms of the detected beat for ECG signals, and the maximum within 50 ms before or 1 second after the detected beat for the ABP or PPG signals. The outputs of all the 20 beat detectors were then fused by adding their binary outputs (with at least 1 beat under AS, at least 2 for other alarms). In the beat classification stage, ECG beat classification was performed for the VFB and VTA alarms only. The beat classifier was a decision tree that utilized features derived from the Stockwell Transform on a 200 ms window. In the alarm classification stage, a decision tree classifier was trained with fivefold cross validation in order to determine the veracity of a beat. The final decision regarding the alarm veracity was made based on a set of heuristics. The proposed algorithm operates on 16 seconds of worth of data prior to the alarm. According to Liu et al., in the pre-processing stage, the ECG and pulsatile signals were band-pass filtered with the passband frequency region of 5 – 40 Hz for the ECGs and a pass-band frequency region of 5 – 35 Hz for the pulsatile waveforms. In the beat detection stage, the authors developed an ECG R wave detection algorithm that used the average maximum amplitude from 6 non-overlapping segments. Pulsatile beats were detected via `wabp`. The final detected beats were validated based on intra-channel and inter-channel verification of the detected beats along with a set of rules involving the number of detected beats, R amplitude, and distance metrics between the heart rate time series. In the beat classification stage, a set of heuristics was applied to classify beats. The features included: morphology analysis based on correlation against template, the ratio between changed beats and total beats in segment, QRS width, and maximum heart rate. In the alarm classification stage, a set of decision rules was applied to channels that passed a data quality check (if the result of the test failed, the alarm was set to false). The features used for the second classification step included number of valid feature points, heart rate, and maximum heart rate at current analysis window. According to Sadr et al., in the pre-processing stage, baseline removal was performed by first estimating the baseline component through median filtering and then subtracting this base-

line component from the original signal. In the beat detection stage, a Hilbert transform based QRS detector based was used for estimating the ECG beats Benitez et al. (2001). The wabp algorithm was used to detect the peaks on the ABP and PPG waveforms, and a quantile algorithm was also used to locate peaks on the PPG waveform. In the alarm classification stage, the alarm verification was performed on a 16 second window of data prior to the alarm. For all of the alarms with the exception of VTA, the alarm data streams had to pass four signal quality checks in order to be deemed a true alarm, otherwise they were tagged as false. Pulsatile signal information was not used for the ETC and VTA alarms. The classification also consisted of decision trees based on several extracted features customized to each alarm type, including: threshold crossing intervals, autocorrelation function values, complexity measures, and QRS template parameters. According to Zong et al., in the pre-processing stage, pulsatile signals were low pass filtered with cuto set to 16 Hz, and a signal quality estimate was obtained using the technique as described in Zong et al. (2004). In the beat detection stage, it was performed with the pulsatile signals using wabp and with a forced detection after a period of 2 seconds from the last detected pulse. In the beat classification stage, the pulsatile beats were classified based on the abnormality index from Sun et al. (2006). In the alarm classification stage, it was achieved using features from pulsatile signals that included: pulse-to-pulse interval, amplitude, maximum slope, signal quality, and rhythm. The classifier was developed based on set of heuristic rules specific to each alarm type. The algorithm was developed and tested using the MIMIC II database [47] rather than the Challenge data, and was not open sourced.

### **2.2.6 Performance Evaluation**

In this study, sensitivity, specificity, positive and negative predictivity and challenge score equation measures were used for performance evaluation of the methods and compare with others in literature. General use of parameters calculation given in the Table 2.3.

The variables and definitions of performance evaluation parameters can be sum-

Table 2.3: General Use of Parameters

Predicted Outcome	Gold Standards	
	True Alarm	False Alarm
True Alarm	TP (True Positive)	FP (False Positive)
False Alarm	FN (False Negative)	TN (True Negative)

marized as follows:

- The gold standard is the best single test (or a combination of tests) that is considered the current preferred method of diagnosing a particular disease (X).
- Sensitivity is the ability of a test to correctly classify an individual as diseased whose equation is given below.

$$Sensitivity = TP/(TP + FN) \quad (2.13)$$

- The ability of a test to correctly classify an individual as disease-free is called the tests specificity and the equation is given below.

$$Specificity = TN/(TN + FP) \quad (2.14)$$

- It is the percentage of patients with a positive test who actually have the disease which's equation is given below.

$$PositivePredictivity = TP/(TP + FP) \quad (2.15)$$

- It is the percentage of patients with a negative test who do not have the disease which's equation is given below.

$$NegativePredictivity = TN/(TN + FN) \quad (2.16)$$

- In Physionet 2015 challenge competitors scored with equation given below. In the score equation more specifically, competitors should attempt to maximize TP and TN while minimizing FP and FN. The scoring will weight FN more heavily than the FP.

$$Score = (TP + TN)/(TP + TN + FP + 5 * FN) \quad (2.17)$$

## CHAPTER 3

### METHODS

This chapter starts with the explanation of the pre-processing stage, followed by the details of the QRS, PPG, ABP detection, feature selection and decision methods implemented in this thesis.

#### 3.1 Pre-Processing

As explained in Section 1.1 in chapter 1, in the dataset used for this study, the alarm starts at the fifth minute and with ten seconds duration for each alarm record in the given database. Moreover, each record has been labeled with only one alarm type in the first five minute (usually in the 4 : 50 – 5 : 00), which means that any other arrhythmias in the first five minutes period was not marked or evaluated. In order to decrease carrying an error from a previous alarm to the following alarm, information from the primitive and repeated alarms are not used. Firstly, all signals in the data set were re-sampled from 12 bit and 250 Hz to 12 bit and 125 Hz frequency for simplicity in computation. ECG signals and PPG/ABP signals are between 0.5 – 40 Hz and 0.5 – 5 Hz respectively, for monitoring case. Therefore, ECG signals are band-pass filtered by using a finite impulse response (FIR) filter designed with two different combinations of specific lower and upper cut-off frequencies (5, 30 *Hz*), which are optimized by trial-and-error method respectively with Hamming window approach to remove baseline wanders, pacemaker noises and power line noises. Coagulation, movement artifacts, line flush, sensor disconnections and other noises may have damaged the pulsatile signals (PPG and ABP). Therefore, the pulsatile signals were band-pass filtered by using a FIR filter designed with specific lower and upper cut-off fre-

frequencies (0.5-5 Hz), which are optimized by trial-and-error method respectively with Hamming window approach. Although these cutoff frequencies corrupt the ECG signal, it is enough for R peak detection and suppressed other redundant (P, T wave and low frequency noises) waves in the ECG signal. These cutoff frequencies are based on analysis and modification of Tsimenidis and Murray researches [74] to apply on our method. Although, there are other filter types like adaptive filters with respect to ECG morphology and noise, they require a large reference signal database and they need high processor power due to their computational complexity (recursive least squares (RLS)). The block diagram of the Pre-processing step shown in Figure 3.1.

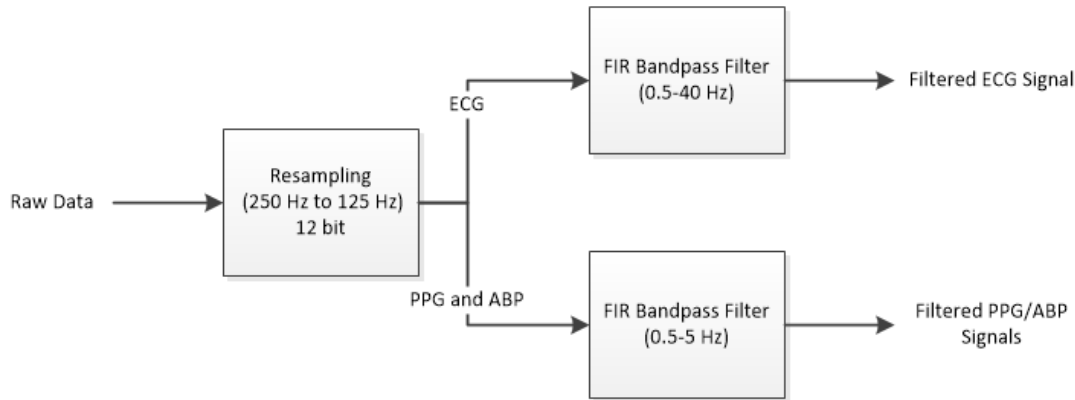


Figure 3.1: Block Diagram of Pre-processing Step

### 3.2 QRS Complex Detection

After the pre-processing step, QRS complex detection algorithm is applied to the filtered ECG signals, which are divided into two parts: signal detection and signal quality index (SQI) calculation. The first step of the signal detection algorithm is to apply an R-peak/ECG pulse peak detection on a sample and to compare the output of the detector with a set of physiologically relevant rules. There are a lot of methods for R or QRS complex peak detection methods. You can see their authors, pre-processing, QRS enhancement and QRS detection methods and their numerical efficiencies in Table 3.1.

These methods performances are shown in Table 3.2, which includes the number

Table 3.1: Summary of various researches for ECG beat segmentation

Authors	QRS Enhancement	QRS Detection	Num. Efficiency
Benitez et al. [11]	Hilbert transform and 1st differential	One adaptive THV and 1st approximation	Medium
Christov et al. [16]	Multiple moving averages, first derivative	Combined three adaptive THV's	High
Chen et al. [14]	Wavelet denoising and moving average filter	One adaptive THV	Medium
Lee at al. [48]	Phase portrait and lowpass filter	Two THVs, refractory blanking and search back	Low
Cvikl et al. [20]	Phase portrait and bandpass filter	two THVs, refractory blanking and search back	Low
Poli et al. [62]	Polynomial filter	Three adaptive THVs	Low
Afonso et al. [3]	Filter bank	Three THVs and timing information	Low
Pan and Tompkins [36]	Morphological processing	Four adaptive THVs and the average RRI information	Medium
Hamilton and Tompkins [35]	Morphological processing	Three adaptive THVs, refractory blanking and search back	Medium

of beats are used for testing, sensitivity rates and positive predictivity rates of them.

Table 3.2: QRS complex performance comparison with several algorithms

Method	Number of beats	Sensitivity	Positive Predictivity
Benitez et al. [11]	45856	99.94	99.93
Cvikl et al. (2007) [20]	109494	99.82	99.82
Pan and Tompkins (1985) [36]	109809	99.75	99.54
Lee at al. (2002) [48]	109486	99.69	99.87
Hamilton and Tompkins (1986) [35]	109267	99.69	99.77
Christov (2004) [16]	110050	99.74	99.65
Poli et al. (1995) [62]	109963	99.60	99.50
Afonso et al. (1999) [3]	90909	99.55	99.59
Chen et al. [14]	100381	99.47	99.54

It is obvious that all these QRS detection algorithms have excellent performances such as over 99% sensitivity and positive predictivity. The QRS detection method, which was proposed by Benitez et al. [11], is slightly the best in all of them and in terms of numerical efficiency, it is proper to implement in a low cost and processor power watch, which is one of our aims in this work. This method is based on Hilbert transform and its flow diagram is shown in Figure 3.2.

Hilbert transform is an odd function, which means that if there is an inflection

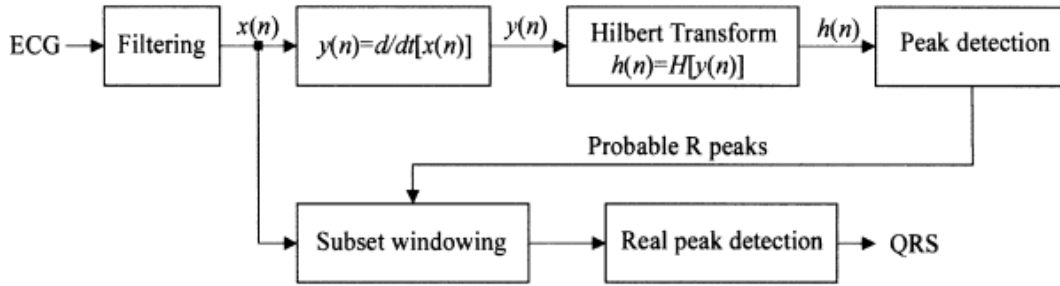


Figure 3.2: Block diagram of Hilbert Detector

point in the original waveform, Hilbert transform of the signal will intersect a zero on the x axis. Similarly, an intersection of the zero between sequential positive and negative inflections in the original waveform will be presented as a peak in its Hilbert transformed conjugate. This interesting feature can be used to implement a simple and easier algorithm to detect peaks of the QRS complexes in the ECG waveform [11]. Correspondence of these zero crossings in its first differential waveform  $d/dt(EGC)$  and peaks in its Hilbert transformed waveforms are shown in Figure 3.3.



Figure 3.3: R wave equivalences in The Approach

In Figure 3.3, top row shows the ECG waveform, the second row shows  $d/dt(EGC)$ , which is the first derivative of original waveform, the third row shows  $H[d/dt(EGC)]$ ,

which is the Hilbert transform of the first derivative of the original signal, the last row shows  $B[d/dt(ECG)]$ , which is the enveloped form of the ECG contributions after HT.

In our work we modified the method [11] above by adding steps to its flow and implemented it. Firstly, for the first derivative step  $d/dt(ECG)$  we used a 2-point first-order differentiator. The  $x(n)$  is the filtered ECG waveform subset sequence. Its first derivative ( $y(t) = d/dt(ECG)$ ) in the discrete domain can be obtained by:

$$y(n) = \frac{1}{2\Delta t}[x(n+1) - x(n-1)] \quad (3.1)$$

for  $n = 0, 1, 2, \dots, m-1$

where:  $m$  is the total number of samples and  $\Delta t$  is the sampling frequency.

The initial value is specified as  $x(-1)$  when  $n = 0$ , and final value is specified as  $x(m)$  when  $n = m-1$ . These preferences are necessary to minimize error at boundaries. The Hilbert transform  $h(n)$  of the sequence  $y(n)$  that represents the first derivative squared of the ECG waveform in this subset is then obtained using the following methodology:

1. Obtain the filtered ECG signal  $x(n)$  after the pre-processing step, which is explained in Section 3.1.
2. Scale the filtered ECG signal  $x(n)$  to have approximately same amplitudes of R points in the signal.
3. Take the derivative of the signal  $x(n)$  with a 2 point 1st order differentiator.
4. Take the Hilbert transform of the first derivative of the signal.
5. Apply squaring function to the Hilbert transform of the signal. This operation makes all the data points in the processed signal positive and amplifies the output of the derivative process nonlinearly. It emphasizes the higher frequencies (QRS complex) and attenuates the lower frequencies (P and T waves) like a low-pass filter.
6. A short sequences of a moving 16 second (2000 point) rectangular window is used to subdivide the input.

7. The rising slope of the R wave will correspond to a maximum in the first derivative sequence and the falling slope of the R wave will correspond to minimum in the first derivative signal. The peak of the R wave will be equivalent to zero crossing between these two positive and negative peaks.
8. Find the standard deviation of the signal and multiply it with  $\beta$  which is the optimized value for the given arrhythmia type to get an adaptive ECG threshold value.
9. By using half of the threshold value, find the minimum peak distances and heights.
10. Calculate the signal quality of the ECG signals by ECG signal quality index (SQI) rules:
  - After the beat detection step, at least  $beatnm_{min}$  number of beats need to be detected.  $beatnm_{min}$  is found by trial and error methods (heuristically) as 2.
  - Maximum RR interval for each ECG signal was calculated. Then the maximum RR interval was compared to the threshold  $RRint_{max}$  (6 s). It should be smaller than  $RRint_{max}$  because RR intervals usually are between 0 – 6 s [64].
  - The standard deviation of the ECG signal should be greater than  $ECGamp_{min}$  (0.05 [64]).
11. If the signal quality of the ECG signal is over the adaptive threshold values, find the parameters related to each arrhythmia type, else disable further analysis and tag the ECG signal as noisy, which means that the ECG signal contains irremovable noise or artifacts.

When two peaks in these Hilbert sequences are located very close to each other (less than 200 ms) only one of the peaks are considered as the real R peak. Then the decision is based on the amplitude of the peak and their position related to the last R peak located using an adaptive time (duration) threshold. This threshold is based on the average of inter beat length (R-R interval) of the previously detected R peaks. The block diagram of the proposed approach is

shown in Figure 3.4.

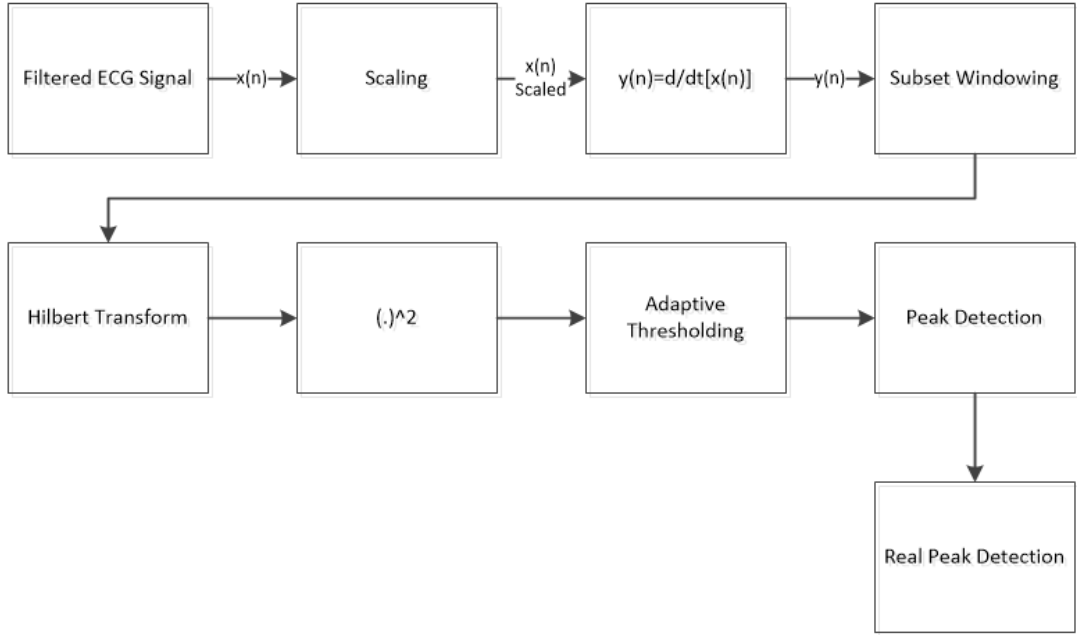


Figure 3.4: Block diagram of the proposed QRS detector

Ventricular tachycardia and ventricular fibrillation/flutter it is unclear if the SQI analysis is appropriate to discriminate these arrhythmias from irremovable artifacts. Our SQI rules for ECG signals gave better result for asystole, bradycardia and tachycardia cases than other arrhythmia cases. The ECG signal was analyzed for non-physiological conditions, such as unusual flat baseline signals, which are resulted from poor electrode contact noise. Therefore, we had a three step SQI analysis:

### 3.3 PPG Detection

PPG detection is divided into three parts: adaptation to ABP signal detection algorithms (explained in section 3.4 ABP Detection), signal detection, feature extraction and signal quality analysis. For the first part, a quantile function is used to separate the signal into three quantiles (0.05, 0.5, and 0.95). The last two parts are implemented by modifying two Physionet open-source algorithms for PPG processing. Then for the second part the wabp.m (algorithm detail are in Appendix Section A) function is used to detect onset points by using the dif-

ference between third quantile and first quantile. These onset point are used to calculate R-R intervals. For the last part, the ppgSQI.m algorithm (algorithm details are in Appendix Section A) is used to compute the SQI (algorithm details are in Appendix Section A). This SQI algorithm is based on beat template correlation. Finally, if the signals have enough quality, the R-R intervals are calculated as the difference of the onset points of the pulses in the signal and compute *high\_hr\_ppg*, *low\_hr\_ppg*, *hr\_max\_ppg*, *hr\_min\_ppg*, *max\_rr\_ppg* parameters for evaluating each arrhythmia type specifically. These parameters are defined as follows:

- *high\_hr\_ppg*: Calculated high heart rate of 17 consecutive beats for Tachycardia case from PPG signal.
- *low\_hr\_ppg*: Calculated low heart rate of 5 consecutive beats for Bradycardia case from PPG signal.
- *hr\_max\_ppg*: The calculated maximum heart rate 16 s before the alarm for decision making from PPG signal.
- *hr\_min\_ppg*: The calculated minimum heart rate 16 s before the alarm for decision making from PPG signal.
- *max\_rr\_ppg*: The calculated maximum RR interval 16 s before the alarm for decision making from PPG signal.

The block diagram of the PPG detection step shown in Figure 3.5.

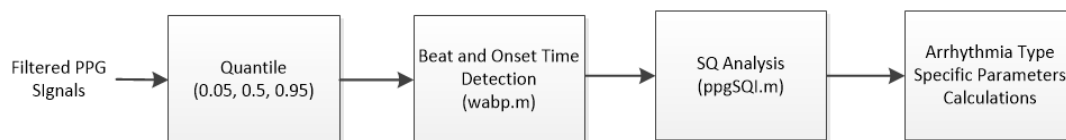


Figure 3.5: Block Diagram of PPG Detection Step

### 3.4 ABP Detection

ABP detection can be divided into three parts as: onset point detection, feature extraction and SQI calculation. These parts are implemented by modifying three Physionet open-source algorithms specialized for ABP processing. For the first part, the `wabp.m` algorithm (algorithm details are in Appendix Section A), which is based on length transform [17], was implemented to detect the onset points of the pulses in the ABP signal [17]. For the second part, the `abpfeature.m` algorithm (algorithm details are in Appendix Section A) was implemented to compute 12 features from ABP signal such as systolic and diastolic pressures, systolic area and mean pressure, etc. from each detected pulse. For last part, the `jSQI.m` algorithm (algorithm details are in Appendix Section A) was applied to evaluate the signal quality of each detected beat of the ABP signal. Output of the algorithm gives an average value between 0 – 1 to each feature of the signal. If the calculated physiological parameter of the signal is in the normal signal levels, the algorithm gives 1. If the calculated physiological parameter is outside of the normal signal levels, algorithm gives 0. Then it sums all scores and computes the mean. It is based on eliminating signals which have physiologically meaningless onset points with respect their signal qualities. Finally, if the signal quality level of the R-R intervals of the signal is over the adaptive threshold, these R-R intervals, which are the time differences of the sequential onset points of the pulses, are used to calculate *high\_hr\_abp*, *low\_hr\_abp*, *hr\_max\_abp*, *hr\_min\_abp*, *max\_rr\_abp* parameters for evaluating each arrhythmia type specifically. These parameters are defined as follows:

- *high\_hr\_abp*: The calculated high heart rate of 17 consecutive beats for Tachycardia case from ABP signal.
- *low\_hr\_abp*: The calculated low heart rate of 5 consecutive beats for Bradycardia case from ABP signal.
- *hr\_max\_abp*: The calculated maximum heart rate 16 s before the alarm for decision making from ABP signal.
- *hr\_min\_abp*: The calculated minimum heart rate 16 s before the alarm

for decision making from ABP signal.

- *max\_rr\_abp*: The calculated maximum RR interval 16 s before the alarm for decision making from ABP signal.

The block diagram of the ABP detection step shown in Figure 3.6.

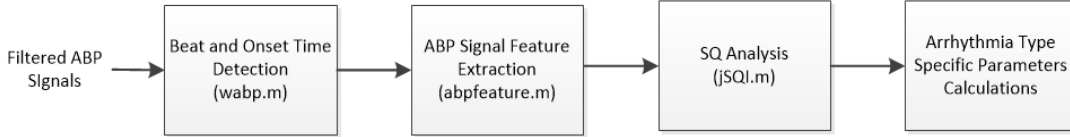


Figure 3.6: Block Diagram of ABP Detection Step

### 3.5 Signal Integration

When various signals are needed to process the outputs, they should be integrated with an integration method to enhance the performance of the approach. Signal fusion is the general name of these methods. There were different methods implemented such as SQI based methods [9], which was modified for this work.

In this study, ECG, PPG and ABP signals were one by one mixed or employed as the most reliable signals and tested to find the best decision logic for each arrhythmia type. The input for the proposed method is the last 16 seconds of each record in the presence of the expected arrhythmia. In this approach, four different fuzzy logic methods are implemented as: "Only ECG" Method, which uses only the ECG signal as input and gives output, "Only PPG or Only ABP" Methods, which use only PPG or ABP signal as the input and gives the output, "Main PPG" or Main ABP-Secondary ECG" Methods, which use firstly PPG or ABP signal and give output with respect to these signals, and if these signals are not available, or their SQ levels are under the thresholds, ECG signal is used as the secondary input, "Main ECG-Secondary PPG or ABP" Algorithms, which use firstly ECG signal as an input and give output with respect to it. If these signals are not available, or its SQ level is under the thresholds, PPG or ABP signal is used as input.

- Only ECG Method:** The block diagram of the Only ECG method is shown in Figure 3.7. First, the ECG signal is extracted from the current arrhythmia data and filtered by specific filters, which was explained in Section 3.1. Then, the signal is evaluated with the degree of signal quality by ECG SQI rules, which are explained in Section 3.2. If the signal SQI degree is over the threshold, it can be used in the alarm decision step by the QRS Complex detection algorithm with specific parameters to the arrhythmia type, which are explained in section 3.6. The output gives the final decision (false or true alarm). If the signal is noisy, which means that the SQI degree of the signal is under the adaptive threshold, the alarm is tagged as false alarm without processed by any other alarm decision step.

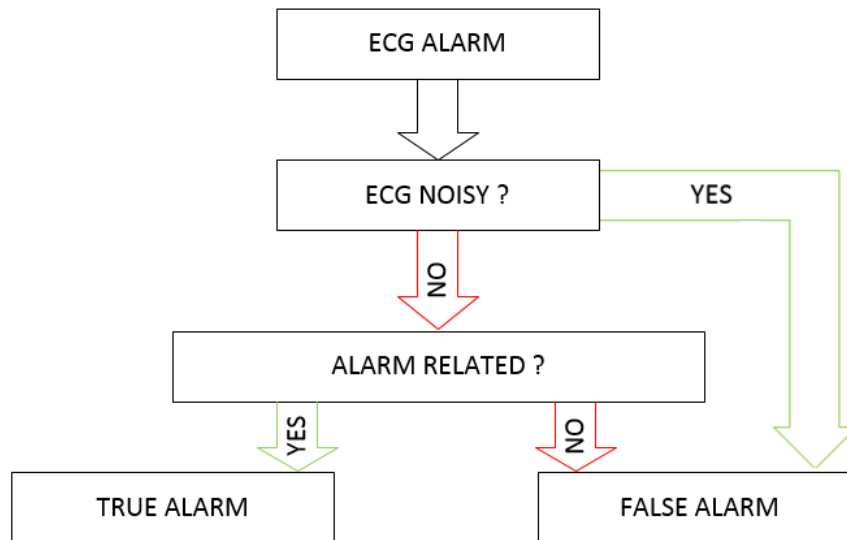


Figure 3.7: Block diagram of Only ECG Method

- Only PPG or ABP Method:** The block diagram of the Only PPG or ABP method is shown in Figure 3.8. First PPG, ABP, or both signals, which are available, are extracted from the current arrhythmia data and filtered by specific filters as explained in section 3.1. Then, signals are evaluated with the degree of SQ by ppgSQI.m, jSQI.m, which are explained in Appendix Section A. If the signals have SQI degrees over the thresholds, it can be used in the alarm decision step by the PPG Detection and ABP Detection methods with specific parameters to the arrhythmia type, which

are explained in Section 3.6. The outputs gives the final decision (false or true alarm) with respect to 'OR' statement between PPG decision and ABP decision rules which are explained in Sections 3.4 and 3.3. If signals are both noisy, which means that both of them have SQI degrees of signals under the adaptive thresholds, the alarm is tagged as false alarm without processed by any other alarm decision step.

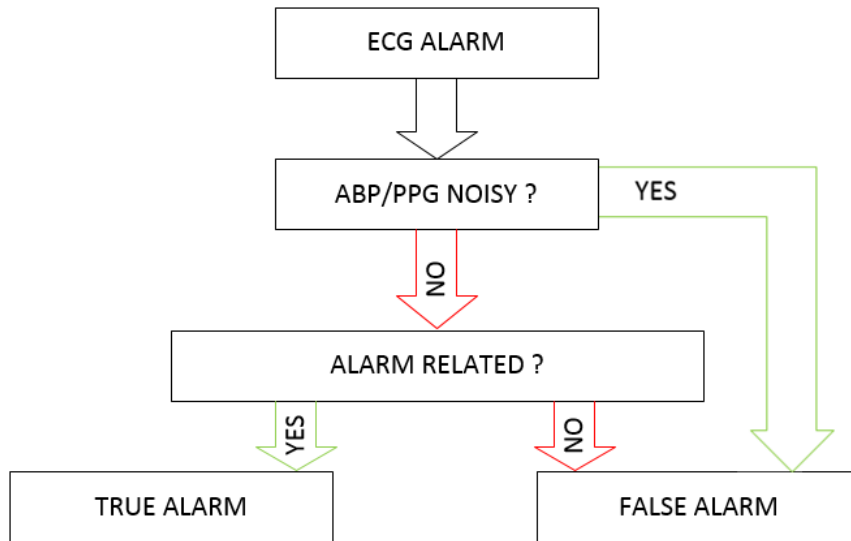


Figure 3.8: Block diagram of Only PPG/ABP Method

- Main PPG or ABP, Secondary ECG Method:** The block diagram of the Main PPG or ABP, Secondary ECG method is shown in Figure 3.9. First ECG, PPG and ABP signals, which are available, are extracted from the current arrhythmia data and filtered by specific filters explained in Section 3.1. Then, PPG, ABP signal qualities are computed by ppgSQI.m, abpSQI.m, which are explained in Appendix Section A. If the signals have SQI degrees over the thresholds, they are evaluated by the PPG detection and ABP detection methods with specific parameter to the arrhythmia type, which are explained in Sections 3.4 and 3.3. The output gives the final decision (false or true alarm) with respect to 'OR' statement between PPG decision and ABP decision. If signals are both noisy, which means that both of their SQI degrees of signals are under the adaptive thresholds, the ECG waveform SQ is computed by ECG SQI rules, which are explained in Section 3.2. If the signal SQI degree is over the threshold, it can be used

in the alarm decision step by the QRS Complex detection algorithm with specific parameters to the arrhythmia type, which are explained in section 3.6. The output gives the final decision (false or true alarm). If the signal is noisy, which means that the SQI degree of the signal is under the adaptive threshold, the alarm is tagged as false alarm without processed by any other alarm decision step.

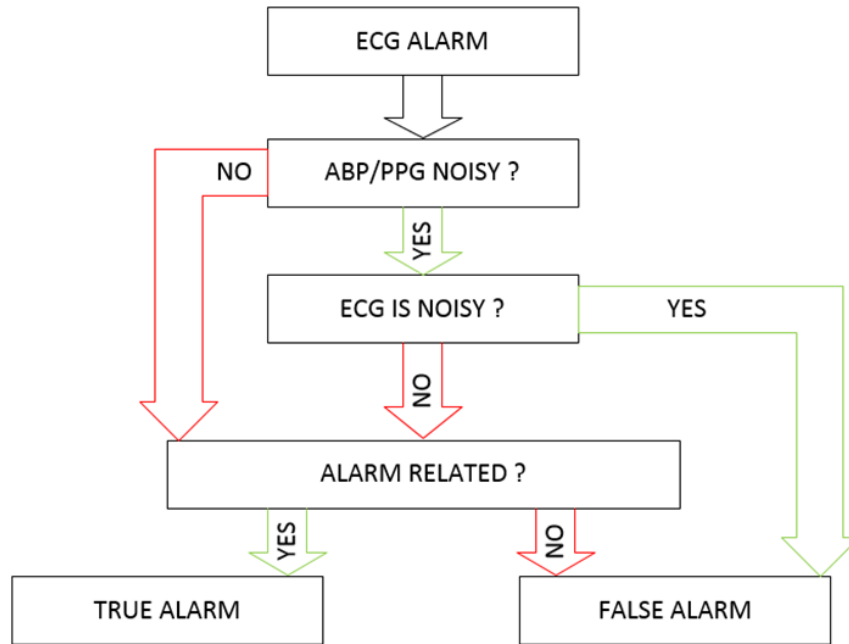


Figure 3.9: Block diagram of Main decider PPG/ABP Secondary Decider ECG Algorithm

- Main ECG, Secondary PPG or ABP Method:** The block diagram of the Main ECG, Secondary PPG or ABP method is shown in Figure 3.10. Firstly available ECG, PPG and ABP signals, which are available, are extracted from the current arrhythmia data and filtered by specific filters explained in Section 3.1. Then, the signal is evaluated with the degree of SQ by ECG SQI rules, which are explained in Section 3.2. If the signal SQI degree is over the threshold, it can be used in the alarm decision step by the QRS Complex detection algorithm with specific parameters to the arrhythmia type, which are explained in section 3.6. The output gives the final decision (false or true alarm). If the ECG signal is noisy, which means that SQI degree is under the adaptive threshold, PPG, ABP signal

qualities are computed by ppgSQL.m, abpSQL.m, which are explained in Appendix Section A. If the signals have SQI degrees over the thresholds, they are evaluated by the PPG detection and ABP detection methods with specific parameter to the arrhythmia type, which are explained in Sections 3.4 and 3.3. The output gives the final decision (false or true alarm) with respect to 'OR' statement between PPG decision and ABP decision. If signals are both noisy, which means that both of their SQI degrees of signals are under the adaptive thresholds, the alarm is tagged as false alarm without processed by any other alarm decision step.

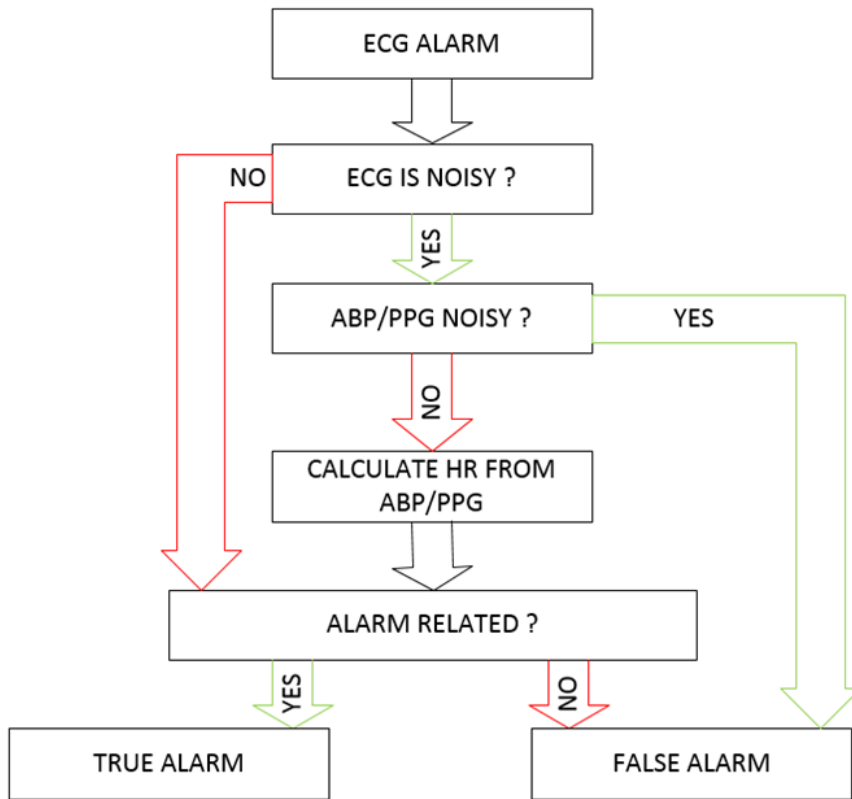


Figure 3.10: Block diagram of Main decider ECG Secondary Decider PPG/ABP Method

### 3.6 Arrhythmia Type Based Processing and Classification

In this section arrhythmias specific parameters and processes (Asystole Processing, Bradycardia Processing, Tachycardia Processing, Ventricular Tachycardia Processing, Ventricular Fibrillation/Flutter) after explained.

### 3.6.1 Asystole Processing

Asystole (*ASY*) is defined as no heart beat for at least four seconds. The block diagram of the Asystole Processing is shown in Figure 3.11. The asystole specific processes are explained as follows:

- Unusual cases like less than 2 beats, adaptive signal amplitude, which blank extreme higher and lower peaks etc. checked for each signal.
- Maximum R-R intervals of signals and their SQIs (explained in Section 3.2 and Appendix Section A) are calculated.

All these results fused with fusion methods, which are explained in Section 3.5. Finally the arrhythmia alarm situation is updated.

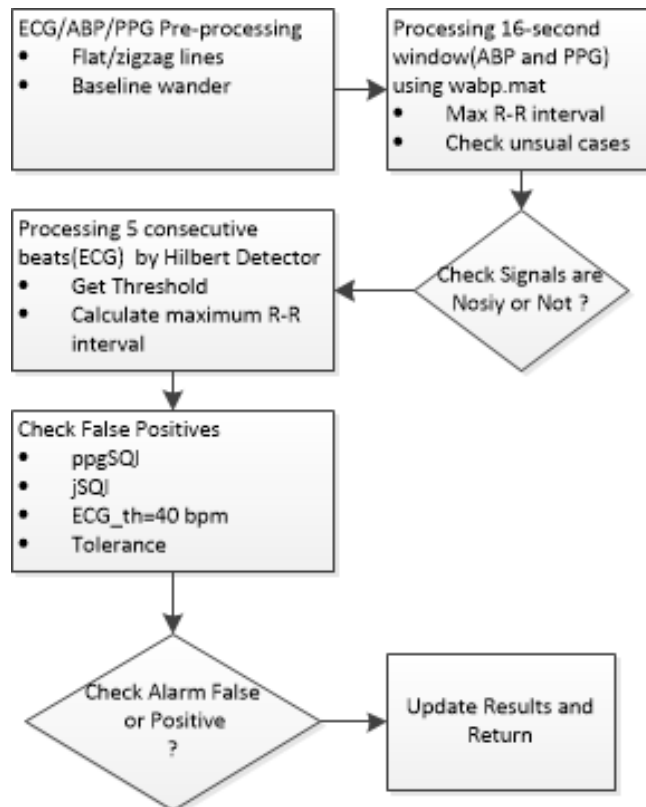


Figure 3.11: Block diagram of Asystole Process

### 3.6.2 Bradycardia Processing

If the heart rate is less than 40 bpm for five consecutive beats, it is defined as Bradycardia (*EBR*). The block diagram of the Bradycardia Processing is shown in Figure 3.12. The bradycardia specific processes are explained as follows:

- Unusual cases like less than 2 beats, adaptive signal amplitude, blank higher peaks etc. checked for each signal.
- The lowest heart rate of each signal type and their SQIs (explained in Section 3.2 and in Appendix Section A) are calculated.

All these results are combined with fusion methods, which are explained in Section 3.5. Finally, the arrhythmia alarm situation is updated.

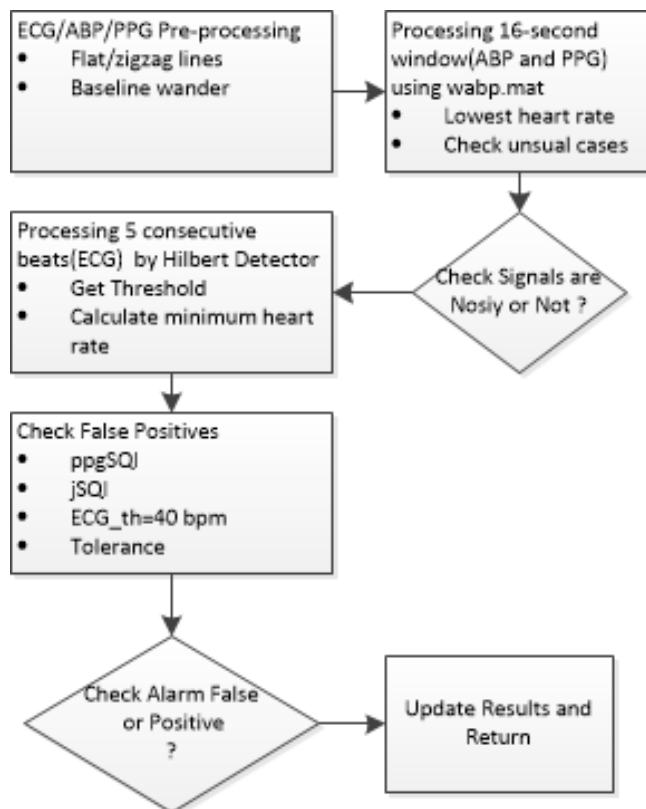


Figure 3.12: Block diagram of Extreme Bradycardia Process

### 3.6.3 Tachycardia Processing

When the heart rate rise to more than 140 bpm for 17 consecutive beats, it is named as Tachycardia (ETC). The block diagram of the Tachycardia Processing is shown in Figure 3.13. The tachycardia specific processes are explained as follows:

- Unusual cases like less than 2 beats, adaptive signal amplitude, blank higher peaks etc. checked for each signal.
- The highest heart rates of each signal type and their SQIs (explained in Section 3.2 and Appendix Section A) are calculated.

All these results are combined with fusion methods, which are explained in Section 3.5. Finally, the arrhythmia alarm situation is updated.

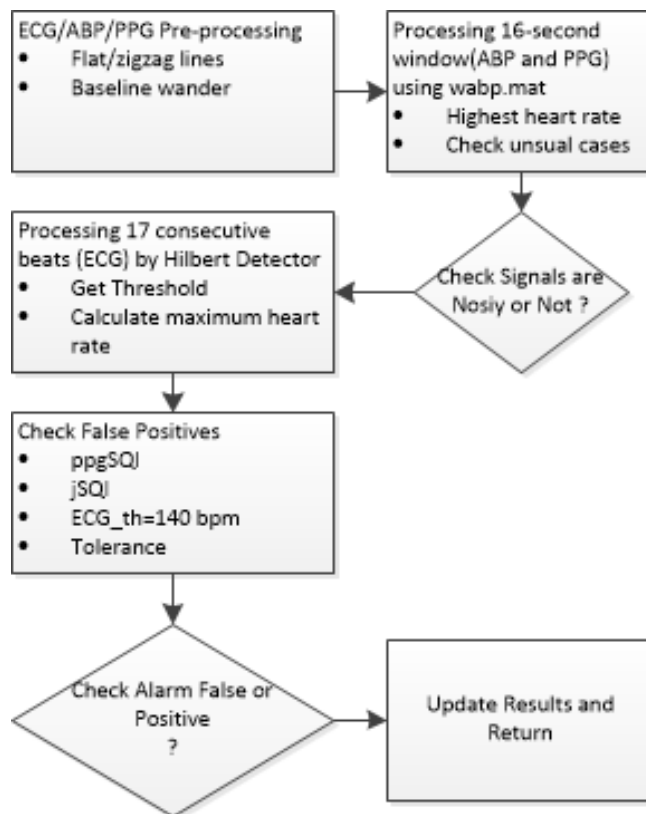


Figure 3.13: Block diagram of Extreme Tachycardia Process

### 3.6.4 Ventricular Tachycardia Processing

Ventricular tachycardia (VTA) defined as five or more ventricular beats with heart rate higher than 100 bpm. The block diagram of the Ventricular Tachycardia Processing is shown in Figure 3.14.

- Unusual cases like less than 2 beats, adaptive signal amplitude, blank higher peaks etc. checked for each signal.
- The maximum heart rates of each signal type and their SQIs (explained in Section 3.2 and Appendix Section A) are calculated.

All these results are combined with fusion methods, which are explained in Section 3.5. Finally, the arrhythmia alarm situation is updated.

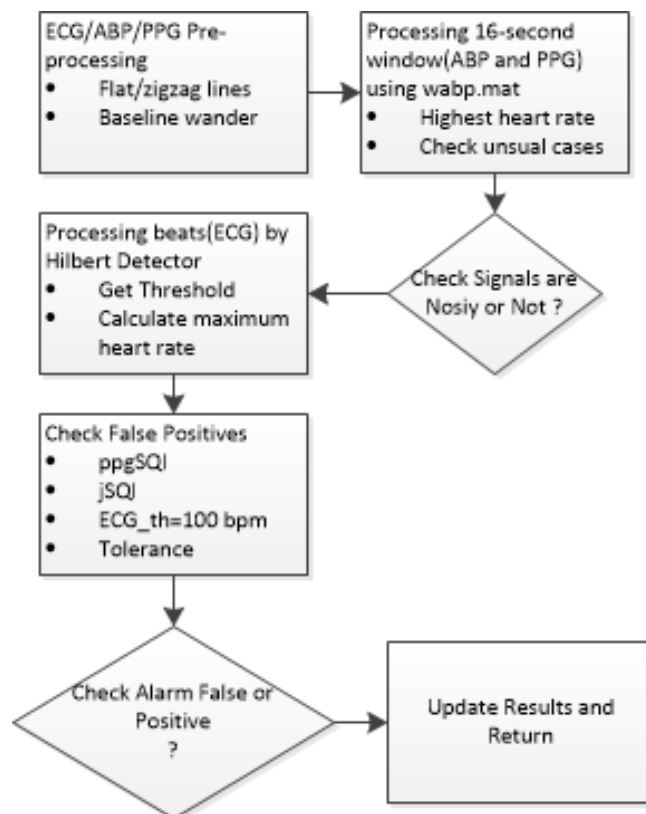


Figure 3.14: Block diagram of Ventricular Tachycardia Process

### 3.6.5 Ventricular Flutter or Fibrillation Processing

Flutter, fibrillatory or an oscillatory waveforms for at least four seconds, it is defined as Ventricular Flutter (VFB). The block diagram of the Ventricular Flutter or Fibrillation Processing model shown in Figure 3.15.

- Unusual cases like less than 2 beats, adaptive signal amplitude, blank higher peaks etc. checked for each signal.
- The maximum heart rates of each signal type and their SQIs (explained in Section 3.2 and Appendix Section A) are calculated.

All these results are combined with fusion methods, which are explained in Section 3.5. Finally, the arrhythmia alarm situation is updated.

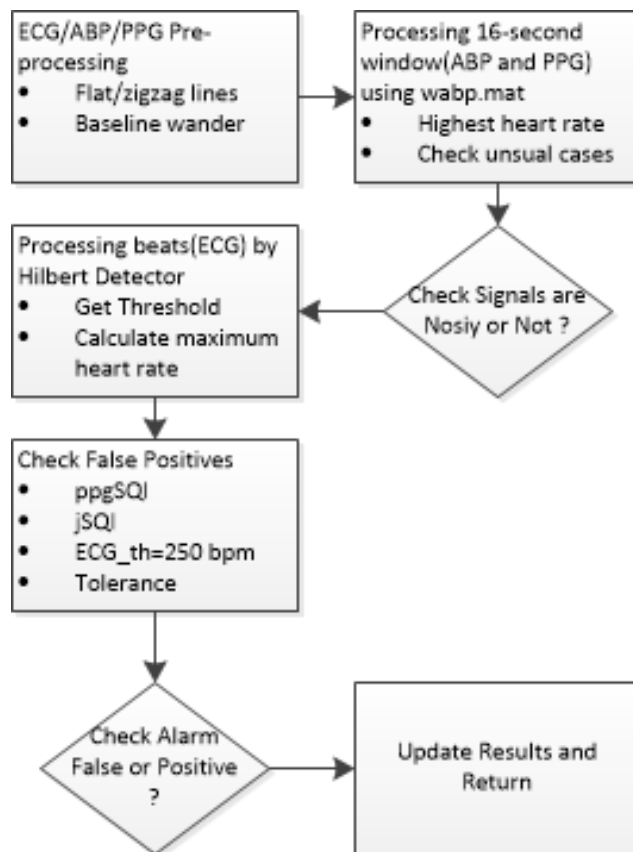


Figure 3.15: Block diagram of Ventricular Flutter/Fibrillation Process



## CHAPTER 4

### PERFORMANCE EVALUATION

In this chapter, our developed algorithms for false arrhythmia alarms reduction were tested on records containing false or true alarms of arrhythmias, such as asystole, bradycardia, tachycardia, ventricular tachycardia, ventricular flutter/fibrillation. Initially, dataset was divided in to two equal numbers of false and true alarms for each arrhythmia cases and labeled as training and test sets. All developed methods, as explained in Section 3.5, were trained and tested with these equal condition (in terms of number of alarms and true and false alarms percentages in the dataset) datasets, which are explained in Section 4.1. These results were analyzed with respect to their powerful parts and limitations in Section 4.1.1. These methods were fused to get the best performance method and to improve the usability in different conditions (such as limited number of physiological signals( Only PPG or ECG and PPG)), for feature health care solutions and improvements, which are explained in 4.1.2. The best part of these methods combination performances were compared with CinC2015 finalists by using the whole dataset for each arrhythmia types, which is explained in Section 4.1.3.

#### 4.1 QRS Complex, PPG, ABP, Detections Performances

In this section, evaluation tests were performed on the last 16 second duration of the alarm records with sampling frequency of 125 Hz, which are modified from Physionet 2015 Challenge training database [17]. There are 3 specific sections: QRS Complex, PPG, ABP, Detection Based Methods Performances (Only ECG Logic, Only PPG/ABP Logic, Main PPG/ABP and Secondary ECG

Logic, Main ECG and Secondary PPG/ABP Logic performances and analysis are explained), METU BEST Methods Performances (METU BEST Method, METU BEST (without ABP signal) Method, METU BEST Generic Method, METU BEST (without ABP signal) Generic Method (for devices unable to measure ABP signals) performances and analysis are explained) performance and analysis are explained). Details of each methods are explained in Section 3.5. Our methods were trained with the training data set. Training dataset features are given in Tables 4.1 and 4.2. All the parameters of our methods were tuned with respect to testing dataset. After tuning our methods were tested with the testing dataset. Testing dataset features are given in Tables 4.1 and 4.2. Our methods were blindly entered to testing dataset. There were 60 records for training dataset (50 false alarm and 10 true alarm) and 60 records for testing dataset (50 false alarm and 10 true alarm) in ASY case. There were 45 records for training dataset (22 false alarm and 23 true alarm) and 45 records for testing dataset (23 false alarm and 22 true alarm) in EBR case. There were 69 records for training dataset (4 false alarm and 65 true alarm) and 70 records for testing dataset (4 false alarm and 66 true alarm) in ETC case. There were 171 records for training dataset (126 false alarm and 45 true alarm) and 172 records for testing dataset (127 false alarm and 45 true alarm) in VTA case. There were 29 records for training dataset (26 false alarm and 3 true alarm) and 29 records for testing dataset (26 false alarm and 3 true alarm) in VFB case. For challenge comparison we used the whole dataset (Training+Testing) for each arrhythmia types.

Table 4.1: Training, Testing and Challenge Datasets Contents [17]

Alarms	Training Set			Testing Set			Challenge Set		
	Total	False	True	Total	False	True	Total	False	True
ASY	60	50	10	60	50	10	120	100	20
EBR	45	22	23	45	23	22	90	45	45
ETC	69	4	65	70	4	66	139	8	131
VTA	171	126	45	172	127	45	343	253	90
VFB	29	26	3	29	26	3	58	52	6

The distribution of the pulsatile waveforms(PPG, ABP) were less than the ECG signals. There were 199 PPG records, with false alarms, and 114 PPG records,

with true alarms for total of all arrhythmia types in the training dataset. There were 115 ABP records, with false alarms, and 56 ABP records, with true alarms total of all arrhythmia types in the training dataset. There were 200 PPG records, with false alarms, and 115 PPG records, with true alarms for total of all arrhythmia types in the testing dataset. There were 116 ABP records, with false alarms, and 58 ABP records, with true alarms in total of all arrhythmia types in the testing dataset.

Table 4.2: Number of PPG/ABP signals in the Training, Testing Datasets [17]

Waveform Groups	Training Set		Testing Set		Challenge Set	
	False	True	False	True	False	True
PPG	113	89	114	89	227	178
ABP	29	31	30	32	59	63
PPG&ABP	86	25	86	26	172	51
Total	229	146	229	146	458	292

#### 4.1.1 QRS Complex, PPG, ABP, Detection Based Methods Performances

In this section we divided our methods with respect to their input signals and evaluate their performances on our given datasets. These methods are: Only ECG Method, Only PPG/ABP Method, Main PPG/ABP and Secondary ECG Method, Main ECG and Secondary PPG/ABP Method. The detailed results of Sensitivity (Sens), Specificity (Spec), Positive Predictivity (+P) and Negative Predictivity (-P) of each arrhythmia type for each method are provided in the following sections. Performance of methods, their detailed results and limitations are explained in the sections below. Arrhythmias thresholds and tolerance limit are given in Table 4.3.

Table 4.3: General Arrhythmias Threshold and Tolerance Limit Parameters

Symbol	Threshold Explanation	Limit
Tolerance	SQ tolerance	%5
$ASY_{th}$	maximum period with with no beats	4 s
$EBR_{th}$	40 beats (maximum number of beats for EBR)	40 bpm
$ETC_{th}$	140 beats (minimum number of beats for ETC)	140 bpm
$VTA_{th}$	100 beats (minimum number of beats for VTA)	100 bpm
$VFB_{th}$	250 (minimum number of beats for VFB)	250 bpm
$beatnm_{min}$	Minimum number of beat	2 bpm
$RRint_{max}$	Maximum period of RR interval	6 s

- Only ECG Method, which was described in Section 3, which was used for false alarm reduction. The methods specific parameters values are given in Table 4.4.

Table 4.4: Only ECG Method Arrhythmia Based Parameters

Parameter	Symbol	Limit
SQ threshold	$SQI_{th}$	0.9
ASY case peak detection threshold constant	$ECC_{th}_{ASY}$	2.5
ASY processing interval	$Window\_length_{ASY}$	5 s
EBR case peak detection threshold constant	$ECC_{th}_{EBR}$	0.625
EBR processing interval	$Window\_length_{EBR}$	16 s
TAC case peak detection threshold constant	$ECC_{th}_{TAC}$	2.5
TAC processing interval	$Window\_length_{TAC}$	16 s
VTA case peak detection threshold constant	$ECC_{th}_{VTA}$	0.625
VTA processing interval	$Window\_length_{VTA}$	16 s
VFB case peak detection threshold constant	$ECC_{th}_{VFB}$	0.625
VFB processing interval	$Window\_length_{VFB}$	16 s

We get results for training and test data as shown in Table 4.5, 4.6.

Table 4.5: Only ECG Method Training Results

Arrhythmia	Sens.(%)	Spec(%)	+P(%)	-P(%)
ASY	80	94.2	72.7	96
EBR	94.7	76	75	95
ETC	95.5	75	98.4	60
VTA	79.3	54.9	26.4	92.9
VFB	100	100	100	100

Table 4.6: Only ECG Method Testing Results

Arrhythmia	Sens.(%)	Spec.(%)	+P(%)	-P(%)
ASY	75	93.7	75	93.8
EBR	92.6	83.3	89.3	88.2
ETC	93.8	40	95.3	33.3
VTA	62.5	54.8	27.8	85
VFB	100	96.4	50	100

There were only 1 – 5% differences between the results of the training and testing sets with respect to arrhythmia types, although the method was tuned with respect to the training set. For comparison with challenge finalists, the method thresholds were tuned with the whole data set (Training + Testing data sets) and our best results are shown as in Table 4.7 with respect to finalists of CinC2015 challenge.

Table 4.7: ONLY ECG Method for Challenge Case and Comparison with CinC2015 Best Results

Alarms	Sens.(%)	Spec.(%)	+P(%)	-P(%)	Best Sens.(%)	Best Spec.(%)
ASY	77.3	94	74	95	100 [46]	97 [46]
EBR	94.4	79	81	94	100 [81]	78 [81]
ETC	95	63	97.3	46	100 [40]	100 [40]
VTA	75	54.1	29	90	90 [40]	71 [40]
VFB	100	98.1	86	100	100 [4]	90 [4]

There were comparable performance results with challenge finalists' results. For EBR and VFB in terms of sensitivity/specificity, we got 94.4%/79% and 100%/98.1% respectively to the challenge case, which are comparable and proper for clinical use (over 90% sensitivity) [33]. We get low results for ASY and VTA due to noise. Because if the method senses noise over the limit flags and go to directly mark the alarm as false. The dataset was prepared for competition; therefore, they add really noisy records which are hard to distinguish. In EBR type of arrhythmia the sensitivity was high enough; however, specificity 79% was not good as the others, because thresholds were optimized to get the highest sensitivity and then we improved specificity. In other words, if we try to increase the specificity percentage more than this the sensitivity start to decrease. The

method fails in ASY provided in Figures 4.1 and 4.2 and in ETC provided in Figures 4.3 and 4.4.

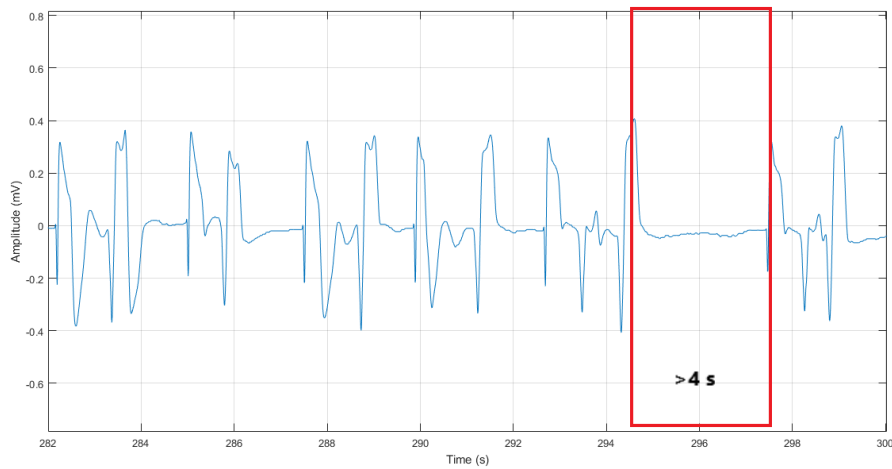


Figure 4.1: Asystole FalsePositive sample(a219l)

In the above asystole alarm FP case Only ECG Method detects the over 4 s period without beat and tagged as it is true alarm. However, as you can see before and after this no beat 4 s period heart beats occurred again, which proved that this was not an asystole. It was probably due to missing beats during ECG recording.

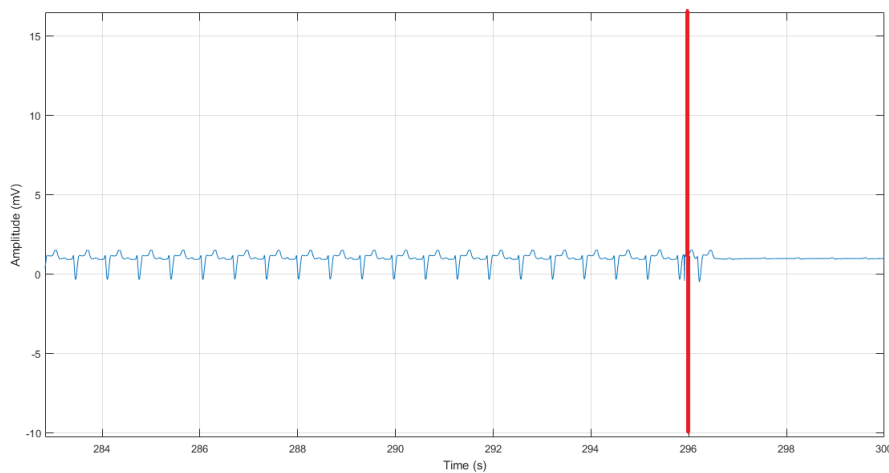


Figure 4.2: Asystole FalseNegative sample(a653l)

In the above asystole alarm FN case Only ECG method could not detect an over 4 s period without beat and tagged as it is false alarm. However,

as you can see that there is a flat line after 296.5 s and it is continuous until the end of the record. Therefore, this is an asystole.

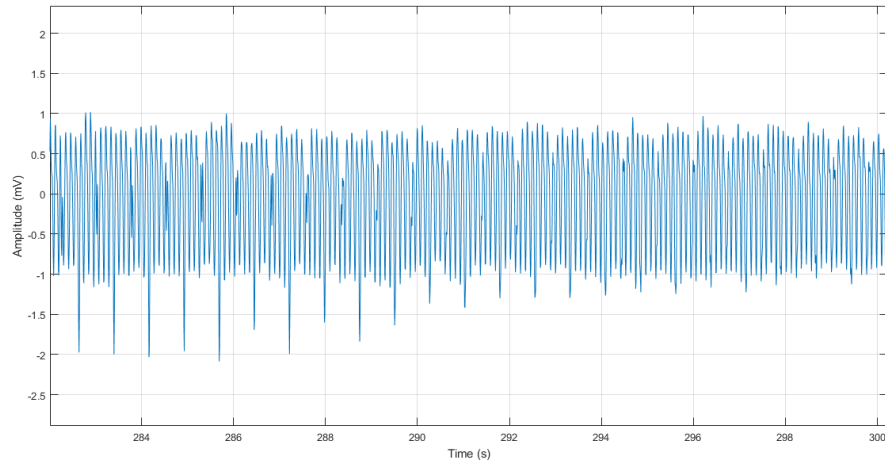


Figure 4.3: Tachycardia FalsePositive sample(t409l)

In the above tachycardia alarm FP case Only ECG Method detects the over 140 beats in 16 s period and tagged as it is true alarm. However, as seen it looks like a continuous noise, probably due to a synchronous motion artifact or noise. It is not possible to remove this type of noises without affecting the original ECG signal with low process power filters. We need to apply mathematical morphology and wavelet transform based filters to remove this type of noises, which need higher processor power than simple filters. Using high processor power algorithms are conflict with our main approaches in this study. In the above tachycardia alarm FN case the signal could not pass the SQ analysis because of the level of noise and artifacts in the signal; therefore, the method tagged as it is false alarm. However, if we analyze the PPG signal of this case, which we did in only PPG/ABP Method, we tagged this alarm as true alarm like the experts.

- When Only PPG/ABP Method, which is described in 3 METHODS section, was used for false alarm reduction. The method specific parameters values are given in Table 4.8.

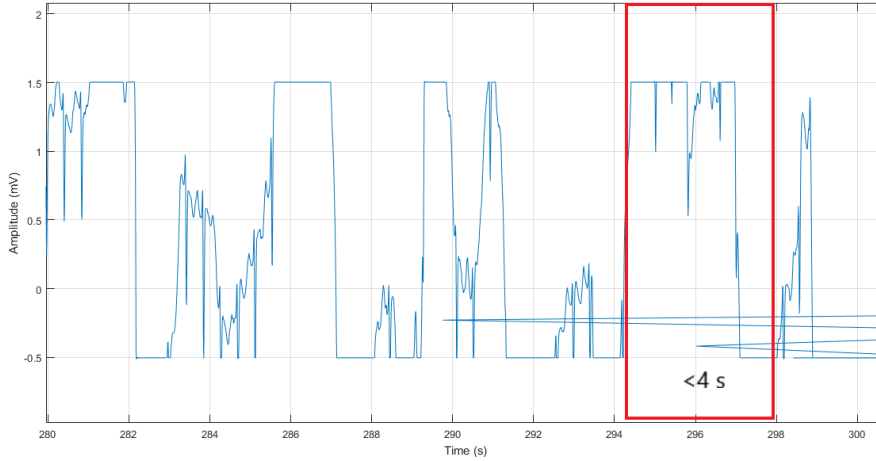


Figure 4.4: Tachycardia FalseNegative sample(t114s)

Table 4.8: Only PPG or ABP Method Arrhythmia Based Parameters

Parameters	Symbol	Limit
SQ threshold	$SQI\_th$	0.9
Minimum required beat number	$beatnm_{min}$	3
Minimum required beat number for EBR	$beatnm\_EBR_{min}$	5
Minimum required beat number for TAC	$beatnm\_TAC_{min}$	17

We got results for training and test data as shown in Table 4.9, 4.10.

Table 4.9: Only PPG/ABP Method Training Results

Alarms	Sens.(%)	Spec.(%)	+P(%)	-P(%)
ASY	100	58.3	38.4	100
EBR	100	65	68.5	100
ETC	85.3	100	100	28.5
VTA	79.3	54.9	26.4	89.5
VFB	100	53.5	11.7	100

Table 4.10: Only PPG/ABP Method Testing Results

Alarms	Sens.(%)	Spec.(%)	+P(%)	-P(%)
ASY	70	54.9	23.4	89.1
EBR	93.6	58.6	77.8	85.3
ETC	84.1	65	97.5	22.5
VTA	79.3	35.2	40.2	76.5
VFB	82	50.4	25.5	94.7

There were around 1 – 30% differences between performance results of training and testing datasets with respect to arrhythmia types, because the whole dataset of PPG and ABP records are not as big as the dataset of ECG signals records, which is explained in Section 4.1. These small dataset was divided in two as training and testing datasets, which also decrease the number of data used in training set for tuning. Moreover, these data sets have not equal number PPG and ABP together, only PPG, only ABP records, which also miss tune our method. For comparison with other finalist we tuned our method with the whole data set (Training + Testing data sets) and our best results are shown in Table 4.11 with respect to finalists of CinC2015 challenge.

Table 4.11: ONLY PPG/ABP Method for Challenge Case

Alarms	Sens.(%)	Spec.(%)	+P(%)	-P(%)	Best Sens.(%)	Best Spec.(%)
ASY	82	54	28.1	93.1	100 [46]	97 [46]
EBR	96	58.1	71	93	100 [81]	78 [81]
ETC	81	75	98	21.4	100 [40]	100 [40]
VTA	83.3	29	22.2	88	90 [40]	71 [40]
VFB	83.3	52	17	96.4	100 [4]	90 [4]

There were lower performance results with respect challenge finalists' results. For VTA and EBR in terms of sensitivity/specificity, it is 83.3%/29% and 96%/58.1% respectively to the challenge case, which are comparable and proper for clinical use. However, we get low results for ASY, ETC and VFB due to generally because of limited number of data includes PPG or ABP signal. Therefore, if the method cannot find any signal, it goes to directly mark the alarm as false. In EBR type of arrhythmia the sensitivity is high enough; however, specificity 58.1% is not good as the others, because thresholds were optimized to get the highest sensitivity then improve specificity. In other words, if we try to increase the specificity percentage more than this the sensitivity start to decrease. The method fails in VTA provided in Figures 4.5 and 4.6, ETC provided in Figures 4.7 and 4.8 and ASY provided in Figures 4.9 and 4.10.

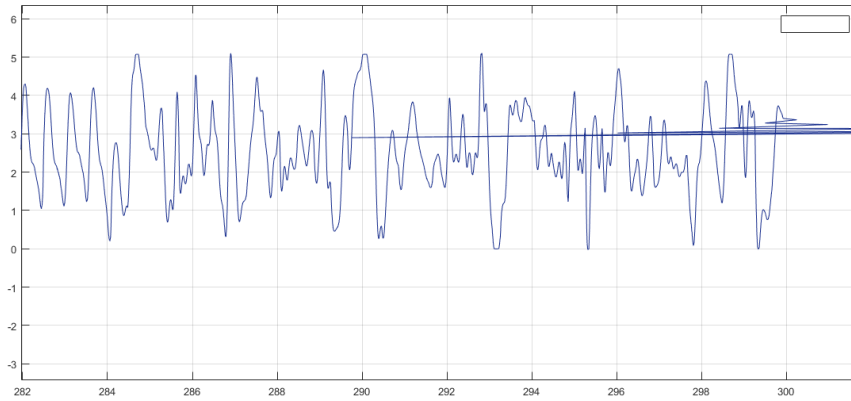


Figure 4.5: Ventricular Tachycardia FalsePositive sample (v100s)

In the above ventricular tachycardia alarm FP case Only PPG/ABP Method detected over 100 beats in 16 s period and tagged as it is true alarm. However, as you can see it looks like that a continuous sinusoidal noise, which is probably due to a synchronous motion artifact or noise is added to the signal. It is not possible to remove noise without affecting the original PPG signal with low process power filters. We need to apply mathematical morphology and wavelet transform based filters to remove this type of noises, which are not proper to use to perform our main approach of this study.

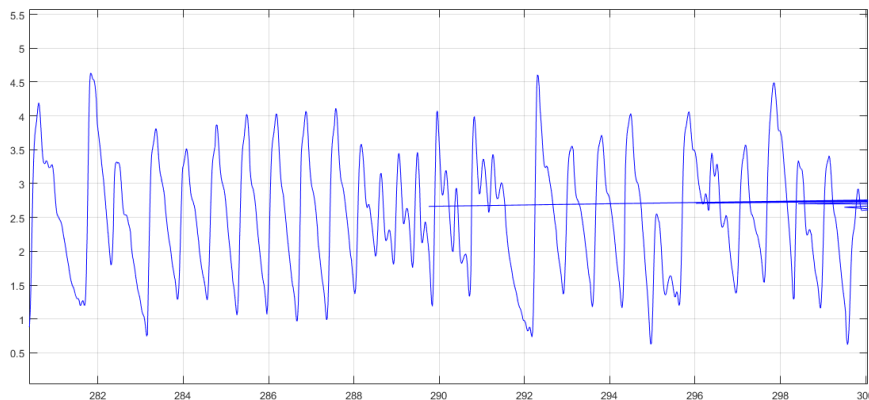


Figure 4.6: Ventricular Tachycardia FalseNegative sample (v206s)

In the above ventricular tachycardia alarm FN case Only PPG/ABP Method could not detect an over 100 heart beats in the 16 s window. Although

our method worked better in 16 s window, if the method particularly investigate the interval between 292 – 300 s it directly tagged it true alarm. without beat and tagged as it is false alarm.

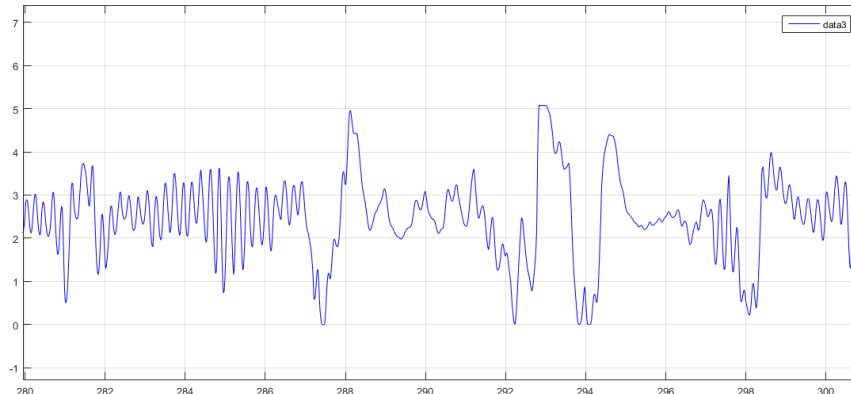


Figure 4.7: Tachycardia FalsePositive sample (t503l)

In the above tachycardia alarm FP case Only PPG/ABP Method detected an over 100 heart beats in the 16 s window and tagged as it is false alarm, although it is a true alarm. In ETC case at low signal amplitude it is hard to distinguish the ECG signal with noise with our low processor power pre-processing methods. We can increase our thresholds to detect this false; however, it affects the overall performance negatively. We need to apply more complex filters and ECG enhancement techniques like mathematical morphology and wavelet transforms, which need more processor power than our pre-processing steps, which conflicts with our main approaches in this thesis.

In the below tachycardia alarm FN case Only PPG/ABP Method detected an over 100 heart beats in the 16 s window and tagged as it is false alarm, although it is a true alarm. We saw that in the last 2 seconds of the alarm there is a low heart rate part, which probably due to weak electrode contact. If we increase the investigation window of our method, we are going to tag this alarm as true. However, it affects the overall performance and numerical efficiency negatively.

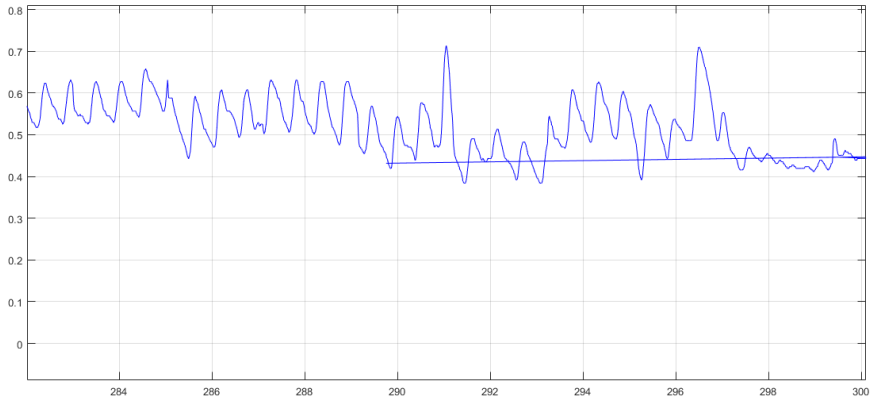


Figure 4.8: Tachycardia FalseNegative sample (t192s)

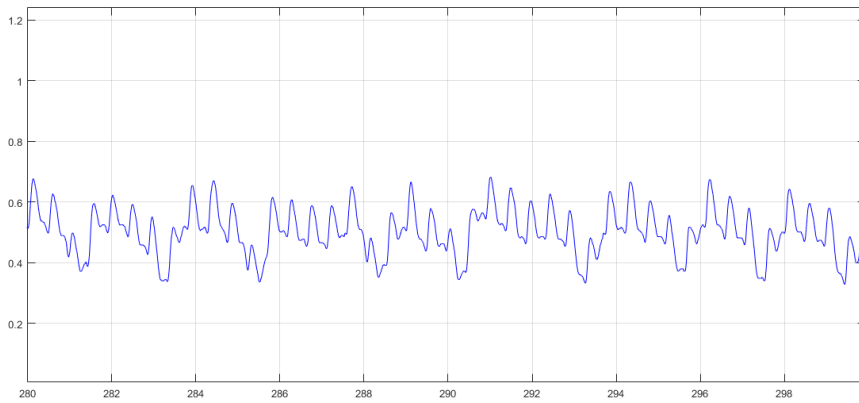


Figure 4.9: Asystole FalsePositive sample (a103l)

In the above asystole alarm FP case Only PPG/ABP Method tagged the signal as noisy because its SQ level is under the  $SQI_{th}$  value. If we decreased the threshold, the alarm would be tagged as false alarm. However, it affects the overall performance and numerical efficiency negatively.

In the below asystole alarm FN case Only ABP/PPG Method could not detect an over 4 s period without beat and tagged as it is false alarm. However, as you can see that there is a no beat interval after the 296.5 s and it is continuous until the end of the record. Therefore, this is an asystole.

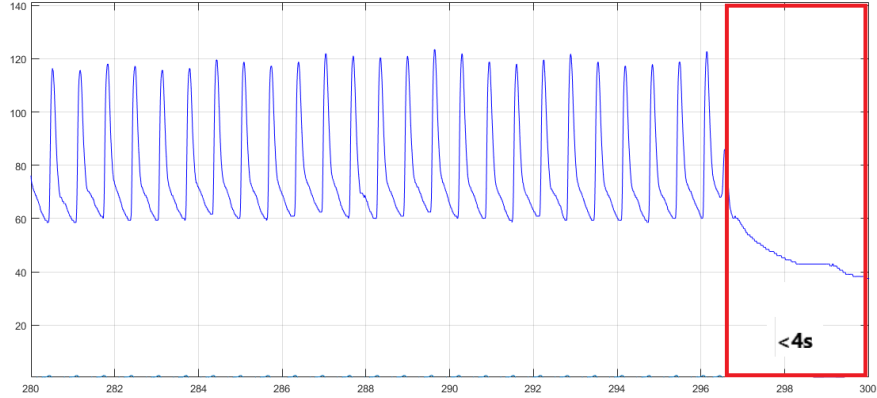


Figure 4.10: Asystole FalseNegative sample (a653l)

- When Main PPG or ABP and Secondary ECG Method, which is described in Section 3, was used for false alarm reduction. The method specific parameters values are given in Table 4.4 and 4.8. We get results for training and testing datasets as shown in Tables 4.12 and 4.13.

Table 4.12: Main PPG/ABP Secondary ECG Method Training Results

Alarms	Sens.(%)	Spec.(%)	+P(%)	-P(%)
ASY	75	70.8	39.1	91.9
EBR	100	72	73.1	100
ETC	78.8	100	100	22.2
VTA	82.8	41.5	22.4	92.2
VFB	100	57.1	7.7	100

Table 4.13: Main PPG/ABP Secondary ECG Method Testing Results

Arrhythmia	Sens.(%)	Spec.(%)	+P(%)	-P(%)
ASY	40	61.4	19	81.8
EBR	88.9	77.8	85.7	82.4
ETC	81.5	60	56.4	20
VTA	76.7	42.3	41.8	77.1
VFB	80	54.2	26.7	92.9

There were 10 – 30 percent differences between results of the training set and testing set because the method was tuned with respect to training set which is not in equal condition with the testing set because of the non-homogeneity of the data features(number data contains PPG+ABP+ECG, PPG/ABP+ECG and only ECG signal). These performance results are low and not eligible to clinical use. In addition, the worst cases of PPG/ABP and ECG data are combined with this method, which is one of the reason for these worst performance results. For comparison with other finalist we tuned our method with the whole data set and our best results for this method are shown in Table 4.14 with respect to finalist of CinC2015 challenge.

Table 4.14: MAIN PPG OR ABP SECONDARY ECG Method for Challenge Case

Alarms	Sens.(%)	Spec.(%)	+P(%)	-P(%)	Best Sens.(%)	Best Spec(%)
ASY	59.1	68	29	88.3	100 [46]	97 [46]
EBR	94	74.4	80	91.4	100 [81]	78 [81]
ETC	80	75	98	21	100 [40]	100 [40]
VTA	83.3	43	26.3	91.3	90 [40]	71 [40]
VFB	83.3	56	18	97	100 [4]	90 [4]

There were the lowest performance results with respect to our methods overall and challenge finalists results. For EBR in terms of sensitivity/specificity, the performance is 94%/74.4% respectively to the challenge case, which are comparable and proper for clinical use. We got very low results for ASY case and average results (around 80% sensitivity) for other arrhythmia types. Because in ASY cases ABP or PPG is not sensitive enough as ECG. In average results group specificity cannot be improved due to the priority of sensitivity in the balance between sensitivity/specificity.

- When Main ECG and Secondary PPG or ABP Method, which is described in 3 METHODS section, was used for false alarm reduction. The method specific parameters values are given in Table 4.15.

We got results for training and test data as shown in Table 4.16, 4.17.

Table 4.15: Main ECG and Secondary PPG or ABP Method Arrhythmia Based Parameters

Parameters	Symbol	Limit
SQ threshold for ASY	$SQI\_th_{ASY}$	0.8
SQ threshold for EBR	$SQI\_th_{EBR}$	0.8
SQ threshold for TAC	$SQI\_th_{TAC}$	0.85
SQ threshold for VTA	$SQI\_th_{VTA}$	0.8
SQ threshold for VFB	$SQI\_th_{VFB}$	0.8

Table 4.16: Main ECG Secondary PPG/ABP Method Training Results

Alarms	Sens.(%)	Spec.(%)	+P(%)	-P(%)
ASY	100	87.5	66.7	100
EBR	100	68	69.2	100
ETC	98.5	75	98.5	75
VTA	86.2	34.5	21.2	92.5
VFB	100	96.4	50	100

Table 4.17: Main ECG Secondary PPG/ABP Method Testing Results

Alarms	Sens.(%)	Spec.(%)	+P(%)	-P(%)
ASY	100	84.6	55.6	100
EBR	92.6	77.8	86.2	87.5
ETC	95.4	40	95.5	50
VTA	70	33.3	36.2	67.3
VFB	100	91.7	71.4	100

There were very similar results while comparing the results of the training and the testing dataset, although the method is tuned with respect to training set. For comparison with other finalist we tuned our method with the whole data set and our best results are shown in Table 4.18 with respect to finalist of CinC2015 challenge.

Table 4.18: MAIN ECG SECONDARY PPG AND ABP Method for Challenge Case

Alarms	Sens.(%)	Spec.(%)	+P(%)	-P(%)	Best Sens.(%)	Best Spec.(%)
ASY	100	94.2	66.7	100	100 [46]	97 [46]
EBR	100	78	79	100	100 [81]	78 [81]
ETC	97.4	63	97.3	50	100 [40]	100 [40]
VTA	83.3	34	24	89.1	90 [40]	71 [40]
VFB	100	94.2	67	100	100 [4]	90 [4]

There were good performance results with respect to our best results for all arrhythmia types. VTA and ETC cases specificity is a little bit low due to noise level. In average results group specificity cannot be improved due to the priority of sensitivity in the balance between sensitivity/specificity. The method worst case is VTA.

#### 4.1.2 METU BEST Methods Performances

In this section we combined our methods which's performances are shown in the previous section and try to get our best performance methods with respect to their usage area. These methods are METU BEST Method, METU BEST (without ABP signal) Method, METU BEST Generic Method, METU BEST (without ABP signal) Generic Method (for devices unable to measure ABP signals).

- When METU BEST Logic Method, which is described in METHODS section, was used for false alarm reduction, we got results for training and testing datasets as shown in Table 4.19, 4.20.

Table 4.19: METU BEST Method Training Results

Alarms	Sens.(%)	Spec.(%)	+P(%)	-P(%)
ASY	100	87.5	66.6	100
EBR	100	72	73.1	100
ETC	98.5	75	98.5	75
VTA	86.2	34.5	21.1	92.5
VFB	100	96.4	50	100

Table 4.20: METU BEST Method Testing Results

Alarms	Sens.(%)	Spec.(%)	+P(%)	-P(%)
ASY	100	78.8	47.6	100
EBR	88.8	77.7	85.7	82.4
ETC	96.9	40	95.5	50
VTA	70	33.3	36.2	67.2
VFB	100	91.7	71.4	100

The method specific parameters values are given in Table 4.21.

Table 4.21: METU BEST Method Arrhythmia Based Parameters

Parameters	Symbol	Limit	Method
SQ threshold for ASY	$SQI\_th_{ASY}$	0.75	ECG + PPG
SQ threshold for EBR	$SQI\_th_{EBR}$	0.8	PPG/ABP + ECG
SQ threshold for ETC	$SQI\_th_{ETC}$	0.95	ECG + PPG
SQ threshold for VTA	$SQI\_th_{VTA}$	0.8	ECG + PPG/ABP
SQ threshold for VFB	$SQI\_th_{VFB}$	0.8	ECG + PPG/ABP

There were very similar performance results when you compare the results of the training set and the testing set, although the method was tuned with respect to training set. For comparison with other finalist we tuned our method with the whole data set and our best results as shown in Table 4.22 with respect to finalist of CinC2015 challenge.

Table 4.22: METU BEST Method for Challenge Case

Alarms	Sens.(%)	Spec.(%)	+P(%)	-P(%)	Best Sens.(%)	Best Spec.(%)
ASY	100	86	61.1	100	100 [46]	97 [46]
EBR	100	78	79	100	100 [81]	78 [81]
ETC	98.2	63	97.4	71.4	100 [40]	100 [40]
VTA	83.3	43	26.3	91.3	90 [40]	71 [40]
VFB	100	98.1	86	100	100 [4]	90 [4]

Weakest part of the method is VTA in terms of sensitivity/specificity like 83.3%/43% respectively to the challenge case, because of limited number of data includes PPG or ABP pulsatile signals, which are more sensitive and less noisy in VTA cases due to their measurement location respect to heart, where the level of noises are low compared to the original heart signals. In the overall results shown Table 4.22 it is better than the challenge finalists results.

Moreover, all the above results are computed from fuzzy logic methods, which were specifically tuned for each arrhythmia type because we know the type of arrhythmia of each alarm data. If we want to implement these methods in an ICU device, we need to optimize these methods with generic thresholds for all arrhythmia types. The training and testing results for Main ECG and Secondary PPG/ABP Method (Generic version of METU BEST Method) with  $SQI_t h = 0.8$  threshold and 10 s window (which is

described in the Association for the Advancement of Medical Instrumentation (AAMI) regulations as alarm must be raised within 10 seconds of an arrhythmia [33] alarm must be raised within 10) until the alarms happens shown in Table 4.23, 4.24.

Table 4.23: METU BEST Generic Method Training Results

Alarms	Sens.(%)	Spec.(%)	+P(%)	-P(%)
ASY	100	87.5	66.6	100
EBR	100	68	69.2	100
ETC	96.9	79	98.4	60
VTA	86.2	34.5	21.2	92.5
VFB	100	96.4	50	100

Table 4.24: METU BEST Generic Method Testing Results

Alarms	Sens(%)	Spec(%)	+P(%)	-P(%)
ASY	100	84.6	66.6	100
EBR	92.6	77.8	86.2	87.5
ETC	93.8	40	95.3	33.3
VTA	70	33.3	36.2	67.3
VFB	100	91.7	71.4	100

- However, except intensive care patients, generally patients in other departments use ICUs without measuring ABP because it is an expensive treatment and not easy to implement to the patient. Therefore, we modified METU BEST Method to become more implementable in clinical use and we got METU BEST (without using ABP signal) Method and if the method cannot find any signal it goes to directly mark the alarm as false. The method specific parameters values are given in Table 4.25.

Table 4.25: METU BEST (without using ABP signal) Method Arrhythmia Based Parameters

Parameters	Symbol	Limit	Method
SQ threshold for ASY	$SQI\_th_{ASY}$	0.8	ECG + PPG
SQ threshold for EBR	$SQI\_th_{EBR}$	0.95	ECG + PPG
SQ threshold for ETC	$SQI\_th_{ETC}$	0.95	ECG + PPG
SQ threshold for VTA	$SQI\_th_{VTA}$	0.85	ECG + PPG
SQ threshold for VFB	$SQI\_th_{VFB}$	0.95	ECG + PPG

We get results for training and test data as shown in Table 4.26, 4.27.

Table 4.26: METU BEST (without using ABP signal) Method Training Results

Alarms	Sens.(%)	Spec.(%)	+P(%)	-P(%)
ASY	100	87.5	66.6	100
EBR	94.7	68	69.2	94.4
ETC	98.5	75	98.5	75
VTA	86.2	32.4	20.7	92
VFB	100	96.4	50	100

Table 4.27: METU BEST (without using ABP signal) Method Testing Results

Alarms	Sens.(%)	Spec.(%)	+P(%)	-P(%)
ASY	100	84.6	55.5	100
EBR	92.6	72.2	83.3	86.6
ETC	98.5	40	95.5	66.7
VTA	71.6	33.3	36.8	68.5
VFB	100	91.7	71.4	100

There were very similar results when you compare the training set and testing dataset, although the method was tuned with respect to training dataset. For comparison with other other finalist we tuned our method with the whole data set and our best results as shown in Table 4.28 with respect to finalist of CinC2015 challenge.

Table 4.28: METU BEST (without using ABP signal) Method for Challenge Case

Alarms	Sens.(%)	Spec.(%)	+P(%)	-P(%)	Best Sens.(%)	Best Spec.(%)
ASY	100	85.3	58.3	100	100 [46]	97 [46]
EBR	93.5	72.1	78.2	91.2	100 [81]	78 [81]
ETC	98.2	63	97.4	71.4	100 [40]	100 [40]
VTA	83.3	32	23	89	90 [40]	71 [40]
VFB	100	96.2	75	100	100 [4]	90 [4]

Weakest part of the method is again VTA in terms of sensitivity/specificity like 83.3%/32% respectively to the challenge case, because of limited number of data includes PPG or ABP pulsatile signals, which are more sensitive and less noisy in VTA cases due to their measurement location respect to heart, where the level of noises are low compared to the original heart signals. In the overall results shown 4.22, it is better than the challenge finalists results. When you compare it with the METU BEST Method, results are similar The differences between their performance results are change between 1 – 5 %. Because we tuned the thresholds to optimize and get the highest sensitivity then improve specificity our best specificity percentages always smaller than sensitivity. In other words, if we try to increase the specificity percentage more than this the sensitivity start to decrease. The method weakest part is ETC and the failed records in ETC provided in Figure 4.11 and Figure 4.12.

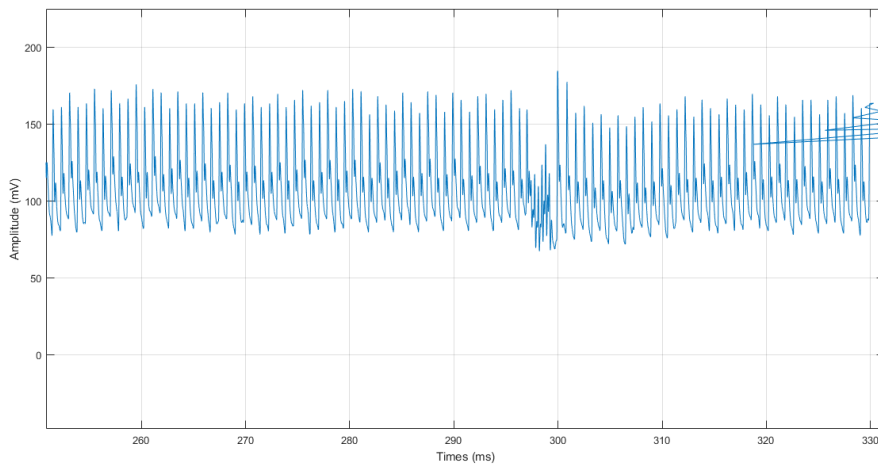


Figure 4.11: Ventricular Tachycardia FalsePositive sample(a3851)

Moreover, all the above results are computed from fuzzy logic methods, which were specifically tuned for each arrhythmia type because we know type of arrhythmia of each alarm data. If we want to implement these methods in an ICU device for general arrhythmia detection, we need to optimize these methods with generic thresholds for all arrhythmia types. The training and testing results for Main ECG and Secondary PPG Method (Generic version of METU

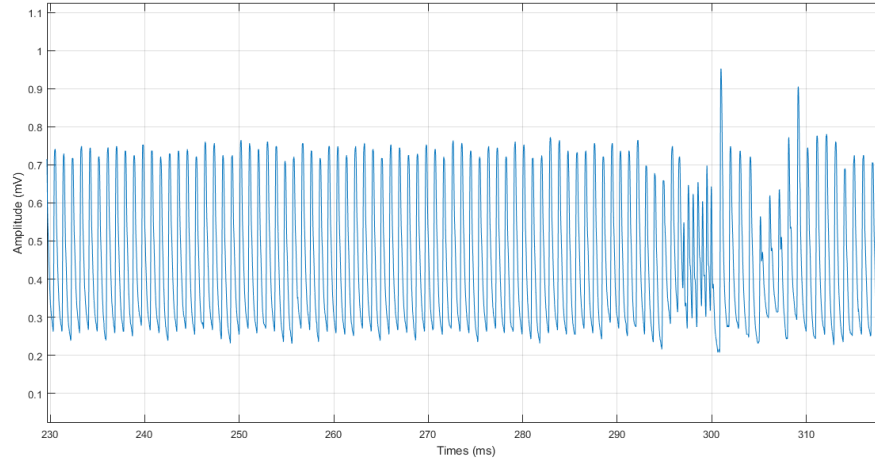


Figure 4.12: Ventricular Tachycardia TrueNegative sample(v1111)

BEST (without using ABP signal) Method) with 0.7 threshold and 10 s window until the alarms happens shown in Table 4.29, 4.30.

Table 4.29: METU BEST (without using ABP signal) Generic Method Training Results

Alarms	Sens.(%)	Spec.(%)	+P(%)	-P(%)
ASY	100	87.5	66.7	100
EBR	94.7	68	69.2	94.4
ETC	96.9	75	98.5	60
VTA	86.2	32.4	20.7	92
VFB	100	96.4	50	100

Table 4.30: METU BEST (without using ABP signal) Generic Method Testing Results

Alarms	Sens.(%)	Spec.(%)	+P(%)	-P(%)
ASY	100	78.8	47.6	100
EBR	92.6	77.8	86.2	87.5
ETC	95.4	40	95.4	40
VTA	71.7	33.3	36.8	68.5
VFB	100	95.8	83.3	100

Table 4.31: METU BEST (without using ABP signal) Generic Method Results in Challenge Case

Alarms	Sens.(%)	Spec.(%)	+P(%)	-P(%)	Best Sens.(%)	Best Spec.(%)
ASY	100	85.3	58.3	100	100 [46]	97 [46]
EBR	93.5	72.1	78.2	91.2	100 [81]	78 [81]
ETC	98.2	63	97.4	71.4	100 [40]	100 [40]
VTA	83.3	32	23	89	90 [40]	71 [40]
VFB	100	96.2	75	100	100 [4]	90 [4]

When Main PPG or ABP and Secondary ECG Logic with 0.8 threshold Method, which is described in Chapter 3, was used for false alarm reduction. There were good performance results with respect to our best results for VTA and EBR in terms of sensitivity/specificity like 83.3%/43% respectively to the challenge case. We got low results for ASY case and average results (around 80% sensitivity) for other arrhythmia types. Because in ASY cases ABP or PPG is not sensitive enough as ECG. In average results group specificity can not be improved due to the priority of sensitivity in the balance between sensitivity/specificity.

#### 4.1.3 Our Best Methods vs Cinc2015 Finalists Performances

The detailed arrhythmia type based comparison, which's main criteria is sensitivity and secondary criteria is specificity, of our best result with CinC2015 finalist are shown below:

- **Asystole:** The sensitivity and specificity of CinC2015 finalist' methods and our methods for asystole case are given in Table 4.32.

Table 4.32: Asystole Case Comparison

Rank	Authors	Sens.(%)	Spec.(%)
1	V. Kresteva et al. [46]	100	97
2	F. Plesinger et al. [61]	100	97
3	<b>METU BEST Method</b>	100	86
4	<b>METU BEST (without ABP signal) Method</b>	100	85.3
5	S. Ansari et al. [4]	94	82
6	C. Daluwatte et al. [17]	91	86
7	W. Zong et al. [81]	89	63
8	L. M. Eerikainen et al. [28]	85	88
9	P. Couto et al. [18]	78	94
10	C. H. Antink et al. [40]	56	94
11	Average	81.2	79.3

In asystole case the average performance of sensitivity/specificity are 81.2%/79.3%. METU BEST Method and METU BEST (without using ABP signal) Method performances are 100%/86% and 100%/85.3%, which are over average performance and they are third and fourth in the ranking in Figure 4.13.

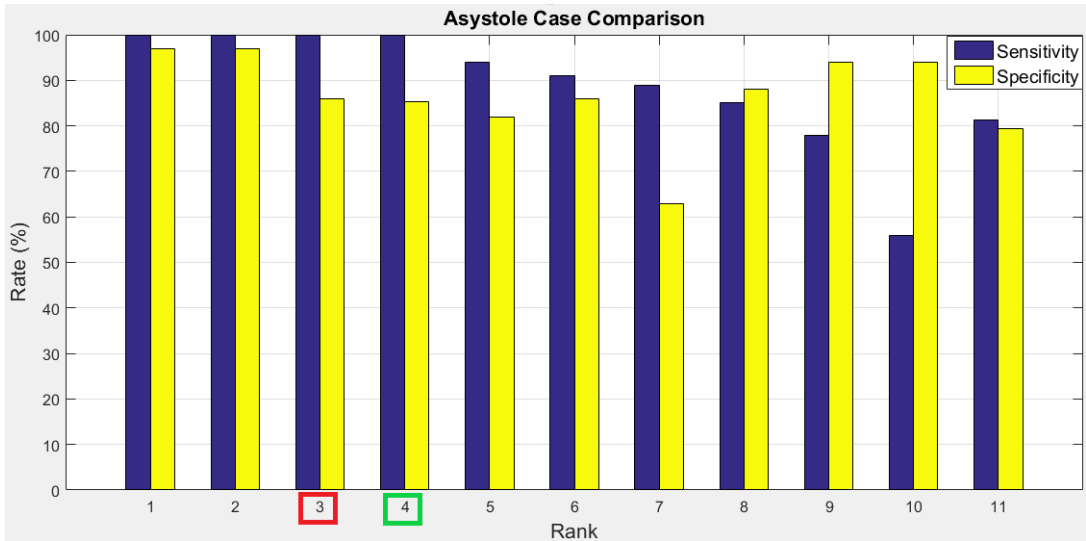


Figure 4.13: Asystole Case Comparison

- **Bradycardia:** The sensitivity and specificity of Cinc2015 finalist's methods and our methods for bradycardia case are given in Table 4.33.

Table 4.33: Bradycardia Case Comparison

Rank	Authors	Sens.(%)	Spec.(%)
1	<b>METU BEST Method</b>	100	78
2	W. Zong et al. [81]	100	78
3	F. Plesinger et al. [61]	100	72
4	C. H. Antink et al. [40]	100	57
5	V. Kresteva et al. [46]	98	86
6	C. Daluwatte et al. [17]	98	44
7	L. M. Eerikainen et al. [28]	96	79
8	P. Couto et al. [18]	95	66
9	<b>METU BEST (without ABP signal) Method</b>	93.5	72.1
10	S. Ansari et al. [4]	77	86
11	Average	87	65.3

In bradycardia case the average performance of sensitivity/specificity are 87%/65.3%. METU BEST Method and METU BEST (without using ABP signal) Method performances are 100%/78% and 93.5%/72.1%, which are over average performance and they are first and ninth in the ranking in Figure 4.14.

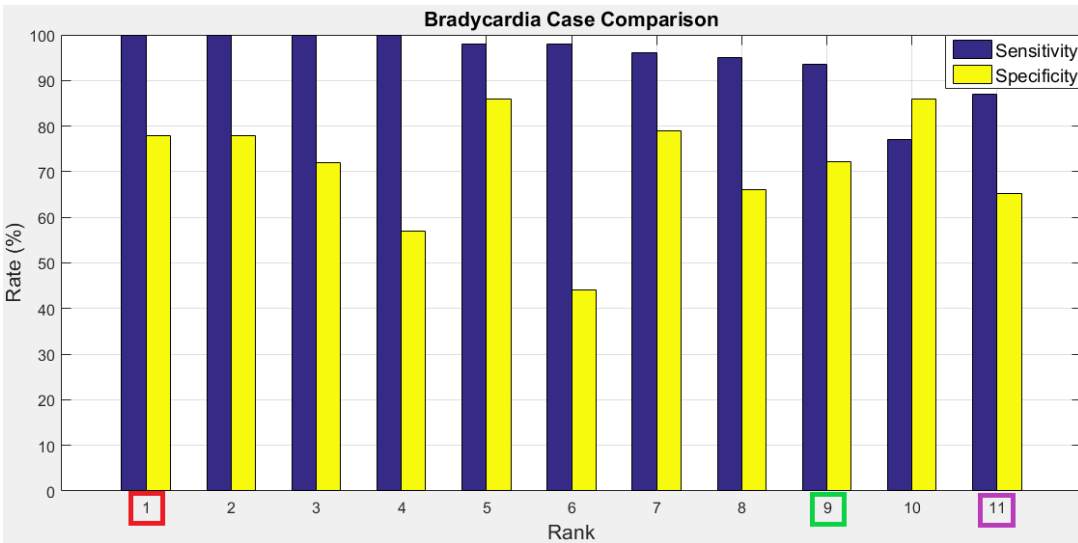


Figure 4.14: Bradycardia Case Comparison

- **Tachycardia:** The sensitivity and specificity of CinC2015 finalist's methods and our methods for tachycardia case are given in Table 4.34.

Table 4.34: Tachycardia Case Comparison

Rank	Authors	Sens.(%)	Spec.(%)
1	C. H. Antink et al. [40]	100	100
2	P. Couto et al. [18]	100	80
3	L. M. Eerikainen et al. [28]	99	99
4	V. Kresteva et al. [46]	99	89
5	<b>METU BEST Method</b>	98.2	63
6	<b>METU BEST (without ABP signal) Method</b>	98.2	63
7	W. Zong et al. [81]	98	80
8	S. Ansari et al. [4]	98	60
9	F. Plesinger et al. [61]	97	100
10	C. Daluwatte et al. [17]	96	78
11	Average	89.4	73.8

In tachycardia case the average performance of sensitivity/specificity are 89.4%/73.8%. METU BEST Method and METU BEST (without using ABP signal) Method performances are 98.2%/63% and 98.2%/63%, which are over average performance and they are first and ninth in the ranking in Figure 4.15.

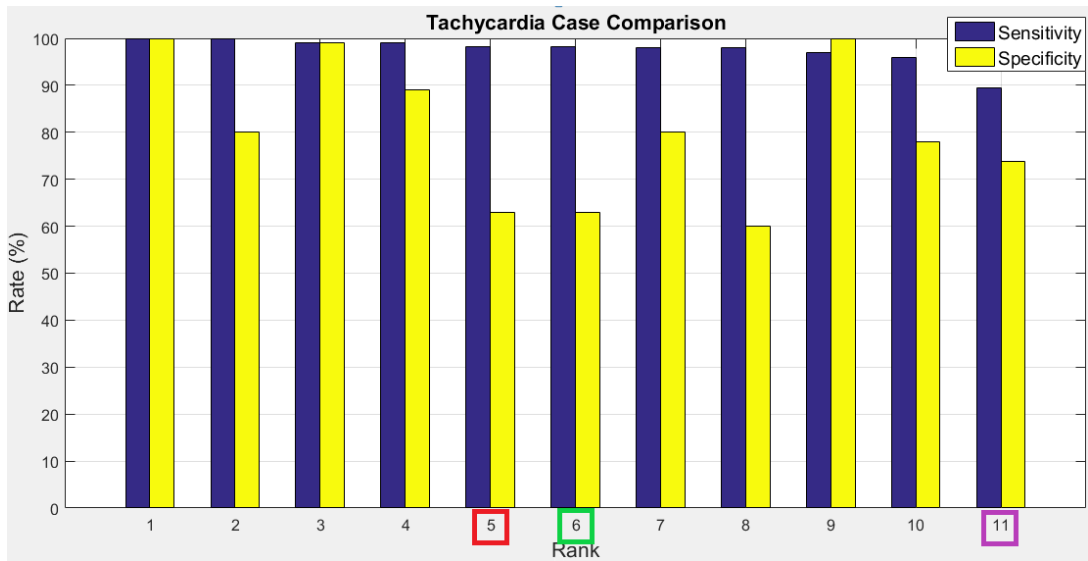


Figure 4.15: Tachycardia Case Comparison

- **Ventricular Tachycardia:** The sensitivity and specificity of CinC2015 finalist's methods and our methods for ventricular-tachycardia case are given in Table 4.35.

Table 4.35: Ventricular-Tachycardia Case Comparison

Rank	Authors	Sens.(%)	Spec.(%)
1	C. H. Antink et al. [40]	90	71
2	F. Plesinger et al. [61]	85	84
3	L. M. Eerikainen et al. [28]	84	74
4	W. Zong et al. [81]	84	43
5	<b>METU BEST Method</b>	83.3	43
6	<b>METU BEST (without ABP signal) Method</b>	83.3	32
7	V. Kresteva et al. [46]	82	71
8	C. Daluwatte et al. [17]	80	82
9	S. Ansari et al. [4]	78	85
10	P. Couto et al. [18]	69	95
11	Average	74.4	55

In tachycardia case the average performance of sensitivity/specificity are 74.4%/55%. METU BEST Method and METU BEST (without using ABP signal) Method performances are 83.3%/43% and 83.3%/32%, which are over average performance and they are fifth and sixth in the ranking in Figure 4.16.

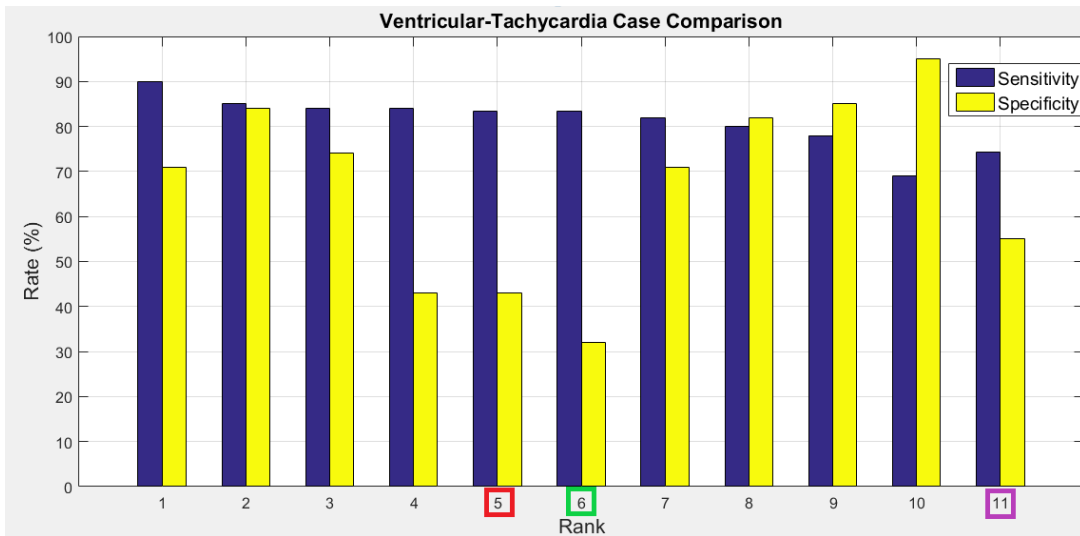


Figure 4.16: Ventricular-Tachycardia Case Comparison

- **Ventricular-Flutter/Fibrillation:** The sensitivity and specificity of Cinc2015 finalist's methods and our methods for ventricular-flutter/fibrillation case are given in Table 4.36.

Table 4.36: Ventricular-Flutter/Fibrillation Case Comparison

Rank	Authors	Sens.(%)	Spec.(%)
1	<b>METU BEST Method</b>	100	98.1
2	<b>METU BEST (without ABP signal) Method</b>	100	96.2
3	S. Ansari et al. [4]	100	90
4	V. Kresteva et al. [46]	100	87
5	C. Daluwatte et al. [17]	100	83
6	P. Couto et al. [18]	89	96
7	W. Zong et al. [81]	89	78
8	L. M. Eerikainen et al. [28]	75	94
9	F. Plesinger et al. [61]	67	100
10	C. H. Antink et al. [40]	67	92
11	Average	80.6	83.1

In ventricular-flutter/fibrillation case the average performance of sensitivity/specificity are 80.6%/83.1%. METU BEST Method and METU BEST (without using ABP signal) Method performances are 100%/98.1% and 100%/96.2%, which are over average performance and they are first and second in the ranking in Figure 4.17.

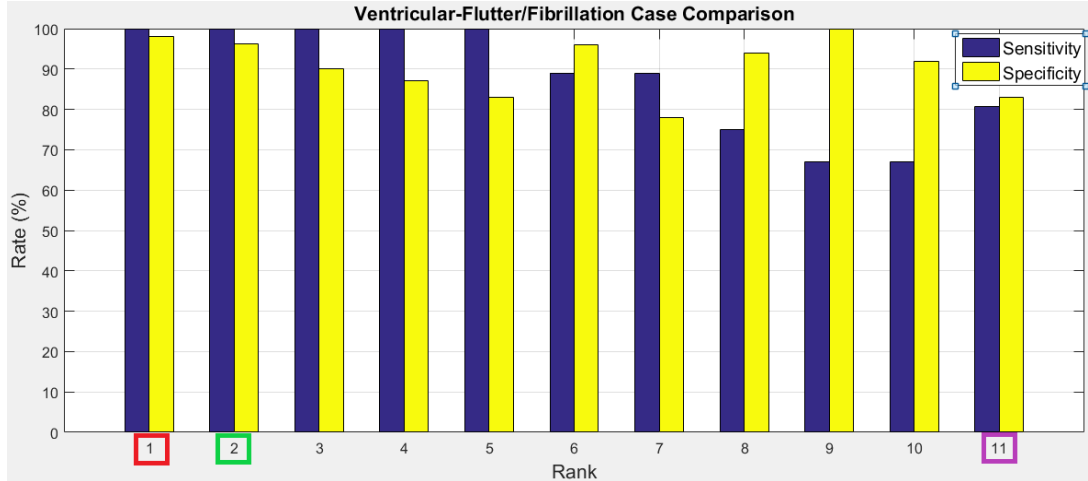


Figure 4.17: Ventricular-Flutter/Fibrillation Case Comparison

## 4.2 Limitations

- Annotations of the alarms were made by individuals who were not involved in the creation of the ECG arrhythmia detection methods, which were used

in the ICU bedside monitors. Therefore, these ECG alarms were annotated using clinical criteria, and our alarm definitions may not be completely consistent with the logic used by the monitoring methods in some cases which decrease the sensitivity and specificity rate of our methods.

- Although heart beat detection on ECG signals was helpful in eliminating stage of false ASY and EBR alarms, heart beat detection on PPG and ABP signals had a significant role in ETC, VTA, VFB alarms because of the high noise levels in the ECG signals. The dataset, which we used in research have a limited number of PPG and ABP records (details are shown in Table 4.2), which decreased our performances on our methods. Therefore, a larger database is needed with more PPG and ABP signals.
- The annotations for the “ventricular tachycardia” alarm category in particular were limited, such as there are total 8 false VTA alarms in the whole dataset, which means that only 4 records were used for tuning, and then this affected our training stage for parameters tuning negatively.
- The monitor method fired an alarm upon the detection of rapid ventricular tachycardia. The clinical annotator labeled rapid ventricular tachycardia as “ventricular tachycardia” and the ventricular fibrillation annotation was reserved for asynchronous ventricular electrical activity. The database did not show any true ventricular fibrillation events. This annotation methodology affects the performance of the PPG signal quality method, ppgSQL.m function.

## CHAPTER 5

### DISCUSSION AND CONCLUSIONS

This chapter starts with a summary of works done followed with the discussion of improvements and limitations end with the conclusion and future works could be implemented in this thesis.

#### 5.1 Summary and Discussions

False arrhythmia alarms of ICUs have been ranked number in the 10 lists of health technology hazards every year, since 2012 (by the ECRI Institute in details [75]). To reduce these alarms, efforts in two aspects are made: a) clinical usage aspect, b) technology aspect. In clinical usage aspect, clinicians, nurses should be aware of the fact that these devices are utilized them only as a tool in the overall assessment of patients conditions and their improper configurations and operations can be resulted negative (adverse) event in hospital. Educations and trainings are useful for proper operation (well integration with other procedures and requirements of patient care), and avoid misconfiguration or false alarms because of the current alarm systems. In technology aspect, especially QRS detection is a mature field since most of the improvements of false alarm reductions are tried and tested on ECG and other waveforms recordings, which are measured from the heart. Their performances are usually above 99% with different amount of computational efforts [11]. However, in literature, only overall results (sensitivity, specificity, etc. parameters) are provided for detection rates without the timings and processor power requirements. Additionally, many of algorithms are not implemented on a standalone device, which makes usability of these algorithms questionable.

In this study, firstly, we pre-processed all signal with specific filters, which are explained in Section 3.1. For QRS detection a modified version of Hilbert transform and a 1st differential method that is known to be successful and numerically efficient (explained in Section 3.2), was implemented and results were compared. For PPG detection Physionet open-source algorithms (ppgSQI.m) were used to process the PPG signal. The process starts with a FIR bandpass filter applied to the PPG signal followed with a quantile function to convert PPG signal to be compliant with wabp.m function for onset point detection. The R-R intervals were calculated from these onset points. Then the ppgSQI.m algorithm was used to estimate the signal quality index to give the decision the alarm was true or false (details are explained in Section 3.3). For ABP detection Physionet open-source algorithms (wabp.m, jSQI.m) were used to process the ABP signal. The process starts with a FIR bandpass filter applied to the ABP signal followed wabp.mat function for computing onset points. The R-R intervals calculated from these onset points. Then the jSQI.m algorithm was used to estimate the signal quality index to give the decision the alarm was true or false (details are explained in Section 3.4).

The signal integration part is based on fuzzy logic with combination of different types signals results and decision rules. Four type of fuzzy logic methods implemented with regard to mix ECG, PPG, ABP signals processing results. These are "Only ECG" Algorithm, which uses only the ECG signal as input and gives output, "Only PPG or Only ABP" Algorithms, which use only PPG or ABP signal as the input and gives the output, "Main PPG" or Main ABP-Secondary ECG" Algorithms, which use firstly PPG or ABP signal and give output with respect to these signals, and if these signals are not available, or their SQ levels are under the thresholds, ECG signal is used as the secondary input, "Main ECG-Secondary PPG or ABP" Algorithms, which use firstly ECG signal as an input and give output with respect to it, and if these signals are not available, or its SQ level is under the thresholds, PPG or ABP signal is used as input. All these methods were trained with training dataset and tested with testing dataset, which are explained in 4.1. The performance results of these methods, are shown that although for QRS and arrhythmia detection, ECG signals are the most reliable signals among the cardiac signals, combination of ECG, ABP, PPG

signals in QRS detection and especially in false arrhythmia alarm reduction give better performance than processing these signals individually. Performance results of them are shown in Section 4.1.1. After evaluation of these methods with respect to Sens, Spec, +P, -P, These methods results also , we compared them with the finalists results in CinC 2015, which are shown in 4.1.1, and we have comparable results. In other words, in some arrhythmia types the performances are better then CinC 2015 finalists performances, in other arrhythmia types the performance are lower than CinC 2015 finalists performances. In order to improve our performance compared with the CinC2015 finalists performances, we combined these methods and got our best performance method, which is named as METU BEST Method. METU BEST Logic, is ranked at the third in ASY case, the first in EBR case, the fifth in ETC case, the fifth in VTA case, the first in VFB case compared to the top 10 methods (our best methods are included) of the CinC2015 challenge finalists according to mainly sensitivity, secondarily specificity. One step further because the ABP signal which is rarely measured from patients, using it in our method limited our method implementation in ICU devices. Therefore, we modified our method like main decider as ECG secondary decider as PPG and it is named as METU BEST (without using ABP) Method. In this way the method increase its usability. When we compared its performance with the CinC2015 finalists performances, METU BEST (without using ABP) Method, is ranked at the third in ASY case, the ninth in EBR case, the fifth in ETC case, the sixth in VTA case, the second in VFB case compared to the top 10 methods (our best methods are included) of the CinC2015 challenge finalists according to mainly sensitivity, secondarily specificity. To achieve a generic arrhythmia alarms detection method, we found generic thresholds for all arrhythmia types and got comparable by modifying METU BEST Logic and METU BEST (Commercial) Logic, which is explained in Section 4.1. We named them as METU BEST Generic Method and METU BEST (without using ABP) Generic Method. It does not have clinically reliable results as METU BEST Generic Method or METU BEST (without using ABP) Generic Method; however, it can be useful for early emergency case detection and continuous tracking for patients who have arrhythmia risks.

## 5.2 Conclusions

The study described in this thesis demonstrated that false alarm suppression methods by using only one or more extra channels of non-ECG information (ABP, PPG or respiration waveform) and fusing them with some fuzzy logic methods allowed for the identification and suppression of the majority of false critical ECG arrhythmia alarms (asystole, bradycardia, tachycardia, ventricular tachycardia, ventricular fibrillation/flutter). These approaches demonstrated the potential of using multiple physiologic waveforms for reducing false alarms in the clinical setting. The best performances of our METU best methods: METU BEST Method, METU BEST (without using ABP) Method have really good performances compared to CinC finalist. METU BEST Method, is ranked at the third ( $Sens/Spec = \%100/\%86$ ) in ASY case, the first ( $Sens/Spec = \%100/\%78$ ) in EBR case, the fifth ( $Sens/Spec = \%98.2/\%63$ ) in ETC case, the fifth ( $Sens/Spec = \%83.3/\%43$ ) in VTA case, the first ( $Sens/Spec = \%100/\%98.1$ ) in VFB case compared to the top 10 methods (our best methods are included) of the CinC2015 challenge finalists according to mainly sensitivity, secondarily specificity. METU BEST (without using ABP) Method, is ranked at the fourth ( $Sens/Spec = \%100/\%85.3$ ) in ASY case, the ninth ( $Sens/Spec = \%93.5/\%72.1$ ) in EBR case, the fifth ( $Sens/Spec = \%98.2/\%63$ ) in ETC case, the sixth ( $Sens/Spec = \%83.3/\%32$ ) in VTA case, the second ( $Sens/Spec = \%100/\%96.2$ ) in VFB case compared to the top 10 methods (our best methods are included) of the CinC2015 challenge finalists according to mainly sensitivity, secondarily specificity. One step further because the ABP signal which is rarely measured from patients, using it in our method limited our method implementation in ICU devices. especially in retaining true alarms while rejecting the false ones. However, due to comparison with other methods this method only tested with 750 alarm records in the comparison with the challenge case and 375 for testing, 375 for training alarm records in the training and testing cases (details are shown in Section 4). Our best methods were modified and specialized with respect their usage area, such as METU BEST Generic Method was developed for clinical use in ICU patient monitors, METU BEST (without using ABP) Generic Method was developed for clinical use in patient monitors, which does

not have ABP measuring option. METU best methods and generic ones have very similar performances only a %1 – 2 changes between them regards to the arrhythmia type. In the ETC and VTA case, our best performances are not good as others performances in CinC2015. They are in the middle level performance with respect to others performances in CinC2015. In some VTA alarm cases, which is the hardest case to classify accurately, in the dataset, because the signals looking more normal and heart rate is very close the threshold limit, it is not possible to detect alarm with not effect the overall performance of our low processor cost algorithms. We may need to use mathematical morphology based neural network approaches, which need more processor power and are explained in Section 2.2. In conclusion, we have presented our effective methods to reduce false critical alarms using waveforms ECG, PPG, and/or ABP signals and modified versions of them for specific usage areas. They are practical on account of its real-time dynamic processing mechanism and computational efficiency.

### 5.3 Recommendations for Future Work

This section summarizes some future research ideas related to the study presented in this thesis. Some of the future work suggestions are:

- A more detailed study on VTA with a bigger dataset, could be increase our sensitivity and specificity rates on VTA (now 83.3%) over 90% which makes our method more reliable to use in clinics (ICUs).
- A more detailed study could be carried out that using wavelet transform for filtering stage and then using Hilbert transform and adaptive thresholding for peak detection as computing techniques for QRS is going to give better and more robust results, although it increase our computational cost.
- A more detailed study could be carried out that using mathematical morphology for QRS detection for VTA cases increase the sensitivity and specificity rates [40] and than using adaptive thresholding for peak detection as computing techniques for QRS is going to give better and more robust results, although it increase our computational cost.

- A bigger database and also pre-clinical test areas, where we can implement our methods parallel to commercial ones on patients to improve the robustness of our method, can improve our results due to the nature of fuzzy logic. Moreover, Our method uses PPG and ABP signals as seconder decision maker which has no difference with using only ECG for evaluation if the data does not contain PPG and ABP signals or contains one of them only, which is an another problem with our database. This inhibits the real performance of our method, because the our decision method tags the alarm as false, if the signal quality level of the waveform is over the threshold.
- Advances in technology have led to much change in the way we collect, store and diagnose ECG signals, especially the use of mobile phones to implement the clinical routine of ECG analysis into everyday life. Therefore, our method need to be optimized to be compliant in terms of memory and processor power of wearable, implantable devices or tele-medicine systems.

## REFERENCES

- [1] Estimation of QRS Complex Power Spectra for Design of a QRS Filter. *IEEE Transactions on Biomedical Engineering*, BME-31(11):702–706, 1984.
- [2] A. Aboukhalil, L. Nielsen, M. Saeed, R. G. Mark, and G. D. Clifford. Reducing false alarm rates for critical arrhythmias using the arterial blood pressure waveform. *Journal of Biomedical Informatics*, 41(3):442–451, 2008.
- [3] V. X. Afonso, W. J. Tompkins, T. Q. Nguyen, and S. Luo. ECG beat detection using filter banks. *IEEE Transactions on Biomedical Engineering*, 46(2):192–202, 1999.
- [4] S. Ansari, A. Belle, and K. Najarian. Multi-modal integrated approach towards reducing false arrhythmia alarms during continuous patient monitoring: The Physionet Challenge 2015. In *Computing in Cardiology*, volume 42, pages 1181–1184, 2015.
- [5] a. Arafat and K. Hasan. Automatic detection of ECG wave boundaries using empirical mode decomposition. *2009 IEEE International Conference on Acoustics, Speech and Signal Processing*, pages 461–464, 2009.
- [6] N. M. Arzeno, Z. D. Deng, and C. S. Poon. Analysis of first-derivative based QRS detection algorithms. *IEEE Transactions on Biomedical Engineering*, 55(2):478–484, 2008.
- [7] N. M. Arzeno, C.-S. Poon, and Z.-D. Deng. Quantitative analysis of QRS detection algorithms based on the first derivative of the ECG. *Conference proceedings : ... Annual International Conference of the IEEE Engineering in Medicine and Biology Society. IEEE Engineering in Medicine and Biology Society. Conference*, 1:1788–91, 2006.
- [8] M. Ayoubi and R. Isermann. Neuro-fuzzy systems for diagnosis. *Fuzzy Sets and Systems*, 89(3):289–307, 1997.
- [9] W. Banasiak, C. Telichowski, K. Kokot, and A. Telichowski. [Diurnal fluctuations of arterial blood pressure and heart rate in patients with atrial fibrillation]. *Wiad Lek*, 45(15-16):584–588, 1992.
- [10] R. Begg, D. T. H. Lai, and M. Palaniswami. *Computational Intelligence in Biomedical Engineering*. 2007.

- [11] D. S. Benitez, P. a. Gaydecki, a. Zaidi, and a. P. Fitzpatrick. A new QRS detection algorithm based on the Hilbert transform. In *Computing in Cardiology*, volume 27, pages 379–382, 2000.
- [12] C. S. Burrus, R. a. Gopinath, and H. Guo. Introduction to Wavelets and Wavelet Transforms: A Primer, 1998.
- [13] M.-C. Chambrin. Alarms in the intensive care unit: how can the number of false alarms be reduced? *Critical Care*, 5(4):184–188, 2001.
- [14] S. W. Chen, H. C. Chen, and H. L. Chan. A real-time QRS detection method based on moving-averaging incorporating with wavelet denoising. *Computer Methods and Programs in Biomedicine*, 82(3):187–195, 2006.
- [15] Chengyu Liu, Peng Li, Lina Zhao, Feifei Liu, and Ruxiang Wang. ECG Quality Assessment for Patient Empowerment in mHealth Applications. In *Computing in Cardiology*, pages 357–360, 2011.
- [16] I. I. Christov. Real time electrocardiogram QRS detection using combined adaptive threshold. *BioMedical Engineering Online*, 3, 2004.
- [17] G. D. Clifford, I. Silva, B. Moody, Q. Li, D. Kella, A. Chahin, T. Kooistra, D. Perry, and R. G. Mark. False alarm reduction in critical care. *Physiological Measurement*, 37(8):E5–E23, 2016.
- [18] P. Couto, R. Ramalho, and R. Rodrigues. Suppression of false arrhythmia alarms using ECG and pulsatile waveforms. In *Computing in Cardiology*, volume 42, pages 749–752, 2015.
- [19] M. Cvach. Monitor alarm fatigue: An integrative review, 2012.
- [20] M. Cvikl, F. Jager, and A. Zemva. Hardware implementation of a modified delay-coordinate mapping-based QRS complex detection algorithm. *Eurasip Journal on Advances in Signal Processing*, 2007, 2007.
- [21] C. Damerval, S. Meignen, and V. Perrier. A fast algorithm for bidimensional EMD. *IEEE Signal Processing Letters*, 12(10):701–704, 2005.
- [22] P. Davey. ECG, 2010.
- [23] A. V. Deshmane. False arrhythmia alarm suppression using ECG, ABP, and photoplethysmogram. *MIT*, pages 1–93, 2009.
- [24] Z. Dokur and T. Ölmez. ECG beat classification by a novel hybrid neural network. *Computer Methods and Programs in Biomedicine*, 66(2-3):167–181, 2001.
- [25] Z. Dokur, T. Ölmez, E. Yazgan, and O. K. Ersoy. Detection of ECG waveforms by neural networks. *Medical Engineering and Physics*, 19(8):738–741, 1997.

- [26] T. L. A. Doyle, E. L. Dugan, B. Humphries, and R. U. Newton. Discriminating between elderly and young using a fractal dimension analysis of centre of pressure. *International Journal of Medical Sciences*, 1(1):11–20, 2004.
- [27] M. J. Drinnan, J. Allen, and A. Murray. Relation between heart rate and pulse transit time during paced respiration. *Physiological measurement*, 22(3):425–432, 2001.
- [28] L. M. Eerikäinen, J. Vanschoren, M. J. Rooijackers, R. Vullings, and R. M. Aarts. Decreasing the false alarm rate of arrhythmias in intensive care using a machine learning approach. In *Computing in Cardiology*, volume 42, pages 293–296, 2015.
- [29] M. Elgendi, M. Jonkman, and F. De Boer. R wave detection using coiflets wavelets. In *Bioengineering, Proceedings of the Northeast Conference*, 2009.
- [30] W. A. H. Engelse and C. Zeelenberg. A single scan algorithm for QRS-detection and feature extraction. *Computers in Cardiology*, 6(9):37–42, 1979.
- [31] S. Fallet and J. M. Vesin. Adaptive frequency tracking for robust heart rate estimation using wrist-type photoplethysmographic signals during physical exercise. In *Computing in Cardiology*, volume 42, pages 925–928, 2015.
- [32] U. Farooq, D. G. Jang, J. H. Park, and S. H. Park. PPG delineator for real-time ubiquitous applications. In *2010 Annual International Conference of the IEEE Engineering in Medicine and Biology Society, EMBC'10*, pages 4582–4585, 2010.
- [33] A. for the Advancement of Medical Instrumentation. Cardiac monitors, heart rate meters, and alarms. *American National Standard (ANSI/AAMI EC13:2002)*, Arlington,;1–87, 2002.
- [34] J. Fraden and M. R. Neuman. QRS wave detection. *Medical & Biological Engineering & Computing*, 18(2):125–132, 1980.
- [35] G. M. Friesen, T. C. Jannett, M. A. Jadallah, S. L. Yates, S. R. Quint, and H. T. Nagle. A Comparison of the Noise Sensitivity of Nine QRS Detection Algorithms. *IEEE Transactions on Biomedical Engineering*, 37(1):85–98, 1990.
- [36] G. S. Furno and W. J. Tompkins. A Learning Filter for Removing Noise Interference. *IEEE Transactions on Biomedical Engineering*, BME-30(4):234–235, 1983.
- [37] E. Grass, R. Morling, and I. Kale. Activity-Monitoring Completion-Detection (AMCD): a new single rail approach to achieve self-timing.

In *Proceedings Second International Symposium on Advanced Research in Asynchronous Circuits and Systems*, number 143, pages 143–149, 2010.

- [38] a. Gund, I. Ekman, K. Lindecrantz, B. a. Sjoqvist, E. L. Staaf, and N. Thorneskold. Design evaluation of a home-based telecare system for Chronic Heart Failure patients. *Conference proceedings : ... Annual International Conference of the IEEE Engineering in Medicine and Biology Society. IEEE Engineering in Medicine and Biology Society. Conference*, 2008:5851–5854, 2008.
- [39] W. P. Holsinger, K. M. Kempner, and M. H. Miller. A QRS Preprocessor Based on Digital Differentiation. *IEEE Transactions on Biomedical Engineering*, BME-18(3):212–217, 1971.
- [40] C. Hoog Antink and S. Leonhardt. Reducing false arrhythmia alarms using robust interval estimation and machine learning. In *Computing in Cardiology*, volume 42, pages 285–288, 2015.
- [41] N. Huang, Z. Shen, S. Long, M. Wu, H. SHIH, Q. ZHENG, N. Yen, C. Tung, and H. Liu. *The empirical mode decomposition and the Hilbert spectrum for nonlinear and non-stationary time series analysis*, volume 454. 1998.
- [42] D.-G. Jang, S. Park, M. Hahn, and S.-H. Park. A Real-Time Pulse Peak Detection Algorithm for the Photoplethysmogram. *International Journal of Electronics and Electrical Engineering*, pages 45–49, 2014.
- [43] B. A. Janz, G. D. Clifford, J. E. Mietus, and R. G. Mark. A multivariable analysis of sedation, activity, and agitation in critically III patients using the riker scale ECG, blood pressure, and respiratory rate. In *Computers in Cardiology*, volume 32, pages 735–738, 2005.
- [44] B. U. Köhler, C. Hennig, and R. Orglmeister. The principles of software QRS detection, 2002.
- [45] B. U. Köhler, C. Hennig, and R. Orglmeister. The principles of software QRS detection, 2002.
- [46] V. Krasteva, I. Jekova, R. Leber, R. Schmid, and R. Abacherli. Real-time arrhythmia detection with supplementary ECG quality and pulse wave monitoring for the reduction of false alarms in ICUs. *Physiological Measurement*, 37(8):1273–1297, 2016.
- [47] J. Lee, D. J. Scott, M. Villarroel, G. D. Clifford, M. Saeed, and R. G. Mark. Open-access MIMIC-II database for intensive care research. In *Proceedings of the Annual International Conference of the IEEE Engineering in Medicine and Biology Society, EMBS*, pages 8315–8318, 2011.

- [48] J. W. Lee, K. S. Kim, B. Lee, B. Lee, and M. H. Lee. A real time QRS detection using delay-coordinate mapping for the microcontroller implementation. *Annals of Biomedical Engineering*, 30(9):1140–1151, 2002.
- [49] Linda S. Costanzo PhD. BRS Physiology, 2014.
- [50] C. Liu, L. Zhao, and H. Tang. Reduction of False Alarms in Intensive Care Unit using Multi-feature Fusion Method. In *Computing in Cardiology*, volume 42, pages 741–744, 2015.
- [51] S. Mallat and W. L. Hwang. Singularity detection and processing with wavelets. *IEEE Transactions on Information Theory*, 38(2):617–643, 1992.
- [52] J. Malmivuo and R. Plonsey. *Bioelectromagnetism: Principles and Applications of Bioelectric and Biomagnetic Fields*. 2012.
- [53] R. G. Mark. *Introduction: The Functional Anatomy of the CV System*. MIT 6.022J Course Reader.
- [54] T. Nguyen. A tutorial on filter banks and wavelets. *Online*. Available: [citeseer.nj.nec.com/nguyen95tutorial.html](http://citeseer.nj.nec.com/nguyen95tutorial.html) 106, 1995.
- [55] M. E. Nygård and L. Sörnmo. Delineation of the QRS complex using the envelope of the e.c.g. *Medical & Biological Engineering & Computing*, 21(5):538–547, 1983.
- [56] M. Okada. A digital filter for the QRS complex detection. *IEEE transactions on bio-medical engineering*, 26(12):700–3, 1979.
- [57] L. Oukhellou, P. Aknin, and E. Delechelle. Railway infrastructure system diagnosis using empirical mode decomposition and Hilbert transform. In *31st IEEE International Conference on Acoustics, Speech and Signal Processing*, 2006.
- [58] D. M. J. Q. P. Morizet-Mahoudex, C. Moreau. Simple microprocessor based system for on-line e.c.g. arrhythmia analysis. pages 19:497–500.
- [59] J. Pan and W. J. Tompkins. A Real-Time QRS Detection Algorithm. *IEEE Transactions on Biomedical Engineering*, BME-32(3):230–236, 1985.
- [60] T. A. Parlikar. *Modeling and monitoring of cardiovascular dynamics for patients in critical care*. PhD thesis, 2007.
- [61] F. Plesinger, P. Klimes, J. Halamek, and P. Jurak. False alarms in intensive care unit monitors: Detection of life-threatening arrhythmias using elementary algebra, descriptive statistics and fuzzy logic. In *Computing in Cardiology*, volume 42, pages 281–284, 2015.

- [62] R. Poli, S. Cagnoni, and G. Valli. Genetic Design of Optimum Linear and Nonlinear QRS Detectors. *IEEE Transactions on Biomedical Engineering*, 42(11):1137–1141, 1995.
- [63] E. D. J. D. P. H. R. Balda, G. Diller. The hp ecg analysis program. pages 197–205.
- [64] N. Sadr, J. Huvanandana, D. T. Nguyen, C. Kalra, A. McEwan, and P. De Chazal. Reducing false arrhythmia alarms in the ICU using multimodal signals and robust QRS detection. *Physiological Measurement*, 37(8):1340–1354, 2016.
- [65] B. Sayadi and S. Marcos. Bayesian multiuser detection based on a Network of NLMS filters. In *European Signal Processing Conference*, 2006.
- [66] B. Scheer, A. Perel, and U. J. Pfeiffer. Clinical review: complications and risk factors of peripheral arterial catheters used for haemodynamic monitoring in anaesthesia and intensive care medicine. *Critical care (London, England)*, 6(3):199–204, 2002.
- [67] C. G. Scully, J. Lee, J. Meyer, A. M. Gorbach, D. Granquist-Fraser, Y. Mendelson, and K. H. Chon. Physiological parameter monitoring from optical recordings with a mobile phone. *IEEE Transactions on Biomedical Engineering*, 59(2):303–306, 2012.
- [68] F. Sufi, Q. Fang, and I. Cosic. ECG R-R peak detection on mobile phones. *Annual International Conference of the IEEE Engineering in Medicine and Biology Society. IEEE Engineering in Medicine and Biology Society.*, 2007:3697–700, 2007.
- [69] Y. Sun, S. Suppappola, and T. A. Wrublewski. Microcontroller-based real-time QRS detection. *Biomedical Instrumentation and Technology*, 26(6):477–484, 1992.
- [70] S. Suppappola and Y. Sun. Nonlinear transforms of ECG signals for digital QRS detection: A quantitative analysis. *IEEE Transactions on Biomedical Engineering*, 41(4):397–400, 1994.
- [71] V. Tanrıverdi. Removal of baseline wandering from the electrocardiogram. Master’s thesis, Middle East Technical University, Ankara, Turkey, June 2006.
- [72] P. E. Trahanias. An Approach to QRS Complex Detection Using Mathematical Morphology. *IEEE Transactions on Biomedical Engineering*, 40(2):201–205, 1993.
- [73] K. K. Tremper. Pulse oximetry. *Chest Journal*, 95(4):713–715, 1989.

- [74] C. Tsimenidis and A. Murray. Reliability of clinical alarm detection in intensive care units. In *Computing in Cardiology*, volume 42, pages 1185–1188, 2015.
- [75] WHO. *World Health Statistics 2012*, volume 27. 2012.
- [76] L. Zapanta, C.-S. Poon, D. P. White, C. L. Marcus, and E. S. Katz. Heart rate chaos in obstructive sleep apnea in children. *Conference proceedings : ... Annual International Conference of the IEEE Engineering in Medicine and Biology Society. IEEE Engineering in Medicine and Biology Society. Conference*, 6:3889–3892, 2004.
- [77] H. ZHOU, K.-M. HOU, and D. ZUO. Real-Time Automatic ECG Diagnosis Method Dedicated to Pervasive Cardiac Care. *Wireless Sensor Network*, 01(04):276–283, 2009.
- [78] Zhou Song-Kai, Wang Jian-Tao, and Xu Jun-Rong. The real-time detection of QRS-complex using the envelope of ECG. *International Conference of the IEEE Engineering in Medicine and Biology Society*, page 38 vol.1, 1988.
- [79] Z. L. H. X. W. L. Zhu H., Zhang Z.M. A novel method for pulse onset detection on photoplethysmogram using changes of waveform trend. In *The International Conference on Health Informatics. IFMBE Proceedings*. Springer, Cham, 2014.
- [80] W. Zong, T. Heldt, G. Moody, and R. Mark. An open-source algorithm to detect onset of arterial blood pressure pulses. In *Computers in Cardiology, 2003*, pages 259–262, 2003.
- [81] W. Zong, L. Nielsen, B. Gross, J. Brea, and J. Frassica. A practical algorithm to reduce false critical ECG alarms using arterial blood pressure and/or photoplethysmogram waveforms. *Physiological Measurement*, 37(8):1355–1369, 2016.



## APPENDIX A

### MATLAB PHYSIONET TOOLBOX ALGORITHMS USED IN THE THESIS

- `jSQI.m`: `jSQI.m` is ABP waveform signal quality index.

$$[BEATQ, R] = jSQI(FEATURES, ONSET, ABP) \quad (A.1)$$

The above function returns a binary signal quality assessment of each beat in ABP. This algorithm relies on detecting abnormalities of numeric values in `FEATURES` and `ONSET`. Written by James Sun ([xinsun@mit.edu](mailto:xinsun@mit.edu))

Table A.1: `jSQI.m`

Input
<code>FEATURES</code> $\langle mx12 \rangle$ — features extracted from ABP using <code>abpfeature.m</code> <code>ONSET</code> $\langle nx1 \rangle$ — onset times of ABP using <code>wabp.m</code> <code>ABP</code> $\langle px1 \rangle$ — arterial blood pressure waveform (125Hz sampled)
Output
<code>BEATQ</code> $\langle nx10 \rangle$ — SQI of each beat: 0=good, 1=bad Col 1: logical OR of cols 2 thru 10 2: P not physiologic ( $<20$ or $>300$ mmHg) 3: MAP not physiologic ( $<30$ or $>200$ mmHg) 4: HR not physiologic ( $<20$ or $>200$ bpm) 5: PP not physiologic ( $<30$ mmHg) 6: abnormal <code>Psys</code> (beat-to-beat change $> 20$ mmHg) 7: abnormal <code>Pdias</code> (beat-to-beat change $> 20$ mmHg) 8: abnormal period (beat-to-beat change $> 1/2$ sec) 9: abnormal <code>P(onset)</code> (beat-to-beat change $> 20$ mmHg) 10: noisy beat (mean of negative <code>dP</code> $< -3$ ) <code>R</code> $\langle 1x1 \rangle$ fraction of good beats in ABP
Usage
- <code>FEATURES</code> must be obtained using <code>abpfeature.m</code> - <code>ONSET</code> must be obtained using <code>wabp.m</code>

on Nov 19, 2005. - v2.0 - 1/18/06 - thresholds updated to reduce false positives - v3.0 - 2/10/06 - added "..101..." detection - see lines 92-96

- `abpfeature.m`: `abpfeature.m` function is a ABP waveform feature extractor.

$$r = abpfeature(ABP, ONSETTIMES) \quad (A.2)$$

The above function extracts features from ABP waveform such as systolic pressure, mean pressure, etc. Written by James Sun (`xinsun@mit.edu`)

Table A.2: `abpfeature.m`

Input
ABP abp signal (125Hz sampled)
ONSETTIMES times of onset (in samples)
Output
Col 1: Time of systole [samples]
2: Systolic BP [mmHg]
3: Time of diastole [samples]
4: Diastolic BP [mmHg]
5: Pulse pressure [mmHg]
6: Mean pressure [mmHg]
7: Beat Period [samples]
8: <i>mean_dyneg</i>
9: End of systole time $0.3 * sqrt(RR)$ method
10: Area under systole $0.3 * sqrt(RR)$ method
11: End of systole time <i>1stmin - slope</i> method
12: Area under systole <i>1stmin - slope</i> method
Usage
- ONSET must be obtained using <code>wabp.m</code>

on Nov 19, 2005.

- `rdmat.m`:

$$[tm, signal, Fs, siginfo] = rdmat(recordName) \quad (A.3)$$

The above function extracts features from ABP waveform such as systolic pressure, mean pressure, etc. Written by Ikaro Silva, 2014

Last Modified: November 17, 2014

Version 1.1

Since 0.9.7

Table A.3: rdmatt.m

Input
recorName String specifying the name of the *.m file
Output
tm A Nx1 array of doubles specifying the time in seconds.
signal A NxM matrix of doubles contain the signals in physical units.
Fs A 1x1 integer specifying the sampling frequency in Hz for the entire record.
siginfo A LxN cell array specifying the signal siginfo.
Currently it is a structure with the following fields:
siginfo.Units
siginfo.Baseline
siginfo.Gain
siginfo.Description

- wabp.m:

$$r = wabp(Araw, Offset, Scale, Fs) \quad (A.4)$$

The above function robustly detects the onset of each beat in the ABP waveform. The basis of Zong's onset detection algorithm is the slope sum function (SSF), which amplifies the rising part of each beat (Figure A.1) [80]. More details can be found in their paper. Gnu Public License

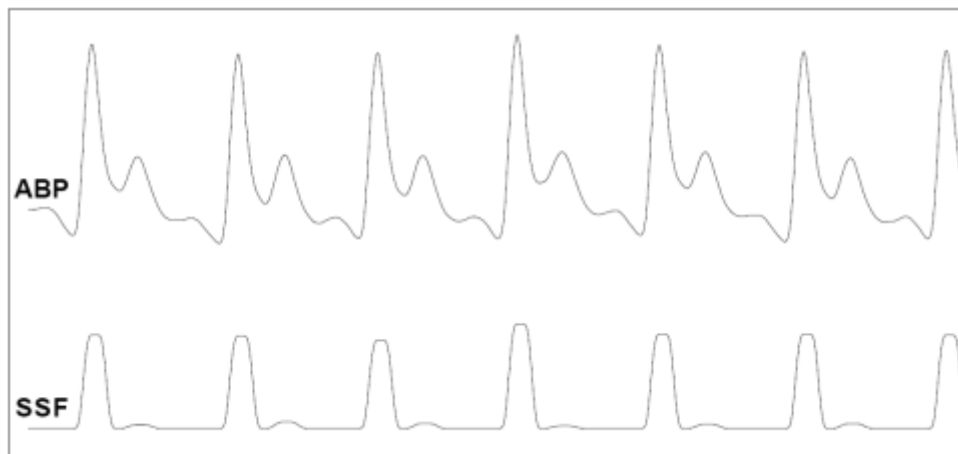


Figure A.1: The slope sum function (SSF),It aids in onset detection [80]

Applies

James Sun Feb 09 2005 with some changes from Gari Clifford based upon wabp.c by Wei Zong ([www.physionet.org](http://www.physionet.org))

- quantile:

Table A.4: wabp.m

Input
Araw (125Hz sampled) waveform in wfdb-MIT format, Offset Scale
Output
The onset times of the input ABP waveform
Usage
Defaults are Offset = 1600; Scale=20; Fs=125 If you pass 0 as the scale then above defaults are invoked

$Y = \text{quantile}(X,p)$  returns quantiles of the values in data vector or matrix  $X$  for the cumulative probability or probabilities  $p$  in the interval  $[0,1]$ .

- If  $X$  is a vector, then  $Y$  is a scalar or a vector having the same length as  $p$ .
- If  $X$  is a matrix, then  $Y$  is a row vector or a matrix where the number of rows of  $Y$  is equal to the length of  $p$ .
- For multidimensional arrays,  $\text{quantile}$  operates along the first non-singleton dimension of  $X$ .

## APPENDIX B

### FEATURE EXTRACTION

For ABP signals feature extraction we used `abpfeature.m` function. This function gets input as ABP (125Hz sampled), times of onset (in samples) and gives a set of features shown in Table B.1.  $P_s$  and  $P_d$  are the local minimum and maximum around the neighborhood of pressure onset point for each beat.  $P_m$  is the mean pressure between sequential onsets. Noise level is defined as the mean of all negative slopes in each beat.

Table B.1: ABP Features

Feature	Description
$P_s$	Systolic Blood Pressure
$P_d$	Diastolic Blood Pressure
$P_p$	Pulse Pressure ( $P_s - P_d$ )
$P_m$	Mean Arterial Pressure
T	Duration of each Beat
f	Heart Rate ( $60/T$ )
w	noise: mean of negative slopes

For ABP we use `jsqi.m` signal quality index algorithm which features and their logic shown in Table B.2.

The first 4 criteria shown in Table B.2 controls signal based on physiological ranges of each feature. The 6th criterion is the noise detector which is based on observation and inspecting ABP data. The Final 3 criteria compare ABP feature between adjacent beats and detect sharp changes in beat-to-beat intervals which are signs of abnormality.

Table B.2: SQI Logic

Feature	Abnormality Criteria
$P_s$	Systolic Blood Pressure
$P_d$	Diastolic Blood Pressure
$P_m$	Pulse Pressure ( $P_s - P_d$ )
f	Mean Arterial Pressure
$P_p$	Duration of each Beat
w	Heart Rate ( $60/T$ )
$P_s(k) - P_s(k - 1)$	$ \delta P_s  > 20mmHg$
$P_d(k) - P_d(k - 1)$	$ \delta P_d  > 20mmHg$
$T(k) - T(k - 1)$	$ \delta T  > 2/3$ sec

Table B.3: Asystole Case Comparison

Authors	Sens.(%)	Spec.(%)
V. Kresteva et al.	100	97
F. Plesinger et al.	100	97
<b>METU BEST Method</b>	100	86
<b>METU BEST Generic Method</b>	100	86
<b>METU BEST (without using ABP) Method</b>	100	85.3
<b>METU BEST (Commercial) Generic Method</b>	100	74
S. Ansari et al.	94	82
C. Daluwatte et al.	91	86
W. Zong et al.	89	63
L. M. Eerikainen et al.	85	88
P. Couto et al.	78	94
C. H. Antink et al.	56	94
Average	81.2	79.3

Table B.4: Bradycardia Case Comparison

Authors	Sens.(%)	Spec.(%)
<b>METU BEST Method</b>	100	78
<b>METU BEST Generic Method</b>	100	78
W. Zong et al.	100	78
F. Plesinger et al.	100	72
C. H. Antink et al.	100	57
V. Kresteva et al.	98	86
C. Daluwatte et al.	98	44
L. M. Eerikainen et al.	96	79
P. Couto et al.	95	66
<b>METU BEST (without using ABP) Method</b>	93.5	72.1
<b>METU BEST (without using ABP) Generic Method</b>	93.5	72.1
S. Ansari et al.	77	86
Average	87	65.3

Table B.5: Tachycardia Case Comparison

Authors	Sens.(%)	Spec.(%)
C. H. Antink et al.	100	100
P. Couto et al.	100	80
L. M. Eerikainen et al.	99	99
V. Kresteva et al.	99	89
<b>METU BEST Logic Algorithm</b>	98.2	63
<b>METU BEST Generic Logic Algorithm</b>	95.6	62.5
<b>METU BEST (without using ABP) Method</b>	98.2	63
<b>METU BEST (without using ABP) Generic Method</b>	98.2	63
W. Zong et al.	98	80
S. Ansari et al.	98	60
F. Plesinger et al.	97	100
C. Daluwatte et al.	96	78
Average	89.4	73.8

Table B.6: Ventricular-Tachycardia Case Comparison

Authors	Sens.(%)	Spec.(%)
C. H. Antink et al.	90	71
F. Plesinger et al.	85	84
L. M. Eerikainen et al.	84	74
W. Zong et al.	84	43
<b>METU BEST Method</b>	83.3	43
<b>METU BEST Generic Method</b>	83.3	43
<b>METU BEST (without using ABP) Method</b>	83.3	32
<b>METU BEST (without using ABP) Generic Method</b>	83.3	28.6
V. Kresteva et al.	82	71
C. Daluwatte et al.	80	82
S. Ansari et al.	78	85
P. Couto et al.	69	95
Average	74.4	55

Table B.7: Ventricular-Flutter/Fibrillation Case Comparison

Authors	Sens.(%)	Spec.(%)
<b>METU BEST Method</b>	100	98.1
<b>METU BEST (without using ABP) Method</b>	100	96.2
<b>METU BEST Generic Method</b>	100	94.2
<b>METU BEST (without using ABP) Generic Method</b>	100	94.2
S. Ansari et al.	100	90
V. Kresteva et al.	100	87
C. Daluwatte et al.	100	83
P. Couto et al.	89	96
W. Zong et al.	89	78
L. M. Eerikainen et al.	75	94
F. Plesinger et al.	67	100
C. H. Antink et al.	67	92
Average	80.6	83.1

## APPENDIX C

### QRS COMPLEX ENHANCEMENT METHODS

ECG signals detection is affected by various kinds of artifacts as mentioned in section 2.1.8. Therefore, ECG signals have to be improved by filtering for noise suppression, R peak enhancement and QRS enhancement stages, which are prerequisites for detecting the QRS complex. This section introduces amplitude thresholding method, first derivative only approach, first and second derivative only approach, digital filters approach, mathematical morphology approach, empirical model decomposition, Hilbert transform approach, filter banks approach and wavelet transform approach.

- **Amplitude Thresholding Method:** Enhancement of R peaks in the ECG signals is the oldest method for detecting R peaks in the ECG signals. Moreover, it is the most common one and still useful for the last 30 years. Sufi et al. [68] used this method in a standalone mobile phone application for QRS detection. This method is usually supported by a first derivative pre-processing step to attenuate P, T waves, and enhance R waves of the signal. After this first derivative process, amplitude thresholding method detects the QRS complex. Formulation is given below:

$$X_{th} = \Lambda \cdot X[n] \quad (\text{C.1})$$

where:

$X[n]$  represents the ECG signal.

$\Lambda$  represents the proportion of the ECG signal, which is useless and contains artifacts.  $\Lambda$  is between 0 – 1.

$X_{th}$  represents the threshold, which should be removed from the ECG signal.

Moreover, different threshold values and formulations has been used. For example, Moriet-Mahoudeaux et al. [58] developed an amplitude threshold algorithm using  $X_{th} = 0.3 \cdot \max X[n]$ , which means 30% of the amplitudes below the maximum positive values are truncated from the whole signal. ECG signal noise is not removed properly. Although it is a simple method, the order of complexity depends on the threshold used and segmentation.

- **First Derivative Only Approach:** First order differentiators for QRS enhancement are commonly used for high-pass filtering which improves baseline wanders and avoid high frequency noises. In addition, ECG signals phases are reconstructed with this process. Moreover, the output ECG signals have zero crossing in the location of the R peaks. In the literature first derivative can be calculated in different ways. Some of these first derivative detection algorithms, introduced in the literature [58] are given below:

$$Y_1[n] = -2X[n - 2] - X[n - 1] + X[n + 1] + 2X[n + 2] \quad (C.2)$$

where:

$Y_1[n]$  represents the first derivative of the ECG signal.

In contrast, Holsinger [39] used a central finite-difference approach as:

$$Y[n] = X[n + 1] - X[n - 1], \quad (C.3)$$

In another study, Okada [56] used a backward difference scheme:

$$Y[n] = X[n] - X[n - 1]. \quad (C.4)$$

This method can not remove high frequency noises. It reduces motion artifacts and baseline drifts. It is a simple method. It contain one equation for feature extraction. The order of complexity depends on the number of the processed segments for each record.

- **First and Second Derivative Approach:** Generally, first and second derivatives of raw ECG signals are computed separately. These computed derivatives are linearly combined and used to enhance the QRS complex part of the ECG signal relative to P and T waves. For example, in the

research of Balda et al. [63], the formulation of First and Second Derivative approach is given below:

$$Y_1[n] = |X[n + 1] - X[n - 1]|, Y_2[n] = |X[n + 2] + X[n - 2]|. \quad (C.5)$$

where:

$Y_2[n]$  represents the second derivative of the ECG signal.

After that, they combined both derivatives according to:

$$Y_3[n] = 1.3Y_1[n] + 1.1Y_2[n]. \quad (C.6)$$

where:

$Y_3[n]$  represents the combination of the first and second derivatives of the ECG signal.

According to Ahlstrom and Tompkins [36] they computed the absolute value of the first derivative of the ECG signal as:

$$Y_1[n] = |X[n + 1] - X[n - 1]|. \quad (C.7)$$

The rectified derivative was modified and improved as:

$$Y_{1mod}[n] = 0.25(Y_1[n - 1] + 2Y_1[n] + Y_1[n + 1]). \quad (C.8)$$

where:

$Y_{1mod}[n]$  represents the modified and rectified version the first derivative of the ECG signal.

Then they calculated the rectified version of the second derivative as:

$$Y_2[n] = |X[n + 2] - 2X[n] + X[n - 2]|. \quad (C.9)$$

Finally, the rectified and modified versions of the first and second derivatives were combined as:

$$Y_3[n] = Y_{1mod}[n] + Y_2[n]. \quad (C.10)$$

where:

$Y_3[n]$  represents the combination of the rectified and modified version of the first and second derivatives of the ECG signal.

This is a simple method, which contains 4 equations for feature extraction.

The order of complexity depends on the derived equations and the number of processed segments.

- **Digital Filters Approach:** There are a lot of useful digital filters, which are used for QRS enhancement [30], [59]. For example, Engelse and Zeelenberg [30] firstly passed the ECG signal through a differentiator:

$$Y_1[n] = X[n] - X[n - 4]. \quad (\text{C.11})$$

Then this signal is passed through a digital low pass filter:

$$Y_3[n] = Y_1[n] + 4Y_1[n - 1] + 6Y_1[n - 2] + 4Y_1[n - 3] + Y_1[n - 4] \quad (\text{C.12})$$

where:

$Y_3[n]$  represents the digital low pass filtered version of the first derivative of the ECG signal.

In [56], a queue digital filter was used. First, a three-point moving average filter is applied to the ECG signal:

$$Y_0[n] = 0.25(X[n - 1] + 2X[n] + X[n + 1]) \quad (\text{C.13})$$

$Y_0[n]$  represents the filtered version of the ECG signal.

Then a low pass filter was applied to the output  $Y_0[n]$  of this filter:

$$Y_1[n] = \frac{1}{2m + 1} \sum_{k=n-m}^{n+m} Y_0[k]. \quad (\text{C.14})$$

The difference of the output and input of this low-pass filter was then squared to suppress low amplitude waves relative to the R peak:

$$Y_2[n] = (Y_0[n] - Y_1[n])^2. \quad (\text{C.15})$$

where:

$Y_2[n]$  represents the combination of the input and output of the low pass filter.

To amplify the QRS complex region compared to P and T wave regions, the squared difference signal  $Y_2[n]$  was filtered.

$$Y_3[n] = Y_2[n] \left( \sum_{k=n-m}^{n+m} Y_2[k] \right)^2 \quad (\text{C.16})$$

where:

$Y_3[n]$  represents the amplified version of the  $Y_2[n]$ .

Multiplication of backward difference (MOBD) approach is also a digital filter approach and has been used (details in [69], [70]). This approach consists of AND gates integration of close magnitude values derivative outputs. The MOBD function is defined as:

$$Z[n] = \prod_{k=0}^{N-1} (X[n-k] - X[n-k-1]). \quad (\text{C.17})$$

where:

$N$  represents the MOBD order,

$Z[n]$  represents the extracted QRS complex, which can be detected by a suitable threshold.

Another approach, which is developed by Dokur et al. [25], contains two separate bandpass filters. Then filtered outputs are multiplied as  $W[n]$  and  $F[n]$ :

$$Z[n] = W[n].F[n]. \quad (\text{C.18})$$

where:

$W[n]$  represents bandpass filter 1.  $F[n]$  represents bandpass filter 2. The approach above relies on the assumption that concurrently resulting frequency components characterize each QRS complex within the pass-band of every filter. The AND combination is performed by the multiplication operation. If the result of AND integration is true, it states a QRS complex. Because of the multiplication operator, if all filter outputs are high then the output is true. Conversely, Pan and Tompkins [34] apply a band-pass digital filter before the derivative operator to the ECG signals. The bandpass filter resulted from a low pass filter  $Y_1[n]$ :

$$Y_1[n] = 2Y_1[n-1] - Y_1[n-2] + X[n] - 2X[n-6] + X[n-12]. \quad (\text{C.19})$$

Then a high pass filter applied as  $Y_2[n]$ :

$$Y_2[n] = 32Y_1[n-16] - (Y_2[n-1] + Y_1[n] - Y_1[n-32]). \quad (\text{C.20})$$

where:

$Y_1[n]$  represents the low pass filtered form of the ECG signal,

$Y_2[n]$  represents the high pass filtered form of  $Y_1[n]$ .

The first derivative ( $Y_3[n]$ ) is obtained after the bandpass filter step was specified as:

$$Y_3[n] = \frac{1}{8}(-Y_2[n-3] - 2Y_2[n-1] + 2Y_2[n+1] + Y_2[n+2]) \quad (C.21)$$

where:

$Y_3[n]$  represents the first derivative of  $Y_2[n]$ .

The last differentiation step emphasizes high frequency signal waves (QRS complex, R wave) and suppresses flat ECG waves, baseline wanders and low frequency noises. This method increases SNR ratio depends on the nature of the filter and its order. It is a simple algorithm, which contains up to 4 equations for feature extraction. The complexity depending on the number of processed segments for each record.

- **Mathematical Morphology Approach:** The details of mathematical morphology approach is provided in [72]. The following theoretical background is a brief summary of detailed works. Its origin came from image processing, later it was applied to enhance ECG signals. There are two main operators, dilation and erosion.

Erosion function is defined as:

$$(f \ominus k)_{(m)} = \min_{n=0,1,\dots,M-1} f[m+n] - k[n] \quad (C.22)$$

for  $N > M$  and  $m=0,\dots,N-M$  where:

$f: F \rightarrow I$ ,

$k: K \rightarrow I$ , (structuring element)

$F=0,1\dots N-1$ ,

$K=0,1\dots M-1$ ,

$m=0,1\dots N-M$ ,

$I$  defined as a set of integer numbers.

$(f \ominus k)$  values are always less than those  $f$  values. Dilation function is defined as:

$$(f \oplus k)_{(m)} = \min_{n=0,1,\dots,M-1} f[n] - k[m-n] \quad (C.23)$$

for  $N > M$  and  $m=M-1,\dots,N-1$

where:

$m=M-1, M \dots N-1,$

These two functions can be combined for additional operations such as Opening (erosion followed by dilation 'o') and Closing (dilation followed by erosion '•'). If Opening is applied to a signal, it removes all peaks. If Closing is applied to a signal, it removes all negative peaks. Trahanias et al. [72] used these functions to suppress noise from the ECG signal:

$$X_{mod}[n] = \frac{[(X[n] \circ k) \bullet k] + [(X[n] \bullet k) \circ k]}{2} \quad (C.24)$$

where:

$X_{mod}[n]$  represents the filtered signal after the noise suppression.

- **Empirical Model Decomposition:** In literature empirical model decomposition (EMD) was introduced by Huang et al. [41] for nonlinear and non-stationary signal analysis. This method is based on the idea that any complex data set can be resolved on a quantifiable and generally small number of intrinsic mode functions (IMFs), which is same as well-behaved Hilbert transforms. Moreover, if IMFs, which are decomposed raw ECG signals, are combined to produce a resulting signal, the QRS complex is more explicit. This approach can also be defined as a type of adaptive filter and have the same behavior of using wavelet transform. Shifting is the main process in EMD. It decomposes the raw signal into a group of IMFs.  $K$  modes  $d_k[n]$  and residual term  $r[n]$ , are the main parameters of this process, [57], [21], which are obtained and expressed by:

$$X[n] = \prod_{k=1}^K d_k + r[n] \quad (C.25)$$

where:

$d_k$  represents  $K$  mode of the IMF.

$r[n]$  represents the residual term of the IMF.

The detailed steps of the EMD approach are given below:

1. Start with the signal  $d_{k=1}[n] = x[n]$ , which followed by the sifting process with  $h_j[n] = d_k[n]$ .

where:

$$j = 0$$

$h_j[n]$  represents sifting process.

2. Calculate all local extrema points of  $h_j[n]$ .
3. Identify the lower (EnvMin) and the upper (EnvMax) envelopes by using cubic spline interpolation of the maxima and minima points.
4. Compute the mean of the upper and lower envelopes as:  $m[n] = \frac{1}{2}(EnvMax[n] + EnvMin[n])$ .
5. Extract the details of  $h_{j+1}[n] = h_j[n] - m[n]$ .
6. If the  $h_{j+1}[n]$  is an IMF, extract the mode  $d_k = h_{j+1}[n]$ ; otherwise, iterate the steps 2, 3, 4, 5 on the signal  $h_{j+1}[n]$ ,  $j = j + 1$  again.
7. Compute the residual  $r_k[n] = x[n] - d_k[n]$ .
8. If the number of extrema points are less than two in  $r_k[n]$ , the extraction process is finished as  $r[n] = r_k[n]$ . Otherwise, return back to step 1 and start from the residual  $r_k[n]$ ,  $k = k + 1$ .

The first several IMFs can filter out the noise and preserve the QRS content compared to other ECG features such as P and T waves. It is a simple algorithm, which contains at least 9 steps with several equations for feature extraction. The complexity of the algorithm increases with the number of processed ECG segments. Its complexity is higher than the other approaches such as derivative based algorithms and digital filters algorithms.

- **Hilbert Transform Approach:** Zhou et al. [78] and Nygard and Srmno et al. [55] proposed and implemented, that Hilbert Transform can be used for QRS detection. Firstly, ECG signals are transformed by output of a filter response as:

$$X_H[t] = H\{X\} = \int_{-\infty}^{+\infty} \frac{X(\tau)}{t - \tau} d\tau \quad (C.26)$$

$$= \frac{1}{\pi} \otimes X(t) \quad (C.27)$$

where:

$X[t]$  represents the ECG signal in continuous time domain.

$H\{X\}$  represents the Hilbert transform operator.

$X_H[t]$  represents the Hilbert transform of  $X[t]$ .

$*$  is the convolution operator.

In the frequency domain, the ECG signal can be transformed with a filter of response:

$$X_H(j\omega) = X(j\omega) * H(j\omega) \quad (\text{C.28})$$

where:

$X(j\omega)$  represents the ECG signal in frequency domain.

Hilbert transform transfer function in frequency domain  $H(j\omega)$  is given as:

$$H(j\omega) = \begin{cases} -j & 0 \leq \omega < \pi, \\ j & -\pi \leq \omega < 0. \end{cases} \quad (\text{C.29})$$

Fast Fourier Transform (FFT) provides numerical efficiency in calculation, which makes it easier to compute the Hilbert transform.  $X_H[n]$  is the Hilbert transform of the ECG signal.  $X[n]$  is utilized for the calculation of the signal.  $Y_e[n]$  is used for the computation of the signal envelope of  $X_H[n]$ , which is discrete Hilbert transform of the ECG signal  $X[n]$ , [55]. For band-limited signals the equation given below:

$$Y_e[n] \approx \sqrt{X^2[n] + X_H^2[n]}. \quad (\text{C.30})$$

For numerical efficiency, the envelope equation is simplified as [55]:

$$Y_e[n] \approx |X[n]| + |X_H[n]| \quad (\text{C.31})$$

Nygards and Srnmo et al. [55] proposed that the envelope is low pass filtered to eliminate ripples and remove ambiguities in the peak level detection. Moreover, they submit a waveform adaptive design for avoiding low-frequency ECG components. The method of Zhou et al. [78] is based on the envelope of the signal is approximated using:

$$Y_e[n] \approx |Y_1[n]| + |Y_2[n]|. \quad (\text{C.32})$$

In the above equation the  $Y_1[n]$  and  $Y_2[n]$  are the outputs of two orthogonal digital filters, which can be defined as:

$$Y_1[n] = X[n] - X[n - 6], \quad (\text{C.33})$$

$$Y_2[n] = X[n] - X[n - 2] - X[n - 6] - X[n - 8]. \quad (\text{C.34})$$

A four-tap moving average filter applied the envelope signal  $Y_e[n]$  to smooth and remove noise. Some researchers use a first derivative before applying the Hilbert transform [6], [11], [7]. Differentiation of the ECG changes its phase by creating a zero crossing at the assumed points of R peaks. Therefore, in order to create a signal with marked peaks at true locations of R peaks, the transformation operation needs to rectify the phase of the signal. Only Hilbert transform (HT) does not improve SNR ratio. Hence, some researchers apply filter to remove the muscular noise and maximize the QRS before using HT. The HT contains at least 9 steps with several equations for feature extraction. However, the main disadvantages of this method are that the computational works require FFT calculations, and the number of processed ECG segments, which increase the complexity compared with time domain approaches. In addition, details and a brief explanation of the application of HT is given in section 3.2 QRS Complex Detection.

- **Filter Banks Approach:** Filter banks divide the input ECG signal, which can be down-sampled, into uniform frequency sub-band signals, because the bandwidth of these sub-band signals have lower amplitude than the input signal. Additionally, the sub-bands carry information from multiple frequency ranges; therefore, this make possible to implement frequency-dependent and time dependent signal processing of the input signal. Filter banks include analysis filters, which divide the input signal into uniform frequency sub-band signals. The input ECG signal is band-passed by these analysis filters to produce sub-band signals as:

$$u_i(z) = H_i(z)X(z). \quad (\text{C.35})$$

where:

$X(z)$  represents the ECG signal in frequency domain.

$H_i(z)$  represents the analysis filters in frequency domain.

$u_i(z)$  represents the decomposed sub-band signals.

The effective bandwidth of  $u_i(z)$  is  $\frac{\pi}{M}$  and  $i = 0, 1, \dots, M - 1$ . Therefore, they can be down-sampled to reduce the total rate. The down-sampled

signal  $w_i(z)$  is:

$$w_i(z) = \frac{1}{M} \sum_{k=0}^{M-1} u_i(z^{\frac{1}{M}} W^k) \quad (\text{C.36})$$

where:

$M$  represent the number of sub-bands (samples) In the above equation  $W = e^{-j(\frac{2\pi}{M})}$ . The sub-bands  $u_i(z)$  and  $w_i(z)$  are band-pass filtered forms of the input.  $u_i(z)$  has a higher sample rate than  $w_i(z)$ . The filtering process can be easily integrated with  $\frac{1}{M}$  of the input ratio because of the advantage of the down-sampling. This method is referred to poly-phase implementation and it plays a central role of computational efficiency of the filter bank algorithms [3]. According to Afonso et al. [3] various features of the ECG complex can be implemented by using sub-bands. For example, a sum of absolute values feature can be computed using sub-bands,  $i = 1, \dots, 4$ . From these sub-bands six features ( $p_1, p_2, p_3, p_4, p_5, p_6$ ) can be derived as follows:

$$\begin{aligned} p_1 &= \sum_{i=1}^3 |w_i(z)|, p_2 = \sum_{i=1}^4 |w_i(z)|, p_3 = \sum_{i=2}^4 |w_i(z)| \\ p_4 &= \sum_{i=1}^3 (w_i(z))^2, p_5 = \sum_{i=1}^4 (w_i(z))^2, p_6 = \sum_{i=2}^4 (w_i(z))^2 \end{aligned} \quad (\text{C.37})$$

These six properties values are proportional to the QRS complex energy. Therefore, these features can be matched with QRS complex by using heuristic beat-detection logic. Digital filters sharply improve the SNR (especially for muscle noise) for Gaussian noise with respect to the mean and median averaging methods. Relatively high computational cost is required because of involvement of a large amount of multipliers in the FIR.

- **Wavelet Transform Approach:** Wavelets have similar features as the filter banks. The wavelet transform (WT) [26] is a function of  $f(t)$ . It is an integral transformation formulated as:

$$W_f(a, b) = \int_{-\infty}^{+\infty} f(t) \psi_{a,b}^*(t) dt. \quad (\text{C.38})$$

where:

$f(t)$  represents the ECG signal in continuous time domain.

the wavelet function is denoted as  $\psi(t)$  and its complex conjugate is denoted as  $\psi^*(t)$ . WT has a time-scale notation, that the short-time Fourier transform (STFT) has similar notation. In contrast to STFT, the WTs perform variable frequency resolution and corresponded time for variable frequency bands by using some analyzing functions. These functions are wave family and they are induced from the same mother wavelet  $\psi(t)$  by:

$$\psi_{a,b}(t) = \frac{1}{\sqrt{2}}\psi\left(\frac{t-b}{a}\right) \quad (\text{C.39})$$

The  $a$  and  $b$  are the scaling (dilation) and shifting parameters respectively. Parameter  $a$  represents the frequency parameter of the STFT. The mother wavelet can be defined as a short oscillation with a zero mean. If  $a$  and  $b$  parameters of WT are discretized, it is transformed to discrete wavelet transform (*DWT*). For example,  $a = 2^j$  and  $b = n(2^j)$  and  $j$  and  $n$  are integers. These parameters turn *DWT* to become dyadic *WT* (*DyWT*) shown below:

$$W_f(2^j, b) = \int_{-\infty}^{+\infty} f(t)\psi_{2^j,b}^*(t)dt, \quad (\text{C.40})$$

$$\psi_{2^j,b}(t) = \frac{1}{2^{\frac{j}{2}}}\psi\left(\frac{t}{2^j} - n\right). \quad (\text{C.41})$$

Although all the equations are shown as an integral transform for *DyWT*, in practice, it is generally implemented as dyadic filter banks with coefficients, which are derived from the wavelet function [12], [54], [29]. Only WT does not improve SNR ratios. However, SNR can be improved by selecting the WT coefficients with the largest amplitude. The length of segment in each segmentation reflects the tradeoff between accuracy and computational time. In general computational cost of WT is the same as digital filter banks and relatively high compared to others.

## C.1 QRS Complex Detection Methods

- **Thresholding:** The set of thresholds that Pan and Tompkins (1985) used for this stage of the QRS detection algorithm were set such that signal peaks (i.e., valid QRS complexes) were detected. Signal peaks are defined as those of the QRS complex, while noise peaks are those of the T waves,

muscle noise, etc. After the ECG signal has passed through the bandpass filter stages, its SNR (signal-to-noise ratio) increases. This permits the use of thresholds that are just above the noise peak levels. Therefore, the overall sensitivity of the detector is improved. It a simple and low complexity method; however, if the SNR of the data is low, performance of this approach is affected negatively. Moreover, choosing the optimal threshold is not easy and you need to optimize it with a huge database.

- **Neural Networks:** Artificial neural networks have been widely applied in nonlinear signal processing, classification and optimization. Generally, their performances are better than classical linear approaches. In ECG signal processing, learning vector quantization (LVQ), radial basis function (RBF) networks and the multilayer perception (MLP) networks are used. In Figure C.1, the MLP network consist of multiple layers of interconnected neurons and each neuron is corresponded by a processing function:

$$y = f(w_0 + \sum_{i=1}^N w_i x_i). \quad (\text{C.42})$$

where:

$w_i$  is the weight assigned to the input  $x_i$  and  $f(\cdot)$  is a linear or nonlinear function.

In the nonlinear case,  $f(\cdot)$  frequently defined as the logistic function  $f(u) = 1/(1 + e^{-u})$  or  $f(u) = \tanh(u)$ . RBF networks are an implementation of the functional equation:

$$y(n) = \sum_{i=1}^N w_i \exp\left(-\frac{x(n) - c_i}{\theta_i}\right) \quad (\text{C.43})$$

where:

$y(n)$  is the RBF network output,

$x(n)$  symbolizes several input of the data vector of the network,

$N$  denotes the quantity of neuron,

$w_i$  denotes the coefficients of the network,

$c_i$  denotes the center vectors,

$\theta_i$  denotes the standard deviations of the network.

The diagram of the MLP shown in Figure C.1: The exponentials may have

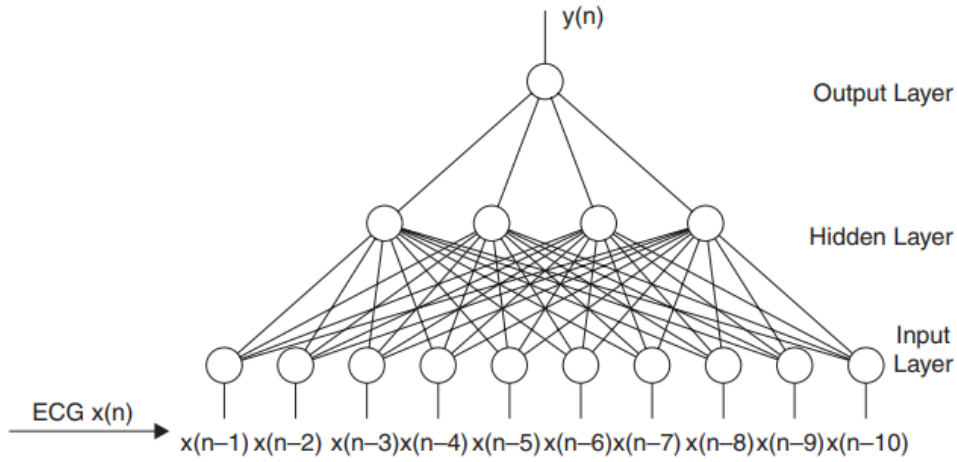


Figure C.1: Multilayer Perceptron [44]

alternative (other) functions to be replaced. In the linear layer a classification is applied, which is based on Euclidean distance method among the competitive neurons. In the final layer, the outputs of the former layer are combined with respect to user defined target classes (similar to fuzzy logic) [8]. The general structure of LVQ network shown in Figure C.2. In addition, despite of the MLP and RBF networks, which are trained by supervised learning algorithms, the LVQ network is tuned in an unmanaged manner [15], [5]. The training stages of these approaches are numerically

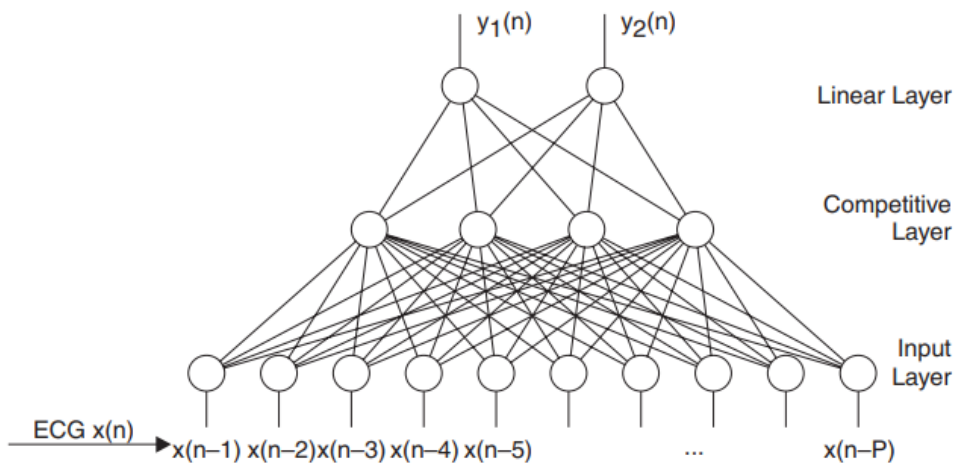


Figure C.2: LVQ Network [44]

in efficient due to an iterative process for adjusting the neural network weights. If the hidden neurons quantity increased the computational load

is also increased. Although you implement these approach on a mobile phone, the amount of memory to store the neuron weights have to be large. In the operating stage a considerable amount of process power is needed for evaluation of nonlinear functions like sigmoid; therefore, it is computationally inefficient.

- **Hidden Markov Models:** In Hidden Markov Models (HMM) the observed data are divided by a probability function, which is based on a Hidden Markov Chain. The objective of the algorithm the HMM method is to understand the primary state sequence in the observed data. For ECG signal processing, probable states are QRS complex, P wave and T wave. In addition, because all states of P waves, QRS complexes and T wave are determined, this method have an important advantage. The disadvantage of this algorithm is including a necessary manual segmentation for training prior to analysis of a record, its patient dependence and the considerable computational complexity even when the computationally efficient Viterby algorithm [76] is applied.

- **Matched Filters:** There are generally neural-network based with linear matched filtering approaches. They improve SNR. Preprocessing steps, such as automatic gain control, are applied to the signal and it is digitized before processing. Then the digitized signal is filtered by a bandpass filter (15 – 40 Hz) with 50 Hz notch. In the final step a matched filter is applied shown below:

$$y(n) = \sum_{i=0}^{N-1} h(i)x(n-i) \quad (\text{C.44})$$

$h(n)$  is the impulse response, which is taken from the first cardiac cycle of the contemporary measurements. Moreover interpolation is used up to four times of the sampling frequency. In final decision step, QRS complex from the filtered signals are separated with respect to fixed threshold. This Method increases timing accuracy of the R wave threshold based detection [24].

According to Lindecrantz et al. [38] research, their algorithm searches from the minimum of average magnitude cross difference (AMCD) instead of using the cross correlation between the signal and the template. The

AMCD equation shown below:

$$AMCD = \sum_{i=1}^N |x(n-i) - h(i)|. \quad (C.45)$$

In the above equation, the ECG signal is defined as  $x(n)$  and the time-reversed variable defined as template. Because there is no multiplication in the equation, computation of the method is easy to implement and computationally inexpensive. Further applications are reported by Grass et. al. [37] in their study, they implemented this method on ICUs for real-time applications. This method is sensitive to noise (such as heart rate variations, baseline wanders). In the operation stage, it evaluates sample by sample moving windows for comparison with the template along the ECG signals, which make this method computationally high.

- **Syntactic Method:** In the syntactic algorithms, signals are examined by a sequence of singularity, which is represented as strings. This representation is solved for search patterns. Therefore, this pattern recognition part is provided by syntactic algorithm with representations. This method is sensitive to noise (such as heart rate variations, baseline wanders).

The specific case of ECG signal processing, the signal divided into short intervals of fixed or variable periods. Each interval is symbolized by a primitive, which is coded with the predefined alphabet [67], [77], [12], [77]. Moreover, These line primitive groups are enlarged by parabolic curves, peaks and features. The computational cost of this algorithm compared to others, because measurements of various parameters have to be performed and semantics are needed to the model of the formulation of the pattern grammar of the specific ECG signal.

- **Zero Crossing:** QRS detection based on zero crossing counts starts with bandpass filtered signal. Then the  $b(n) = k(n)(-1)^n$  is a high frequency sequence, which is added to the filtered signal  $y_1(n)$ :

$$y_2(n) = y_1(n) + b(n). \quad (C.46)$$

The amplitude of the high-frequency sequence  $k(n)$  is computed by a running average of the factor of the band-pass filtered ECG  $|y_1(n)|$ . Since the

amplitude of  $k(n)$  is lower than the amplitude of the QRS complex, the number of zero crossing is large in the period of non-QRS segments and low in the period of the QRS complex. Computing [1] a running average of the number of zero crossings results in a robust feature  $z(n)$  for the QRS complexes. An adaptive threshold is used to check the feature signal  $z(n)$  for the detection of QRS complex. Then a maximum points search in the bandpass filtered signal is used to find the temporal location of the R-wave around a detected QRS candidate. It is a simple algorithm with an inefficient computational cost, because of the time consuming stages in the maxima and minima search for temporal localization of R wave in the ECG signal.

- **Singularity:** The algorithm first applied to QRS detection by Mallat Hwang [51]. The R peaks are found by using local maxima of the wavelet coefficient signals [1]. This method is sensitive to noise (such as heart rate variations, baseline wanders). In this method the correspondence between singularities of a function  $f(t)$  and local maxima in its wavelet transform  $Wf(a, t)$  is investigated. The singularities correspond to pairs of modulus maxima across several scales. A point to point mapping between a signal with its singularities and wavelet coefficients are shown in Figure C.3. The computation of the singularity degree (peakiness) used for peak

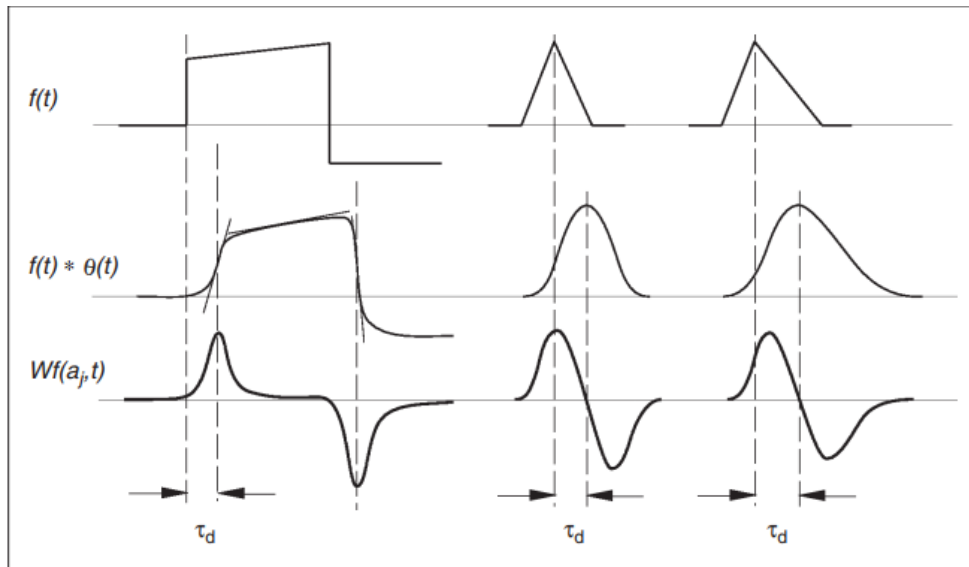


Figure C.3: Singularity Work Flow [44]

classification. The local Lipschitz regularity  $\alpha$  must be greater than zero for a valid R-peak.  $\alpha$  is computed by from the decline of the wavelet coefficients of the signal as [1]:

$$\alpha_j = \log_2 |Wf(2^{j+1}, n^{j+1})| - \log_2 |Wf(2^j, n^j)| \quad (\text{C.47})$$

$$\alpha = \frac{\alpha_1 + \alpha_2}{2} \quad (\text{C.48})$$

It is computationally inefficient because of the time consuming stage of the search and optimization for detecting R waves in ECG segments.